

A NOVEL NEURAL NETWORK BASED APPROACH FOR DIRECTION OF
ARRIVAL ESTIMATION

A THESIS SUBMITTED TO
THE GRADUATE SCHOOL OF NATURAL AND APPLIED SCIENCES
OF
MIDDLE EAST TECHNICAL UNIVERSITY

BY

SELÇUK ÇAYLAR

IN PARTIAL FULFILLMENT OF THE REQUIREMENTS
FOR
THE DEGREE OF DOCTOR OF PHILOSOPHY
IN
ELECTRICAL AND ELECTRONICS ENGINEERING

SEPTEMBER 2007

Approval of the thesis:

A NOVEL NEURAL NETWORK BASED APPROACH FOR DIRECTION OF
ARRIVAL ESTIMATION

submitted by **SELÇUK ÇAYLAR** in partial fulfillment of the requirements for the
degree of **Doctor of Philosophy in Electrical and Electronics Engineering**
Department, Middle East Technical University by,

Prof. Dr. Canan Özgen _____
Dean, Graduate School of **Natural and Applied Sciences**

Prof. Dr. İsmet Erkmén _____
Head of Department, **Electrical and Electronics Engineering**

Prof. Dr. Gülbin Dural _____
Supervisor, **Electrical and Electronics Eng. Dept., METU**

Prof. Dr. Kemal Leblebiciođlu _____
Co-supervisor, **Electrical and Electronics Eng. Dept., METU**

Examining Committee Members

Prof. Dr. Altunkan HIZAL (METU, EE) _____
Electrical and Electronics Eng. Dept., METU

Prof. Dr. Gülbin DURAL (METU, EE) _____
Electrical and Electronics Engineering Dept., METU

Prof. Dr. Ayhan ALTINTAŞ (Bilkent, EE) _____
Electrical and Electronics Eng. Dept., Bilkent University

Prof. Dr. Kemal LEBLEBİCİOĐLU (METU, EE) _____
Electrical and Electronics Eng. Dept., METU

Assoc. Prof. Dr. Seyit Sencer KOÇ (METU, EE) _____
Electrical and Electronics Engineering Dept., METU

Date: _____
03 / 09 / 2007

I hereby declare that all information in this document has been obtained and presented in accordance with academic rules and ethical conduct. I also declare that, as required by these rules and conduct, I have fully cited and referenced all material and results that are not original to this work.

Name, Last name : Selçuk ÇAYLAR

Signature :

ABSTRACT

A NOVEL NEURAL NETWORK BASED APPROACH FOR DIRECTION OF ARRIVAL ESTIMATION

Çaylar, Selçuk

Ph.D., Department of Electrical and Electronics Engineering

Supervisor: Prof. Dr. Gülbin DURAL

Co-supervisor: Prof. Dr. Kemal LEBLEBİCİOĞLU

September 2007, 109 pages

In this study, a neural network(NN) based algorithm is proposed for real time multiple source tracking problem based on a previously reported work. The proposed algorithm namely modified neural network based multiple source tracking algorithm (MN-MUST) performs direction of arrival(DoA) estimation in three stages which are the detection, filtering and DoA estimation stages. The main contributions of this proposed system are: reducing the input size for the uncorrelated source case (reducing the training time) of NN system without degradation of accuracy and insertion of a nonlinear spatial filter to isolate each one of the sectors where sources are present, from the others.

MN-MUST algorithm finds the targets correctly no matter whether the targets are located within the same angular sector or not. In addition as the number of targets exceeds the number of antenna elements the algorithm can still perform sufficiently well. Mutual coupling in array does not influence MN-MUST algorithm performance.

MN-MUST algorithm is further improved for a cylindrical microstrip patch antenna array by using the advantages of directive antenna pattern properties. The new algorithm is called cylindrical patch array MN-MUST(CMN-MUST). CMN-MUST algorithm consists of three stages as MN-MUST does. Detection stage is exactly the same as in MN-MUST. However spatial filtering and DoA estimation stage are reduced order by using the advantages of directive antenna pattern of cylindrical microstrip patch array.

The performance of the algorithm is investigated via computer simulations, for uniform linear arrays, a six element uniform dipole array and a twelve element uniform cylindrical microstrip patch array. The simulation results are compared to the previously reported works and the literature. It is observed that the proposed algorithm improves the previously reported works. The algorithm accuracy does not degrade in the presence of the mutual coupling. A uniform cylindrical patch array is successfully implemented to the MN-MUST algorithm. The implementation does not only cover full azimuth, but also improve the accuracy and speed. It is observed that the MN-MUST algorithm provides an accurate and efficient solution to the target-tracking problem in real time.

Keywords: Direction Finding, Target Tracking, Beam Forming, Direction of Arrival Estimation, Neural Network, Spatial Filtering.

ÖZ

AKILLI ANTENLER İLE HEDEF İZLEME

Çaylar, Selçuk

Doktora, Elektrik ve Elektronik Mühendisliği Bölümü

Tez Yöneticisi: Prof. Dr. Gülbin DURAL

Ortak Tez Yöneticisi: Prof. Dr. Kemal LEBLEBİCİOĞLU

Eylül 2007, 109 sayfa

Bu çalışmada, daha önce geliştirilen bir algoritmaya dayanan, gerçek zamanlı çoklu hedef takibi problemi için yapay sinir ağı kullanan yeni bir algoritma önerilmiştir. Önerilen, geliştirilmiş yapay sinir ağına dayalı çoklu hedef izleme(GY-ÇHİ) algoritması üç bölümden, kestirim, konumsal süzgeçleme ve yön bulma katlarından oluşmaktadır. Önerilen sistemin ana katkısı bir birinden ilintisiz hedefler olması durumunda yapay sinir ağlarının giriş ölçeklerinin düşürülmesi ile birden çok sektörde hedef bulunması durumunda her bir sektörü diğer sektörlerden yalıymak amacıyla ilave edilen küresel süzgeçleme katıdır.

GY-ÇHİ algoritması, hedefler birden çok açısal bölgede olsa bile bulabilmektedir. Ayrıca hedef sayısı anten dizini elamanı sayısını geçmesi durumunda bile algoritma hedefleri doğru olarak bulabilmektedir. Anten dizininde meydana gelecek girişimler GY-ÇHİ algoritmasının performansını etkilememektedir.

GY-ÇHİ algoritması, yönlü anten yayılım karakteristiği kullanılarak silindirik microstrip patch anten dizini için daha fazla iyileştirilmiştir. Yeni algoritma silindirik microstrip patch dizini ile GY-ÇHİ(SGY-ÇHİ) algoritması olarak isimlendirilmiştir. SGY-ÇHİ, GY-ÇHİ gibi üç bölümden oluşur. Kestirim bölümü GY-ÇHİ ile

tamamem aynıdır. Konumsal süzgeçleme ve yön bulma katları ise yönlü antenin avantajlarını kullanarak sade bir yapıda önerilmiştir.

Algoritmanın performansı, bilgisayar benzetimleri ile düzgün doğrusal anten dizini, altı elemanlı düzgün bir dairesel dipole anten dizini ve on iki elemanlı düzgün bir silindirik microstrip patch anten dizini için ayrı ayrı incelenmiştir. Benzetim sonuçları daha önce geliştirilen algoritmalar ve literatürde yer alan geleneksel yöntemler ile karşılaştırılmıştır. Önerilen algoritmanın daha önce geliştirilen algoritmaları iyileştirdiği gözlemlenmiştir. Anten dizininde oluşacak girişimler, algoritmanın kestirim doğruluğunu düşürmemektedir. On iki elemanlı düzgün silindirik bir patch anten dizinine SGY-ÇHI algoritmasına başarıyla uygulanmıştır. Uygulama yalnızca tüm yatay açıyı kestirmekle kalmayıp, aynı zamanda kestirim doğruluğunu ve hızı iyileştirirken yapay sinir ağ boyutunu küçültmektedir. SGY-ÇHI algoritmasının gerçek zamanlı hedef izleme problemine doğru ve etkin çözüm sağladığı gözlemlenmiştir.

Direction Finding, Target Tracking, Beam Forming, Direction of Arrival Estimation, Neural Network, Spatial Filtering.

Anahtar Kelimeler: Yön Bulma, Hedef İzleme, Huzme Şekillendirme, Geliş Yönü Tahmini, Yapay Sinir Ağı, Konumsal Filtreleme.

To My Family: Yasemin, Oğuz Mert, Mine Ezgi aylar

ACKNOWLEDGMENTS

The author wishes to express his deepest gratitude to his supervisor Prof. Dr. Gülbin Dural and co-supervisor Prof. Dr. Kemal Leblebiciođlu for their guidance, advice, criticism, encouragements and insight throughout the research.

The author would like to thank Prof. Altunkal Hızal, Prof. Ayhan Altıntaş and Assoc. Prof. Dr. Seyit Sencer Koç for their suggestions and comments.

The author also would like to thank Ebru Serttaş for her editorial guidance.

He also would like to acknowledge the encouragement, patience and sacrifice made by his wife Yasemin Çaylar, his son Ođuz Mert Çaylar and his daughter Mine Ezgi Çaylar.

TABLE OF CONTENTS

ABSTRACT	iv
ÖZ	vi
DEDICATION	viii
ACKNOWLEDGMENTS	ix
TABLE OF CONTENTS	x
1 INTRODUCTION.....	1
2 DIRECTION FINDING.....	5
2.1 Direction Finding Problem.....	6
2.2 Conventional DoA Estimation Methods	8
2.2.1. Bartlett DoA Estimation.....	8
2.2.2. Capon DoA Estimation	9
2.2.3. Linear Prediction DoA Estimate	10
2.2.4. Maximum Entropy DoA Estimate	11
2.2.5 Pisarenko Harmonic Decomposition(PHD) DoA Estimate	11
2.2.6 Min-Norm DoA Estimate.....	11
2.2.7 MUSIC DoA Estimate	13
2.2.8 Root-MUSIC DoA Estimate	14
2.2.9 ESPRIT DoA Estimate.....	16
2.3 Neural Network Based Algorithms for DoA	20
2.3.1. Multilayer Perceptron Method	21
2.3.2. Hopfield Method	23

2.3.3. Radial Basis Function Network Method	24
2.3.4. Principal Component Analysis Based Neural Method.....	24
2.3.5. Fuzzy Neural Method.....	26
2.4. Discussion	27
3 NEURAL NETWORK-BASED DIRECTION FINDING	29
3.1 Problem Formulation for Uniform Linear Array	30
3.2 Modified Neural Multiple Source Tracking (MN-MUST) Algorithm	34
3.2.1 Detection Stage	34
3.2.2 Spatial Filtering Stage.....	35
3.2.3 DoA Estimation Stage.....	37
3.3 MN-MUST Algorithm Features.....	38
3.3.1. Sampled Data Processing.....	38
3.3.2. Correlation Matrix.....	39
3.3.3. Signal and Noise Model.....	40
3.3.4. Radial Basis Function Applied to MN-MUST Algorithm.....	41
3.3.4.1. Detection Stage RBFNN Training and Performance Phase.....	43
3.3.4.2. Spatial Filtering Stage RBNN Training and Performance Phase .	44
3.3.4.3. DoA Estimation Stage RBNN Training and Performance Phase .	45
3.4 MNMUST Algorithm for Circular Array in The Presence of Mutual Coupling.....	46
3.4.1 Problem Formulation for Circular Array	47
3.4.2. Mutual Coupling	51

3.4.3. Problem Formulation in the Presence of Mutual Coupling for Circular Array	52
3.5 MN-MUST Algorithm for Cylindrical Microstrip Patch Array	54
3.5.1 Cylindrical Microstrip Patch	55
3.5.2 Cylindrical Microstrip Patch Radiation Pattern	58
3.5.3 Cylindrical Microstrip Patch Array	59
3.5.4 MN-MUST Implementation to Cylindrical Array	64
3.5.4.1 Spatial Filtering Stage	64
3.5.4.2 Reduced Order Sectoral DoA Estimation Stage	67
4 SIMULATIONS	68
4.1 Simulations Features	69
4.2 Cramer-Rao Bound	70
4.3 Neural Network Training Mean Squared Error Effects	72
4.4 Number of Antenna Elements	73
4.5 MN-MUST and N-MUST Comparison	74
4.6 SNR Level	79
4.8 Effect of Angular Separation of the Targets	82
4.9 Effect of the Mutual Coupling under UCA Implementation	83
4.10 Cylindrical Patch Array Implementation	85
5 CONCLUSIONS	89
REFERENCES	92
APPENDICES	
A. CORRELATION MATRIX	106

B. MUTUAL IMPEDANCE MATRIX FOR 6 ELEMENT CIRCULAR ARRAY WITH HALF-WAVELENGTH DIPOLES	108
VITA	109

LIST OF FIGURES

Figure 2.1 M -element array with arriving signals.....	7
Figure 2.2 Doublet composed of two identical displaced arrays.	17
Figure 2.3 DoA neural network model.	20
Figure 2.4 Neural architecture.	21
Figure 2.5 MLP architecture.	22
Figure 2.6 Hopfield network.	23
Figure 2.7 Architecture of the RBFN.....	24
Figure 2.8 PCA network.	25
Figure 3.1 Array structure.	31
Figure 3.2 The block diagram of DoA estimation problem (Fig. 1. of [57])......	33
Figure 3.3 The modified neural multiple source tracking architecture.....	36
Figure 3.4 Radial basis neural network structure.....	42
Figure 3.5 Circular array structure.....	49
Figure 3.6 Geometry of cylindrical micro strip patch antenna.	56
Figure 3.7 The total electrical field pattern of a patch at $\theta = 90^\circ$ (E -plane) with $h = 1.6mm$, $\epsilon_r = 4.4$, $L = 38.3mm$, $\theta_0 = 9.1848^\circ$ and $a = 38.3mm$	61
Figure 3.8 The geometry of 12 element uniform cylindrical patch array with $h = 1.6mm$, $\epsilon_r = 4.4$, $L = 38.3mm$, $\theta_0 = 9.1848^\circ$ and $a = 38.3mm$	62
Figure 3.9 The individual element electrical field patterns of 12 element patch array given in Fig. (3.8).....	63

Figure 3.10 Geometry of a circular array (m -th incident wave on n -th antenna element).....	63
Figure 3.11 The twelve cylindrical patch pattern is divided into 12 equal sectors....	65
Figure 3.12 The CMN-MUST algorithm architecture.	66
Figure 4.1 MN-MUST performance comparison with MUSIC algorithm and CRB for 0° for three different SNR.....	70
Figure 4.2 MN-MUST performance comparison with MUSIC algorithm and CRB for 2° for three different SNR.....	71
Figure 4.3 DoA estimation RMS error for three elements ULA, three and four sources cases tested on a MN-MUST algorithm DoA estimation stage NN trained under the goal of 20, 50, 100 and 150 mean squared error.....	72
Figure 4.4 DoA estimation RMS error for five element ULA, three and four sources cases tested on a MN-MUST algorithm DoA estimation stage NN trained under the goal of 20, 50, 100 and 150 mean squared error.....	73
Figure 4.5 DoA estimation RMS error vs. number of antenna elements used in ULA, three source, 20 dB SNR, constant training RBNN parameter.	74
Figure 4.6 Training time vs. antenna elements size (MN-MUST algorithm to N-MUST algorithm)	75
Figure 4.7 Error performance of MN-MUST algorithm and N-MUST algorithm	76
Figure 4.8 Memory requirements comparison of the neural networks for MN-MUST algorithm and N-MUST algorithm.....	76
Figure 4.9 Three targets in three sectors in a three-element array (Targets are at 1, 15 and 24 degrees)	77

Figure 4.10 Three targets in one sector in a five-element array (Targets are at 22, 24 and 29 degrees). Targets are of equal power and 5 dB higher than noise power.....	78
Figure 4.11 Four targets in one sector in a three-element array (Targets are at 21, 24, 27 and 29 degrees). Targets are of equal power and 5 dB higher than noise power..	79
Figure 4.12 Twelve-element ULA , tested for three sources.	80
Figure 4.13 Three-element ULA, tested for three sources.....	80
Figure 4.14 RMS value of DoA estimation error v.s. number of snapshots for a 8-element ULA with $\lambda / 2$ distance and tested for 3 targets. Targets are of equal power and 20 dB higher than noise power.....	82
Figure 4.15 RMS value of DoA estimation error v.s. angular separation for an 8-element ULA with $\lambda / 2$ distance. There are three targets, of equal power and 20 dB higher than noise power.	83
Figure 4.16 Two targets in six-element half-wave dipole uniform circular array (Targets are at 21 and 25 degrees). MN-MUST DoA Networks are trained in PMC.	84
Figure 4.17 Two targets in a six-element half-wave dipole uniform circular array (Targets are at 21 and 25 degrees). MN-MUST DoA Networks are trained in the absence of mutual coupling.....	85
Figure 4.18 DoA estimation two targets are in angular Sector 1 (Targets are at 348 and 3 degrees). CMN-MUST DoA estimation stage of Sector-1 run with a 30 dB SNR level (estimated values of the targets is the one close to the center).....	87
Figure 4.19 CMN-MUST DoA estimation error RMS values versus 20, 30, 50 dB SNR. Two target case run for angular Sector 1.	88

Figure 4.20 Two targets are in two different sectors. The spatial filtering stage run after the detection stage for Sector 1. The filtered output is the input for DoA estimation stage for Sector 1. DoA estimation results for Sector 1 and actual targets in the same axes (targets at 5 and 164 degrees). SNR is 30 dB. 88

LIST OF TABLES

Table C.1 Coupling Impedance Matrix for a 6 elements halfwavelength dipole array with a radius $a = \frac{3\lambda}{2\pi}$	108
---	-----

CHAPTER 1

INTRODUCTION

Direction finding is one of the major problems for many applications such as radar, navigation, mobile communications, electronic warfare systems, sonar and seismology. Direction finding algorithms have also been known as spectral estimation, direction-of-arrival (DoA) estimation, angle of arrival (AoA) estimation, or bearing estimation. The goal of DoA estimation algorithm is to estimate the direction of the signal of interest from a collection of noise “contaminated” set of received signals.

The early direction finding methods were based on creating a pencil beam, then mechanically steering that beam into the angular region of interest. Arrays were used to create the desired beam. Later, mechanical steering is replaced by electronic beam steering with the advances in antenna manufacturing and signal processing.

Direction finding have followed an evolutionary trend. In the previous decade some powerfull and high-resolution methods for DoA estimation such as MUSIC and ESPRIT [1-3] had already been developed. However, these conventional methods were typically linear algebra based methods requiring computationally intensive matrix inversions. Furthermore there were some drawbacks such as the number of arriving sources must be less than the number of antenna array elements and a accuracy degradation of DoA estimation under low SNR. Therefore they were not able to meet real-time requirements.

Rapid growth in wireless communication accelareted the demand for DoA estimation. Neural networks (NN) evolved into powerful tools in various fields in the past few decades. Within the last decade quite a few number of NN based DoA estimation algorithms have been developed to overcome the drawbacks of conventional methods and respond the demand [4-57]. The main advantages of the NN methods are that they outperform conventional linear algebra based methods in

both speed and accuracy, since NN methods avoid the cumbersome eigen-decomposition processes. Apart from being computationally efficient, NN methods have been observed to be more immune to noise and are found to yield better performance in the presence of correlated arrivals. However, in this study, proposed algorithm improvement in neural network size is developed for uncorrelated source case.

In a recently published work, a NN algorithm, namely the Neural Multiple-Source Tracking (N-MUST) algorithm, was presented for locating and tracking angles of arrival from multiple sources [57]. The algorithm employs a neural network operating in two stages and is based on dividing the field of view of the antenna array into angular sectors. Each network in the first stage of the algorithm is trained to detect signals generated within its sector. Depending on the output of the first stage, one or more networks of the second stage can be activated to estimate the exact location of the sources. Main advantages of the N-MUST algorithm were presented as significant reduction in the size of training set and the ability of locating more sources than there are array elements.

The algorithm proposed in this thesis [58-63], namely the Modified Neural Multiple Source Tracking Algorithm (MN-MUST), consists of three stages that are classified as the detection, filtering and DoA estimation stages. Similar to [57], a number of Radial Basis Function Neural Networks (RBFNN) are trained for detection of the angular sectors which have source or sources. A spatial filter stage is applied individually to the every angular sector which is classified in the first stage as having source or sources. Each individual spatial filter is designed to filter out the signals coming from the all other angular sectors outside the particular source detected angular sector. This stage considerably improves the performance of the algorithm in the case where more than one angular sector have source or sources at the same time. Insertion of this spatial filtering stage is one of the main contributions of this thesis. The third stage consists of a Neural Network trained for DoA estimation. In all three stages Neural Network's size and the training data size is considerably reduced as

compared to the previous approach [57] for uncorrelated sources, without loss of accuracy.

Within the scope of the thesis, the target tracking problem is examined for a linear array with uniform isotropic elements, a circular array with uniform dipole elements and a cylindrical patch array to demonstrate the performance of the algorithm. The ambiguity problem can arise for ULA and UCA applications. Therefore for UCA and ULA implementation of the MN-MUST algorithm is considered only for a limited angular sector. However, ambiguity is not a problem for cylindrical microstrip patch array, while covering the full azimuth.

In Chapter 1, a general introduction to DoA estimation, evolution of the algorithms is given.

In Chapter 2, the direction finding problem is defined. The conventional methods in the literature have been discussed in an orderly manner. The advances and drawbacks of the conventional algorithms have been reviewed. Neural network algorithms for DoA estimation is presented and each NN algorithm has been reviewed separately. The aim of the thesis is also explained in this chapter.

In Chapter 3, the problem formulation is presented and the neural networks for the problem of DoA estimation are established for the case of a linear array of isotropic sources. Then the proposed algorithm is discussed for a linear array. The proposed algorithm is implemented on a uniform circular dipole array in the presence of mutual coupling. Mutual coupling matrix and mutual coupling impedance have been studied for a 6-six element uniform circular dipole array. Then the algorithm is tested in the presence of mutual coupling. In the last section of the chapter proposed algorithm is applied on a twelve-element cylindrical patch array. The proposed algorithm is simplified for cylindrical arrays because of the pattern characteristics, while covering the whole azimuth.

In Chapter 4, simulation results are obtained to evaluate the performance of the proposed algorithm. Simulations have been made for linear, circular and cylindrical arrays examined in Chapter 3.

The performance of the algorithm is also tested in the presence of mutual coupling and different noise level. Simulation results are compared with conventional and neural network algorithms in the literature.

In Chapter 5, conclusive remarks are provided.

CHAPTER 2

DIRECTION FINDING

In many applications such as radar, navigation, mobile communications, electronic warfare systems, sonar and seismology, direction finding is one of the major problems. A variety of techniques for its solution have been proposed over past decades.

Direction finding algorithms have also been known as spectral estimation, angle of arrival (AoA) estimation, direction-of-arrival (DoA) estimation or bearing estimation. The goal of DoA estimation algorithms is to estimate the direction of the signal of interest from a collection of noise “contaminated” set of received signals in an array.

DoA estimation algorithms have been developed following an evolutionary trend. In the previous decade some powerful and high-resolution methods for DoA such as MUSIC and ESPRIT had already been developed. However, these conventional methods were typically linear algebra based methods requiring computationally intensive matrix inversions. Furthermore there were some drawbacks such as the number of arriving sources must be less than the number of antenna array elements and an accuracy degradation of DoA estimation under low SNR. Therefore they were not able to meet real-time requirements. Neural Networks (NN) evolved into powerful tools in various fields in the past few decades. Within the last decade quite a few number of NN based DoA estimation algorithms have been developed to overcome the drawbacks of conventional methods.

An extensive survey on the evolution of conventional DoA estimation algorithms is provided in [1], where conventional DoA estimation algorithms are classified. Conventional DoA estimation classifications can be found in [2] and [3] as well. The DoA algorithm classification discussed in this chapter is parallel to [1-3] to a large extent.

Neural network based methods have recently been developed for real-time DoA estimation problem requirements [4-57]. A survey of neural network based methods for array signal processing including DoA estimation methods is presented in [4]. The main advantages of the neural methods are that they outperform conventional linear algebra based methods in both speed and accuracy. Since neural methods avoid the cumbersome eigen-decomposition processes they are found to be far quicker than conventional methods. Apart from being computationally efficient, neural methods have been observed to be more immune to noise and are found to yield better performance in the presence of correlated arrivals. However, a drawback of the neural schemes is the selection of the network size which is usually done by trial and error.

This thesis is motivated around the Neural Multiple-Source Tracking (N-MUST) algorithm [53-57]. The proposed algorithm is based on N-MUST and is called Modified Neural Multiple Source Tracking (MN-MUST) and published in [58-63].

2.1 Direction Finding Problem

DoA estimation problem in generalized form is to be defined in order to review the evolution of the DoA estimation algorithms. Notations used in this section are parallel to those given in [2].

Fig. (2.1) shows a receiving array with incident plane waves from various directions. There are K signals arriving from K directions. Signals received by M antenna elements in the array are multiplied by M potential weights. Each received signal $S_m(k)$ includes additive, zero mean, Gaussian noise. Time is represented by the k -th time sample. Thus the array output Y can be given as

$$Y(k) = W^T X(k) \tag{2.1}$$

where

$$\begin{aligned}
 X(k) &= [a(\theta_1) \quad a(\theta_2) \quad \dots \quad a(\theta_K)] \begin{bmatrix} S_1(k) \\ S_2(k) \\ \vdots \\ S_K(k) \end{bmatrix} + N(k) \\
 &= AS(k) + N(k)
 \end{aligned} \tag{2.2}$$

$S(k)$ is a vector of K signals at time k , $N(k)$ is a noise vector at each array element m , zero mean, variance σ^2 , $a(\theta_i)$ is a M -element array steering vector for the θ_i direction of arrival, A is an $M \times K$ matrix of steering vectors $a(\theta_i)$.

It is assumed that the directions of incident signals are not changed for a period of time. The received signals are also considered as time varying and thus the calculations are based upon snapshots of them.

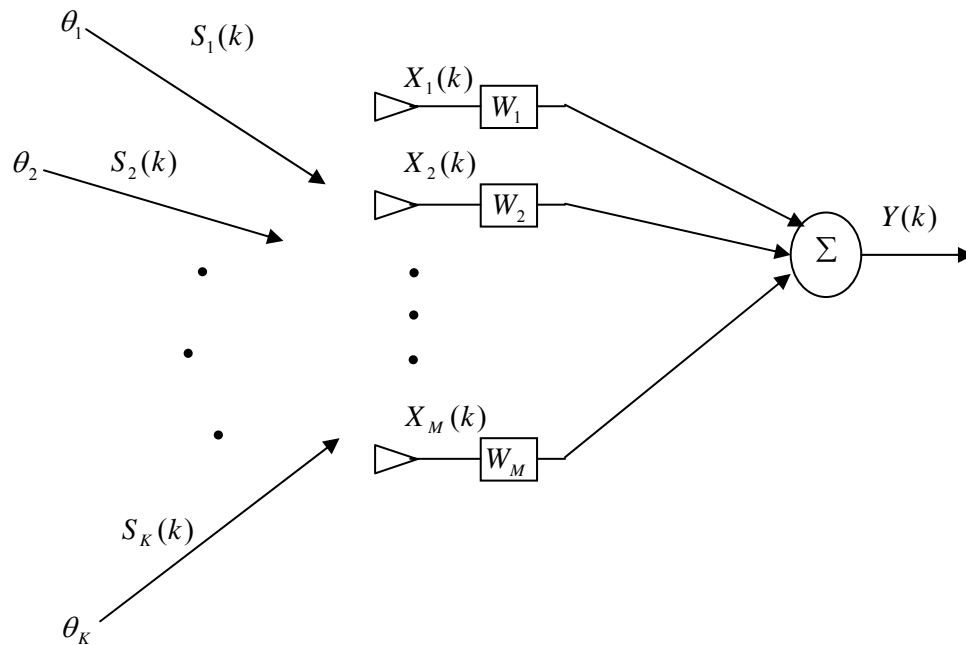


Figure 2.1 M -element array with arriving signals.

The correlation matrix based on Eq. (2.2) can be defined as,

$$\begin{aligned}
R &= E\{XX^H\} \\
&= E\{(AS + N)(AS + N)^H\}A^H \\
&= AE\{SS^H\}A^H + E\{NN^H\} \\
&= AR_s A^H + R_n
\end{aligned} \tag{2.3}$$

where R_s is an $K \times K$ source correlation matrix, $R_n = \sigma^2 I$ is a $M \times M$ noise correlation matrix, I is an $M \times M$ identity matrix.

2.2 Conventional DoA Estimation Methods

Conventional DoA estimation algorithms have been developed in the previous three decades. It is possible to group these algorithms in several different ways. The goal of this section is to give a general idea about the evolution of the conventional methods; that is the reason why the details of the algorithms are not given explicitly. However, the last two algorithms, i.e., MUSIC and ESPRIT algorithms have been reviewed thoroughly as they are the most advanced conventional methods. The methods are given in an evolutionary and historical order.

The goal of conventional DoA estimation techniques is to define a function that gives an indication of the angles of arrival based upon maxima vs. angle. This function is traditionally called the pseudospectrum $P(\theta)$ and the units can be in energy or in watts (or at times energy or watts squared). The pseudospectrum will be used for all conventional algorithms except ESPRIT.

2.2.1. Bartlett DoA Estimation

Bartlett DoA method is one of the earliest methods. Uniform weighting is applied to the array. This method estimates the mean power expression of pseudospectrum $P_B(\theta)$ [64] such as

$$P_B(\theta) = a(\theta)^H R_X a(\theta) \quad (2.4)$$

Under the conditions that the source signals are uncorrelated and there is no system noise, Eq. (2.4) is equivalent to

$$P_B(\theta) = \left| \sum_{i=1}^K \sum_{m=1}^M e^{j(m-1)kd(\sin\theta - \sin\theta_i)} \right|^2 \quad (2.5)$$

The peditogram is equivalent to the spatial finite Fourier transform of all arriving signals.

The main limitation of Bartlett approach for DoA estimation is the resolution of arrival angles. It is limited by the array half power beam width [1].

2.2.2. Capon DoA Estimation

The Capon DoA estimation [65-66] is known as a minimum variance distortionless response. It is alternatively a maximum likelihood estimate of power arriving from one direction while all other sources are considered as interference. The goal is to maximize the signal-to-interference ratio (SIR) while passing the signal of interest undistorted in phase and amplitude. This maximized SIR is accomplished with a set of array weights, W , is given by

$$W = \frac{R_X^{-1} a(\theta)}{a(\theta)^H R_X^{-1} a(\theta)} \quad (2.6)$$

where R_X is the unweighed array correlation matrix.

Substituting Eq. (2.6) into the array given in Fig. (2.1), the pseudospectrum $P_C(\theta)$ is obtained,

$$P_C(\theta) = \frac{1}{a(\theta)^H R_X^{-1} a(\theta)} \quad (2.7)$$

Capon DoA estimate has much greater resolution than the Bartlett DoA estimate. However, Capon resolution will not work in the case of highly correlated sources exist. The main advantage of Capon estimate is that one does not need a priori knowledge of specific statistical properties [2].

2.2.3. Linear Prediction DoA Estimate

The goal of the linear prediction method is to minimize the prediction error between the output of the m -th sensor and the actual output [67]. In order to accomplish this goal it needs to find the weights that minimize the mean-squared prediction error. The solution for the array weights is given as

$$W = \frac{R_X^{-1} U_m}{U_m^T R_X^{-1} U_m} \quad (2.8)$$

where U_m is the Cartesian basis vector which is the m -th column of the $M \times M$ identity matrix.

Substituting of the Eq. (2.8) into pseudo-spectrum, it can be shown that, P_{LP_m} is given by

$$P_{LP_m}(\theta) = \frac{U_m^T R_X^{-1} U_m}{|U_m^T R_X^{-1} a(\theta)|^2} \quad (2.9)$$

The particular choice for which m -th element output for prediction is random. However, its selection affects the resolution capability and bias in estimate. Linear prediction methods perform well in a moderately low SNR environment and are a good compromise in situations where sources are coherent and equal power. Linear prediction estimate can also provide signal strength information.

2.2.4. Maximum Entropy DoA Estimate

The goal of maximum entropy DoA estimate is to find a pseudospectrum that maximizes the entropy function subject to constraints [68-70]. The pseudospectrum, P_{ME_m} , is given by

$$P_{ME_m}(\theta) = \frac{1}{a(\theta)^H C_j C_j^H a(\theta)} \quad (2.10)$$

where C_j is the j -th column of the inverse array correlation matrix(R_x^{-1}).

2.2.5 Pisarenko Harmonic Decomposition(PHD) DoA Estimate

The goal is to minimize mean-squared error of the array output under the constraint that the norm of the weight vector be equal to unity. The eigenvector that minimizes the mean-squared error corresponds to the smallest eigenvalue [71-72]. Pisarenko harmonic decomposition pseudospectrum, P_{PHD} , is given by

$$P_{PHD}(\theta) = \frac{1}{|a^H(\theta)e_1|^2} \quad (2.11)$$

where e_1 is the eigen vector associated with the smallest eigenvalue λ_1 . Pisarenko harmonic decomposition method provides the better solution than linear prediction and maximum entropy methods.

2.2.6 Min-Norm DoA Estimate

The minimum-norm method is only valid for uniform linear arrays (ULA) [72-75]. The min-norm algorithm optimizes the weight vector by solving the following optimization problem,

$$\min_w W^H W \quad \text{such that} \quad E_S^H W = 0 \quad W^H U_1 = 1 \quad (2.12)$$

where

W is array weights, E_S subspace of K eigenvectors such as

$$E_S = [e_{M-K+1} \quad e_{M-K+2} \quad \dots \quad e_M]$$

M is the number of array elements, K is the number of arriving signals, and $U_1 = [1 \quad 0 \quad \dots \quad 0]^T$

The solution to the optimization yields the min-norm pseudospectrum; P_{MN} ,

$$P_{MN}(\theta) = \frac{(U_1^T E_N E_N^H U_1)^2}{|a(\theta)^H E_N E_N^H U_1|^2} \quad (2.13)$$

where E_N is subspace of $M - K$ noise vectors

$$E_N = [e_1 \quad e_2 \quad \dots \quad e_{M-K}]$$

$a(\theta)$ is array steering vector.

Numerator of Eq. (2.13) is constant, so the pseudospectrum can be normalized such that

$$P_{MN}(\theta) = \frac{1}{|a(\theta)^H E_N E_N^H U_1|^2} \quad (2.14)$$

It should be noted that the pseudospectrum from the min-norm method is almost identical to the PHD pseudospectrum. The min-norm method combines all noise eigenvectors whereas the PHD method only uses the first noise eigenvector.

2.2.7 MUSIC DoA Estimate

MUSIC is an acronym for Multiple Signal Classification. MUSIC is a popular high resolution exigent structure method [76]. It promises to provide unbiased estimates of number of signals, the angles of arrival, and the strengths of the waveforms. MUSIC makes the assumption that the noise in each channel is uncorrelated making the noise correlation matrix diagonal. The incident signals may be somewhat correlated creating a nondiagonal signal correlation matrix.

The number of incoming signals is known or eigenvalues must be searched to determine the number of incoming signals. If the number of signals K , the number of signal eigenvalues and eigenvectors K , and the number of noise eigenvalues and eigenvectors is $M - K$ (M is the number of array elements), then the array correlation matrix can be calculated based on the assumption of uncorrelated noise and equal variances.

$$R_X = AR_S A^H + \sigma^2 I \quad (2.15)$$

The next step is to find eigenvalues and eigenvectors. Then K eigenvectors associated with the signals and $M - K$ eigenvectors associated with the noise are produced. Then the eigenvectors associated with the smallest eigenvalues are chosen. For uncorrelated signals, the smallest eigenvalues are equal to the variance of noise. Then the $M \times (M - K)$ subspace spanned by the noise eigenvectors is constructed as shown below:

$$E_N = [e_1 \quad e_2 \quad \dots \quad e_{M-K}] \quad (2.16)$$

The noise subspace eigenvectors are orthogonal to the array steering vectors at the angles of arrival $\theta_1, \theta_2, \dots, \theta_K$. Because of this orthogonality condition, Euclidean distance becomes $d^2 = a(\theta)^H E_N E_N^H a(\theta) = 0$ for every arrival angle $\theta_1, \theta_2, \dots, \theta_K$. Placing this distance expression in the denominator creates

sharp peaks at the angles of arrival. The MUSIC pseudospectrum, P_{MU} , is then given as

$$P_{MU}(\theta) = \frac{1}{|a(\theta)^H E_N E_N^H a(\theta)|} \quad (2.17)$$

For a single source case and a high SNR, MUSIC algorithm approaches the CRLB. When using large number of snapshots, MUSIC algorithm gets the best solution [1]. However for low SNR and correlated sources case the performance diminishes.

2.2.8 Root-MUSIC DoA Estimate

The MUSIC algorithm in general can be applied to any arbitrary array regardless of the position of the array elements. Root-MUSIC implies that the MUSIC algorithm is reduced to finding roots of a polynomial as opposed to merely plotting the pseudospectrum or searching for peaks in the pseudospectrum.

One can simplify Eq. (2.17) by defining the matrix $C = E_N E_N^H$ which is Hermitian. This leads to the root-MUSIC expression [70],

$$P_{MU}(\theta) = \frac{1}{|a(\theta)^H C a(\theta)|} \quad (2.18)$$

If we have an ULA, the m th element of the array steering vector is given by

$$a_m(\theta) = e^{jkd(m-1)\sin\theta} \quad m = 1, 2, \dots, M \quad (2.19)$$

The denominator in Eq. (2.18) can be written as

$$\begin{aligned}
a_m(\theta)^H C a(\theta) &= \sum_{m=1}^M \sum_{n=1}^M e^{-jkd(m-1)\sin\theta} C_{mn} e^{jkd(n-1)\sin\theta} \\
&= \sum_{l=-M+1}^{M-1} C_l e^{jkd l \sin\theta}
\end{aligned} \tag{2.20}$$

where C_l is the sum of the diagonal element of C along the l th diagonal such that

$$C_l = \sum_{n-m=l} C_{mn} \tag{2.21}$$

It should be noted that the matrix C has off-diagonal sums such that $C_0 > |C_l|$ for $l \neq 0$. Thus the sum of off-diagonal elements is always less than the sum of the main diagonal elements. In addition, $C_l = C_{-l}^*$.

Eq. (2.20) can be simplified to be in the form of a polynomial whose coefficients are C_l ,

$$D(z) = \sum_{l=-M+1}^{M-1} C_l z^l \tag{2.22}$$

where $z = e^{-jkd \sin\theta}$

The roots of $D(z)$ that lie closest to the unit circle correspond to the poles of the MUSIC pseudospectrum. Thus, this technique is called root-MUSIC. The polynomial Eq. (2.22) has an order of $2(M-1)$ and thus has roots of $z_1, z_2, \dots, z_{2(M-1)}$. In the fields of complex numbers, each root can be represented in polar form as

$$z_i = |z_i| e^{j \arg(z_i)} \quad i = 1, 2, \dots, 2(M-1) \tag{2.23}$$

where $\arg(z_i)$ is the phase angle of z_i .

Exact zeros in $D(z)$ exist when the root magnitudes $|z_i|=1$. DoA can be calculated by comparing $e^{j\arg(z_i)}$ to $e^{jkd\sin\theta_i}$ to get

$$\theta_i = -\sin^{-1}\left(\frac{1}{kd}\arg(z_i)\right) \quad (2.24)$$

Root-MUSIC method has a better solution than MUSIC for a ULA case.

2.2.9 ESPRIT DoA Estimate

ESPRIT stands for Estimation of Signal Parameters via Rotational Invariance Techniques. The goal of ESPRIT is to exploit the rotational invariance in the signal subspace which is created by two arrays with a translational invariance structure [77 and 78]. ESPRIT inherently assumes narrowband signals so it is assumed that there are $K < M$ narrow-band sources centered at the center frequency f_0 . These signal sources are assumed to be of a sufficient range so that the incident propagation field is approximately planar. The sources can be either random or deterministic and the noise is assumed to be random with zero mean. ESPRIT assumes multiple identical arrays called doublets. These can be separate arrays or can be composed of subarrays of one larger array. These arrays are displaced translationally. An example is shown Fig. (2.2) where a four element linear array is composed of two identical three-element subarrays or two doublets. These two subarrays are translationally displaced by the distance d . Arrays are labeled as array 1 and array 2.

The signals induced on each the arrays are given by

$$\begin{aligned} X_1(k) &= [a_1(\theta_1) \quad a_1(\theta_2) \quad \dots \quad a_1(\theta_K)] \begin{bmatrix} S_1(k) \\ S_2(k) \\ \dots \\ S_K(k) \end{bmatrix} + N_1(k) \\ &= A_1 S(k) + N_1(k) \end{aligned} \quad (2.25)$$

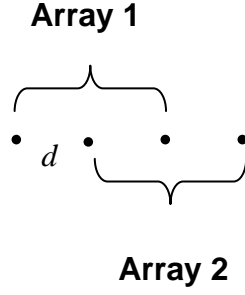


Figure 2.2 Doublet composed of two identical displaced arrays.

$$\begin{aligned} X_2(k) &= A_2 S(k) + N_2(k) \\ &= A_1 \Phi S(k) + N_2(k) \end{aligned} \quad (2.26)$$

where $\Phi = \text{diag}\{e^{jkd \sin \theta_1}, e^{jkd \sin \theta_2}, \dots, e^{jkd \sin \theta_K}\}$ is a $K \times K$ diagonal unitary matrix with phase shifts between the doublets for each DoA. A_i is a Vandermonde matrix of steering vectors for sub arrays $i = 1, 2$.

The complete received signals considering the contributions of both sub-arrays is given as

$$X(k) = \begin{bmatrix} X_1(k) \\ X_2(k) \end{bmatrix} = \begin{bmatrix} A_1 \\ A_1 \Phi \end{bmatrix} S(k) + \begin{bmatrix} N_1 \\ N_2 \end{bmatrix} \quad (2.27)$$

Correlation matrix for either the complete array or for the two subarrays can be computed. The correlation matrix for the complete array is given by

$$R_X = E\{XX^H\} = AR_S A^H + \sigma^2 I \quad (2.28)$$

The correlation matrices for the two sub arrays are given by

$$R_1 = E\{X_1 X_1^H\} = A_1 R_S A_1^H + \sigma^2 I \quad (2.29)$$

$$R_2 = E\{X_2 X_2^H\} = A_1 \Phi R_s \Phi^H A_1^H + \sigma^2 I \quad (2.30)$$

Each of the full rank correlation matrices given in Eq. (2.29) and (2.30) has a set of eigenvectors corresponding to the K sources. Creating the signal subspace for two subarrays results in the two matrices E_1 and E_2 . Creating the signal subspace for entire array results in the one signal subspace given by E_x . Because of the invariance structure of the array, E_x can be decomposed into the subspaces E_1 and E_2 .

Both E_1 and E_2 are $M \times K$ matrices whose columns are composed of the K eigenvectors corresponding to the latest eigenvalues of R_1 and R_2 . Since the arrays are translationally related, the subspaces of eigenvectors are related by a unique non-singular transformation matrix Ψ such that

$$E_1 \Psi = E_2 \quad (2.31)$$

There must also exist a unique non-singular transformation matrix T such that

$$E_1 = AT \quad (2.32)$$

and

$$E_2 = A\Phi T \quad (2.33)$$

By substituting Eqs (2.31) and (2.32) into Eq. (2.33) and assuming that A is full-rank, then one can write,

$$T\Psi T^{-1} = \Phi \quad (2.34)$$

Thus, the eigenvalues of Ψ must be equal to the diagonal elements of Φ such that $\lambda_1 = e^{jkd \sin \theta_1}$, $\lambda_2 = e^{jkd \sin \theta_2}$, ..., $\lambda_K = e^{jkd \sin \theta_K}$ and the columns of T must be the eigenvectors of Ψ . Ψ is a rotation operator that maps the signal subspace E_1 into the signal subspace E_2 . The only remaining thing left is to estimate the eigenvalues of rotational operator Ψ . Following steps outlines the details of the estimation.

Step-1: Estimate the array correlation matrices R_1, R_2 from the data samples.

Step-2: Estimate the total number of sources by the number of large eigenvalues of either R_1 or R_2 .

Step-3: Calculate the signal subspaces E_1 and E_2 based upon the signal eigenvectors of R_1 and R_2 .

Step-4: Form a $2K \times 2K$ matrix using the signal subspaces such that

$$C = \begin{bmatrix} E_1^H \\ E_2^H \end{bmatrix} \begin{bmatrix} E_1 & E_2 \end{bmatrix} = E_C \Lambda E_C^H \quad (2.35)$$

where the matrix E_C is from the eigenvalue decomposition (EVD) of C such that $\lambda_1 \geq \lambda_2 \geq \dots \geq \lambda_{2K}$ and $\Lambda = \text{diag}\{\lambda_1, \lambda_2, \dots, \lambda_{2K}\}$.

Step-5: Partition E_C into four $K \times K$ submatrices such that

$$E_C = \begin{bmatrix} E_{11} & E_{12} \\ E_{21} & E_{22} \end{bmatrix} \quad (2.36)$$

Step-6: Estimate the rotation operator Ψ by

$$\Psi = -E_{12} E_{22}^{-1} \quad (2.37)$$

Step-7: Calculate the eigenvalues of Ψ , $\lambda_1, \lambda_2, \dots, \lambda_K$

Step-8: Estimate the angles of arrival, given that $\lambda_i = |\lambda_i e^{j \arg(\lambda_i)}|$

$$\theta_i = \sin^{-1} \left(\frac{\arg(\lambda_i)}{kd} \right) \quad i = 1, 2, \dots, K \quad (2.38)$$

ESPRIT [1] is a computationally efficient and robust method of DoA estimation. However it requires the prior knowledge of number of sources. The number of sources needs to be less than the total number of elements in the array.

ESPRIT and MUSIC algorithms are the most advanced conventional methods. There are also available some more hybrid methods but the general drawbacks still remain.

2.3 Neural Network Based Algorithms for DoA

Neural network (NN) based DoA methods is reviewed by [4] thoroughly. The notations and classifications of NN DoA methods in this section are parallel to those given in [4].

The DoA problem aims to get the DoA of signals from the measurement of the array output Fig. (2.3). For an antenna array system, a neural network is first trained, which then performs the DoA estimation.

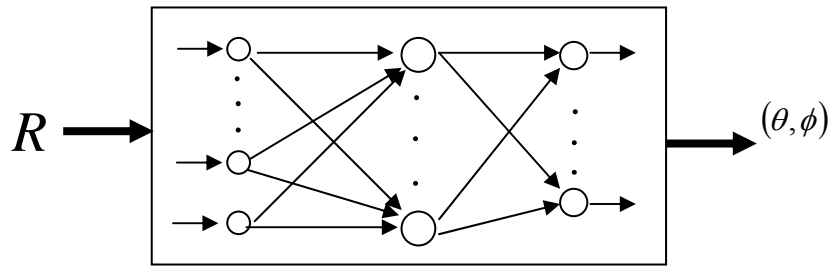


Figure 2.3 DoA neural network model.

A typical architecture of a neural processor is displayed in Fig. (2.4). The network computational structure is composed of input preprocessing for antenna measurements, a neural network to perform the inversion, and output post processing. Input preprocessing is used to remove redundant or irrelevant information to reduce the size of the network, and hence to reduce the dimensionality of the signal parameter space. Post processing the output node information yields the desired information. For example, for the DoA problem, the initial phase contains no

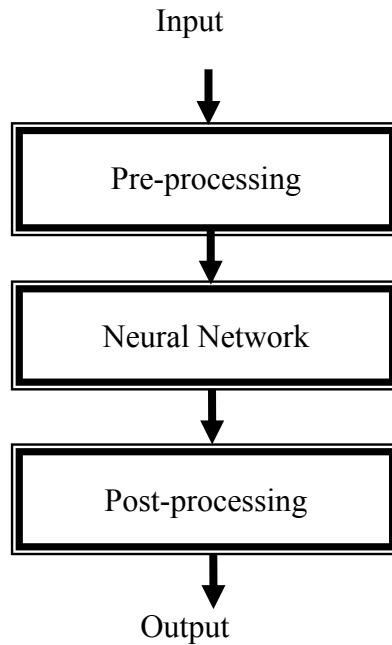


Figure 2.4 Neural architecture.

information about the DoA and can be eliminated at the preprocessing phase. The input of the network can also be normalized since the signal gain does not affect the detection of the DoA. [4] Classifies NN methods for DOA into five different methods.

2.3.1. Multilayer Perceptron Method

The multilayer perceptron (MLP) has strong classification capabilities, and is a universal approximator with a three-layer topology [79, 80]. The architecture of the MLP is shown in Fig. (2.5), where $g(\cdot)$ represents the sigmoid relation. The MLP is very efficient for function approximation in high dimensional spaces. The convergence rate of the MLP is independent of the input space dimensionality, while the rate of the error convergence of polynomial approximators decreases with the input dimensionality, while the rate of the error convergence of polynomial

approximators decreases with the input dimensionality. The MLP with the back propagation (BP) learning rule is one of the most widely used networks. The BP is a supervised gradient-descent technique wherein the squared error between the actual output of the network and the desired output is minimized. It is prone to local minima.

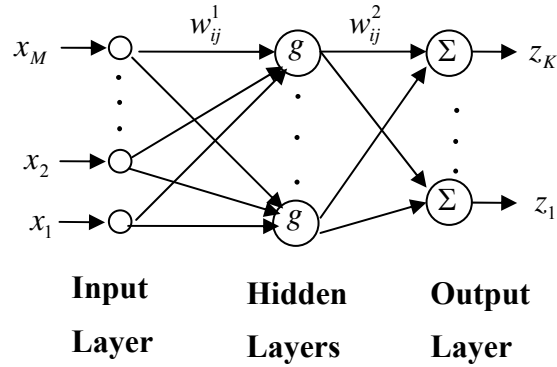


Figure 2.5 MLP architecture.

For a given problem, there is a set of training vectors X , such that for every vector $x \in X$ there is a corresponding desired output vector $d \in D$, where D is the set of the desired output. The error E_p is defined as

$$E_p = \frac{1}{2} \|d_p - z_p\| \quad (2.39)$$

where subscript p represents the p th desired output, $\|\cdot\|$ denotes the Euclidean norm.

The total error is defined $E_T = \sum_p E_p$, where p is the cardinality of X . The BP algorithm is defined as

$$\Delta w(t) = -\eta \frac{\partial E_p}{\partial w} + \alpha \Delta w(t-1) \quad (2.40)$$

where η is the learning rate, α is the momentum factor, and w represents any single weight in the network. When $\alpha \neq 0$, it is called the momentum method; for $\alpha = 0$, it is the BP algorithm. In [81, 82] MLP with the BP rule have been implemented for DoA problem.

2.3.2. Hopfield Method

The Hopfield network [83] is a two-layered fully interconnected recurrent neural network. The structure of the network is shown in Fig. (2.6). The input layer only collects signals from the feedback of the output layer. Due to recurrence, it remembers cues from the past and does not appreciably complicate the training procedure. This network is considered as a stable dynamic system in which the forward and backward paths will cause the processing of the network to converge to a stable fixed point.

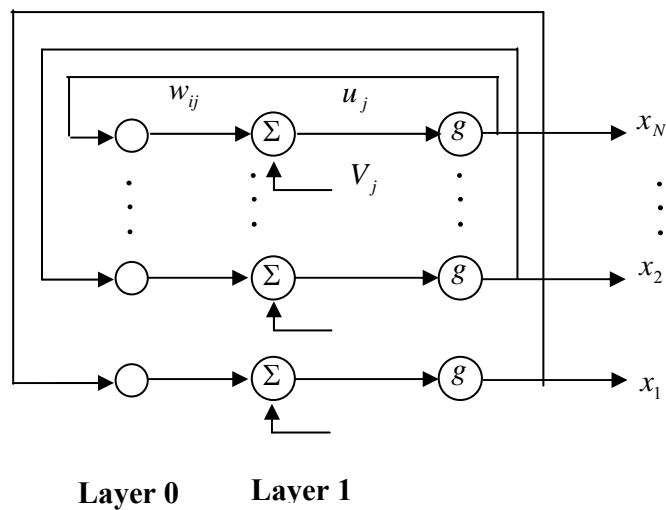


Figure 2.6 Hopfield network.

2.3.3. Radial Basis Function Network Method

The radial-basis function network (RBFN) is a three-layered feed forward network, and is shown in Fig. (2-7).

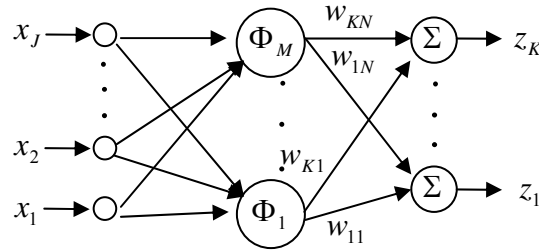


Figure 2.7 Architecture of the RBFN.

It has universal approximation and regularization capabilities [84]. It has been proved that the RBFN can theoretically approximate any continuous function [84, 85]. The RBFN is a type of receptive field network, or a localized network. The localized approximation method provides the strongest output when the input is near a node centroid. It has a faster learning speed as compared to global methods, such as the MLP with the BP rule, and only part of the input space needs to be trained. It has been reported that the RBFN requires orders-of-magnitude less iterations for convergence than the popular MLP with the BP rule using the sigmoid activation function [52]. In [52-87] RBFN is implemented for DoA problem. RBFN is employed in this thesis and it will be discussed in more detail in Chapter 3.

2.3.4. Principal Component Analysis Based Neural Method

The principal component analysis (PCA) is a well-known statistical criterion. This criterion turns out to be closely related to the Hebbian learning rule. The PCA is directly related to the Karhunen–Loeve transform (KLT) and singular value decomposition (SVD) [4].

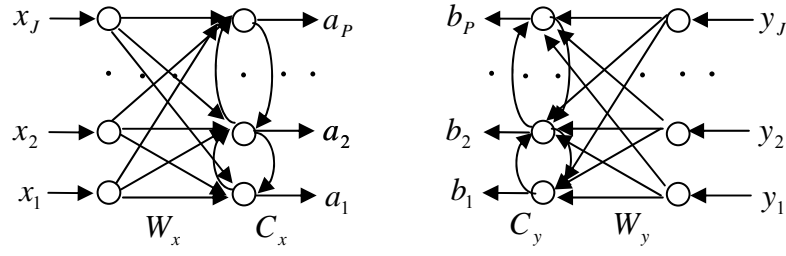


Figure 2.8 PCA network.

The PCA can be used as a solution to the maximization problem when the weight W in Eq. (2.1) is the eigenvector corresponding to the largest eigenvalue of the correlation matrix R . The cross-correlation asymmetric PCA network consists of two sets of neurons laterally connected mutually. The topology of the network is shown in Fig. (2.8). The two sets of neurons are with cross-coupled Hebbian learning rules orthogonal to each other. This model is extracts the SVD of the cross-correlation matrix of two stochastic signals. The exponential convergence has been demonstrated by simulation. In Fig. (2.8), x and y are input signals to the network, $W_x = [w_{x1}, w_{x2}, \dots, w_{xp}]$ and $W_y = [w_{y1}, w_{y2}, \dots, w_{yp}]$ are the network connection weights, the lateral connection weights are C_x and C_y . The network is described by the following relations:

$$a = W_x^T x \quad (2.41)$$

$$b = W_y^T y \quad (2.42)$$

Thus

$$ab^T = W_x^T xy^T W_y \quad (2.43)$$

The learning rules are as follows:

$$w_{xp}(k+1) = w_{xp}(k) + \beta [y(k) - w_{xp}(k)b_p(k)] a'_p(k) \quad (2.44)$$

$$w_{yp}(k+1) = w_{yp}(k) + \beta [x(k) - w_{yp}(k)a_p(k)] b'_p(k) \quad (2.45)$$

$$c_{xpi}(k+1) = c_{xpi}(k) + \beta [b_i(k) - c_{xpi}(k) b_p(k)] a'_p(k) \quad (2.46)$$

$$c_{ypi}(k+1) = c_{ypi}(k) + \beta [a_i(k) - c_{ypi}(k) a_p(k)] b'_p(k) \quad (2.47)$$

where

$$a'_p = a_p - \sum_{i < p} c_{xpi} a_i, \quad a_i = W_{xi}^T x, \quad i \leq p \quad (2.48)$$

$$b'_p = b_p - \sum_{i < p} c_{ypi} b_i, \quad b_i = W_{yi}^T x, \quad i \leq p \quad (2.49)$$

and β is the learning rate. In the above algorithm, W_x and W_y will approximate the left and right singular vectors of R_{xy} respectively, as $k \rightarrow \infty$. When $x = y$, it reduces to the conventional symmetric PCA [88].

2.3.5. Fuzzy Neural Method

In feedback control systems, fuzzy logic is a very popular tool. Usually, the inputs to the system are the error and the change in error of the feedback loop, while the output is the control action. The data flow in a fuzzy logic system involves fuzzification, rule base evaluation, and defuzzification [89]. The fuzzy neural network (FNN) is a neural network structure constructed from fuzzy reasoning. The FNN acquires the fuzzy rules and tunes the membership functions based on the learning ability of the neural network, and is a synergy of the two paradigms, which captures the merits of both the fuzzy logic and the neural networks. Expert knowledge is expressed by using the fuzzy IF-THEN rules, and is put into the network as a priori knowledge, which can increase the learning speed and estimation accuracy.

A typical FNN structure includes an input layer, an output layer, and several hidden rule nodes. The FNN employs the same network topologies as the ordinary neural networks, such as the multi-layer perceptron-structured FNN, RBFN-structured FNN, and recurrent FNN. Fundamentals in fuzzy neural synergisms for modeling and control have been reviewed in [90].

In [26] the authors have applied the six-layered, self-constructing neural fuzzy inference network (SONFIN) [91] to the DoA problem. The SONFIN is a feed forward multi-layer network that integrates the basic elements and functions of a traditional fuzzy system into a connectionist structure. It can find the proper fuzzy logic rules dynamically, and can find its optimal structure and parameters automatically. It always produces an economical network size, and its learning speed and modeling ability are superior to the ordinary neural networks. The input to the network is the phase difference, which experiences the same input preprocessing as in [52], and thus the method is useful only for single source case.

2.4. Discussion

Due to its general-purpose nature and proven excellent properties, the neural method provides a powerful means to solve DoA problems. The neural method outperforms the conventional linear algebra-based method in both the accuracy and speed, although each specific application has its own limitation [4]. It is especially suitable for hardware implementation. Among the neural models, the Hopfield network is suitable for hardware implementation and can converge in the same order of time as the hardware time constant; the RBFN method is much faster than the MLP method, and is receiving more attention in recent years. the PCA-based neural method deserves attention since it provides a general method for treating the computationally intensive SVD or eigen decomposition, which is common in linear algebra-based methods; the FNN method is a synergy of the neural method and fuzzy logic, which captures the merits of both methods. It can achieve a faster convergence speed with smaller network size, and represents a direction of research interests.

A DoA estimation scheme based on a radial basis function neural network (RBFNN) is presented in [57]. Here the DoA estimation problem is viewed as a function approximation problem, and the RBFNN is trained to perform the mapping from the space of the sensor array output to the space of DoAs. It exploits the universal function approximation capability of RBFNNs to estimate the DoAs and a successful classification of closely separated sources (2 degrees) has been reported. Further, this RBFNN based method has been compared with the conventional MUSIC algorithm for different levels of source correlations and it has been shown to produce better results. We propose a modified version N-MUST algorithm in this thesis. Details of the proposed algorithm are given in Chapter III for ULA, UCA and uniform cylindrical patch arrays, simulation results are provided in Chapter IV. Publications related with the proposed algorithm are given in [58-63].

CHAPTER 3

NEURAL NETWORK-BASED DIRECTION FINDING

Direction of Arrival (DoA) estimation and Direction Finding algorithms have been classified in general and overviewed in Chapter 2. DoA estimation and target tracking problems have been studied for years and several different adaptive algorithms have been developed within the last two decades [1]. However, since adaptive algorithms require extensive computation time, it is difficult to implement them in real time in general [92]. In recent years application of Neural Network (NN) algorithms in both target tracking problem and DoA estimation [4-63] and [78-92] have become popular because of the increased computational efficiency.

In a recently published work, a NN algorithm, namely the Neural Multiple-Source Tracking (N-MUST) algorithm, is presented for locating and tracking angles of arrival from multiple sources [57]. N-MUST algorithm has a neural network operating in two stages and is based on dividing the field of view of the antenna array into angular sectors. Each network in the first stage of the algorithm is trained to detect signals generated within its sector. Depending on the output of the first stage, one or more networks of the second stage can be activated to estimate the exact location of the sources. Main advantages of the N-MUST algorithm were presented as significant reduction in the size of training set and the ability of locating more sources than there are array elements.

The algorithm proposed in this thesis, namely the Modified Neural Multiple Source Tracking Algorithm (MN-MUST), consists of three stages those are classified as the detection, filtering and DoA estimation stages [58-63]. Similar to [57], a number of Radial Basis Function Neural Networks (RBFNN) are trained for detection of the angular sectors which have source or sources. A spatial filtering stage is applied individually to every angular sector which is classified in the first stage as having source or sources. Each individual spatial filter is designed to filter out the signals coming from all other angular sectors outside the particular source detected angular

sector. This stage considerably improves the performance of the algorithm in the case where more than one angular sector have source or sources at the same time. Insertion of this spatial filtering stage is one of the main contributions of this thesis. The third stage consists of a Neural Network trained for DoA estimation. In all three stages Neural Network's size and the training data are considerably reduced as compared to the previous approach [57] for uncorrelated sources, without loss of accuracy. Reduced size neural network approach is also applicable to beam forming and direction of arrival estimation algorithms presented in [53-56].

In this chapter first the problem is established for a linear array with uniform isotropic point source elements, then the problem is examined for a uniform circular array with dipole elements in the presence of mutual coupling, eventually problem is tested for a cylindrical microstrip patch array. MN-MUST algorithm is adapted to cylindrical patch array implementation. This adaptation reduced the size of NNs in filtering and DoA estimation stages.

3.1 Problem Formulation for Uniform Linear Array

The notations and symbols used in this section are parallel to [57] where NN-based multiple source tracking algorithm is introduced. The problem is formulated as follows: M isotropic antenna elements are placed along a line and separated by a uniform distance d as shown in Fig. (3.1). The number of sources (targets) is K , where K is not known and it is allowed to exceed M . The antenna elements are assumed to be omni-directional point sources. The angle of incidence of each source is Θ_i , $i = 1, 2, \dots, K$ which are required to be determined.

The sources are assumed to be located in the far field of the antenna array, so the difference in the aspect angle of a given source by the different antenna element is neglected. The signal received on each antenna element can be written as

$$X_i(t) = \sum_{m=1}^K S_m(t) e^{-j(i-1)k_m} + n_i(t) \quad i = 1, 2, \dots, M \quad (3.1)$$

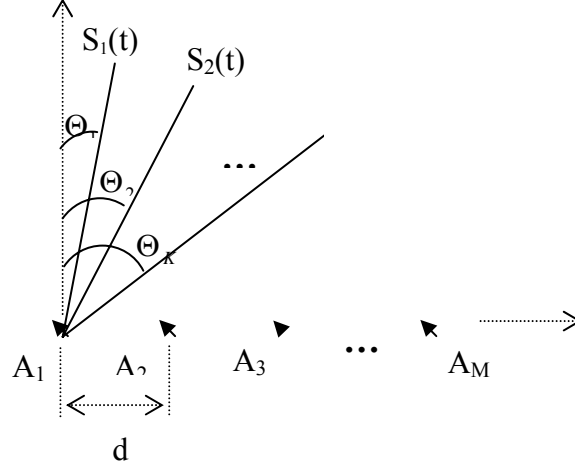


Figure 3.1 Array Structure.

where $n_i(t)$ is the noise signal received by the i -th antenna element and $k_m = \frac{\omega_0 d}{c} \sin(\Theta_m)$, d is the spacing between the elements of array, c is the speed of light in free-space, and ω_0 is the angular center frequency of the signal.

In matrix form,

$$X(t) = AS(t) + N(t) \quad (3.2)$$

where

$$\begin{aligned} X(t) &= [X_1(t) \ X_2(t) \ \dots \ X_M(t)]^T, \\ N(t) &= [n_1(t) \ n_2(t) \ \dots \ n_M(t)]^T, \\ S(t) &= [S_1(t) \ S_2(t) \ \dots \ S_K(t)]^T, \end{aligned} \quad (3.3)$$

and each entry of A can be defined as;

$$A_{im} = e^{-j(i-1)k_m} \quad (3.4)$$

The noise signals, $\{n_i(t), i = 1 : M\}$ received at different antenna elements of the array are assumed to be statistically independent zero mean white noise signals with variance σ^2 independent of $S(t)$. The spatial correlation matrix R of the received signal is given by

$$\begin{aligned} R &= E\{X(t)X(t)^H\} \\ &= AE\{S(t)S(t)^H\}A^H + E\{N(t)N(t)^H\} \end{aligned} \quad (3.5)$$

here “ H ” denotes the conjugate transpose.

It is shown in Appendix A that all entries of the correlation matrix R starting from the second row are arithmetic combinations of the entries in the first row. Therefore, it will be sufficient to calculate only the first row to represent the overall correlation matrix.

Based on Eq. (3.2), the array can be considered as a mapping, $G : R^K \rightarrow C^M$, from the space of DoA's $\{\theta_1, \theta_2, \dots, \theta_K\}^T$, to the space of antenna element output $\{X_1(t), X_2(t), \dots, X_M(t)\}^T$. In order to construct the inverse mapping, $F : C^M \rightarrow R^K$, a multistage architecture using NNs are employed. The block diagram of DoA estimation and MN-MUST algorithm architecture are given in Figs. (3.2) and (3.3), respectively.

In general, array-processing algorithms utilize correlation matrix for direction of arrival estimation instead of the actual array output $X(t)$. In this thesis a similar approach is followed with an improvement in the DoA estimation stage by using a three-stage algorithm consisting of preprocessing, neural network and the post processing stages (Fig. (3.2)). In the preprocessing stage the input to the spatial filtering stage is obtained from the antenna element signals $X(t)$ given by Eq. (3.2).

Upper triangular part of the correlation matrix R is used for the DoA estimation applications in [53-57]. Based on Eq. (A.10), in this study, only the first row of correlation matrix is used to represent the signals in the antenna elements for the case of uncorrelated sources exist. Then the input of neural networks is given as

$$R = \begin{bmatrix} R_{11} & R_{12} & R_{13} \\ R_{21} & R_{22} & R_{23} \\ R_{31} & R_{32} & R_{33} \end{bmatrix} \quad b = [R_{11} \quad R_{12} \quad R_{13}]$$

$$Z = \frac{b}{\|b\|} \quad (3.6)$$

The first entry of R , R_{11} is real and all the other entries are complex. NN algorithms deals with only real entries so the entries with complex parts are considered as two different numbers. Therefore the size of Z is $2M - 1$ where M is the number of elements of the array structure. On the other hand, in the N-MUST algorithm [53-57], the size of Z is given to be $M \times (M + 1)$. For example, for an $8 \times 8 = 64$

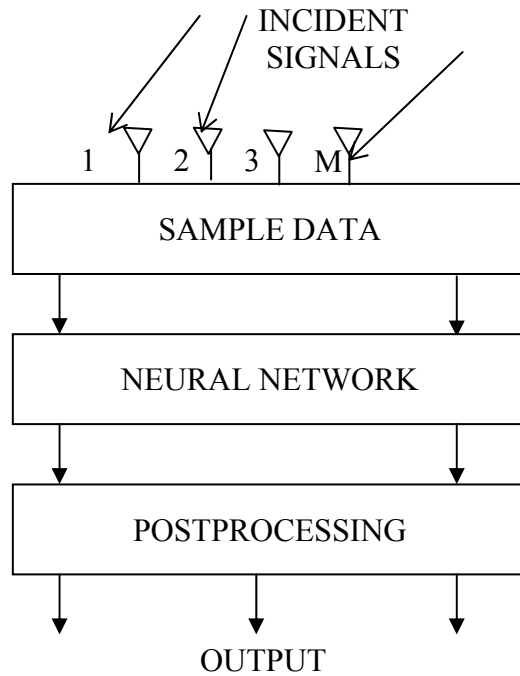


Figure 3.2 The block diagram of DoA estimation problem (Fig. 1. of [57]).

element planner smart array structure, the NN input sizes of the MN-MUST and N-MUST are $2 \times 64 - 1 = 127$ and $64 \times (64 + 1) = 4160$, respectively, while the output sizes of both NNs are the same. Obviously a considerable reduction in the training time is obtained with the use of MN-MUST algorithm.

3.2 Modified Neural Multiple Source Tracking (MN-MUST) Algorithm

MN-MUST algorithm consists of three stages those are the detection stage, the filtering stage and the DoA estimation stage as shown in Fig. (3.3). In the first stage a number of Radial Basis Function Neural Networks (RBFNN)'s are trained for detection similar to the N-MUST algorithm [57] but with reduced input size as discussed in the previous section. In the spatial filtering stage, the angular sector of interest is isolated from the others so as to improve the detection accuracy. The third stage is dedicated to DoA estimation by a NN whose input size is much smaller than the input size of N-MUST algorithm. Third stage is also similar to the N-MUST algorithm [57] except the size of NN.

3.2.1 Detection Stage

In this stage first, the entire angular spectrum is divided into P subsectors. For each subsector p , ($1 \leq p \leq P$) an RBFNN is trained to determine if any source exists within the sector. Depending on whether sources are present in the corresponding sector or not, the sectorial NN will produce "1" or "0" as its output, respectively. This information is then transferred to the "Filtering" stage. In the detection stage the input vector Z is supposed to have size $2M - 1$ as mentioned in the previous section. Network training and test (generalization) phase in training are similar to those of N-MUST algorithm except the input size of the network. The test phase produces the

input vector Z , presents it to the RBFNN's of the detection stage and then sends the output of each subsector, that is "1" or "0", to the next stage.

3.2.2 Spatial Filtering Stage

This stage is one of main the contributions of the thesis. The spatial filtering stage aims to isolate each one of the sectors where sources are present from the other sectors. A separate nonlinear (band-pass) filter is designed for each sector and activated depending on whether or not target exists in that sector. All these filters are multilayer perceptron type NN's with input size of $2M - 1$ and output size of $2M - 1$. The Spatial Filtering stage is basically a NN system. The inputs for the Spatial Filter Network are similar to the vector Z as of detection stage in [57]. The output of the spatial filter network for sector- i is Z_{fi} which does not include the signals from other sectors. In the training phase Z_{fi} pairs are processed discarding the signals outside the i -th angular sector. It is assumed that $\{S_1(t), S_2(t), \dots, S_K(t)\}$ are the signals impinging on the array and $\{S_t(t), S_q(t), S_l(t)\}$ are the only signals coming from direction of angular sector- i where $t, q \& l \leq K$. The input of the NN, Z is computed through Eq. (3.6) having $\{S_1(t), S_2(t), \dots, S_K(t)\}$ signal pair while the output of NN, Z_{fi} is computed through Eq. (3.6) again but the signal pair is $\{S_t(t), S_q(t), S_l(t)\}$ this time. Filtering stage filters out the $\{S_1(t), S_2(t), \dots, S_K(t)\} - \{S_t(t), S_q(t), S_l(t)\}$ signal pair for subject training example. In the training phase NN generalizes the input-output ($Z \rightarrow Z_{fi}$) relations. In the testing phase, one can have a generalized response to inputs that it has not seen before.

The filtered Z , which is Z_{fi} will be the input DoA Estimation Network for Sector- i . In order to understand the spatial filtering stage's function, let us assume it were not used and there were sources in other angular sectors as well as in sector- i .

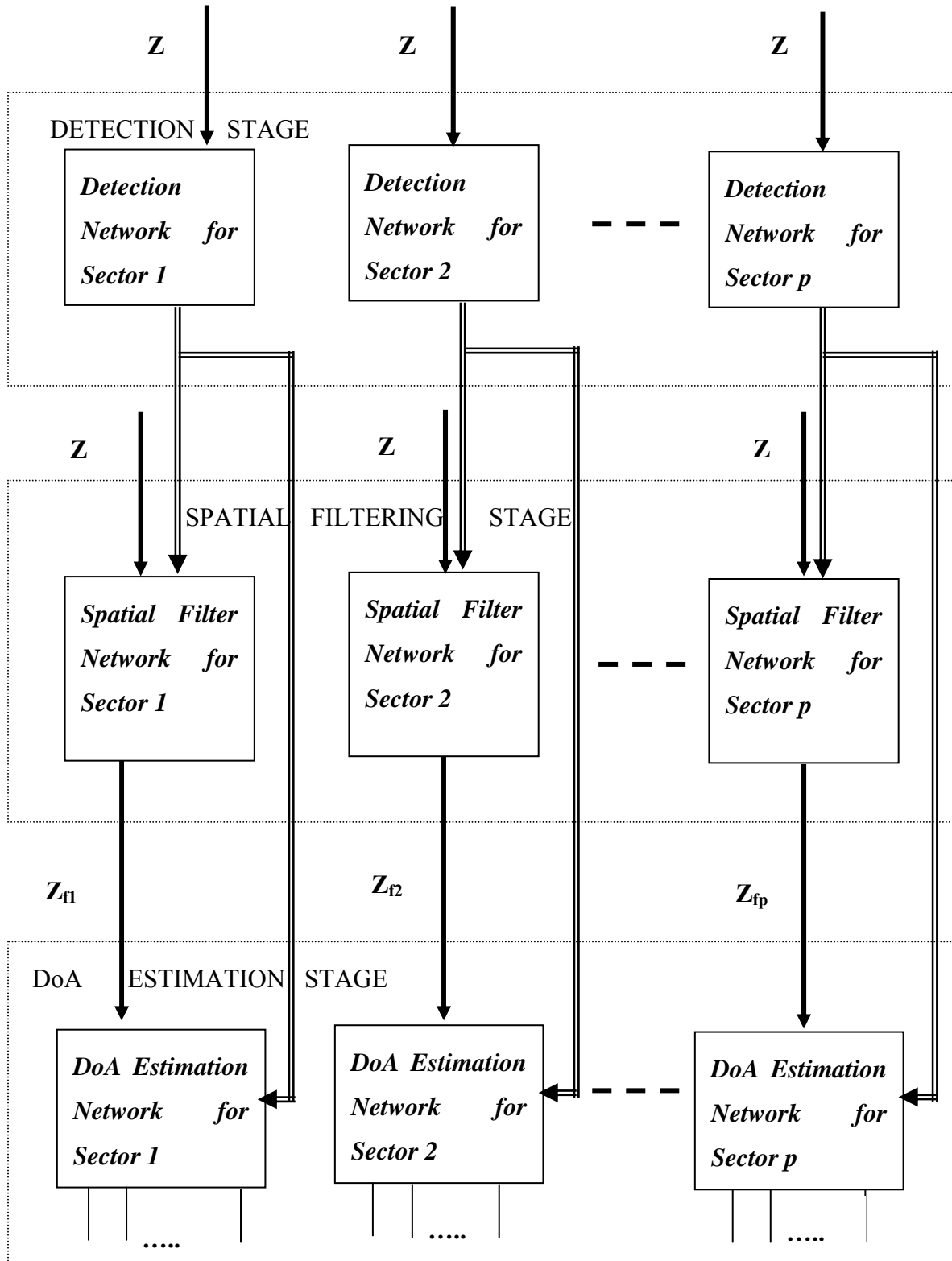


Figure 3.3 The modified neural multiple source tracking architecture

The algorithm described in [57] can be used; in other words, the algorithm with detection stage first and DoA estimation stage next. After the detection stage the angular sectors having the sources would have been identified correctly, but in DoA Estimation stages for the neighboring angular sectors, the correct source angles would not be found because the NN was trained in such a way that sources were present only in a specific angular sector. At a first glance it may seem that the filtering stage inserted in this study makes the algorithm more complicated with respect to the one in [57], but in reality, it is not so. A single NN is trained for a sector and the others have been obtained by spatial shifting. The selection of number of angular sectors basically depends on the total angular range we are looking for and the angular resolution. In this thesis one degree angular resolution is preferred.

3.2.3 DoA Estimation Stage

DoA estimation stage consists of a NN that is trained to perform the actual direction of arrival estimation. When the output of one or more networks of sectors from the first stage is “1”, the corresponding second stage network(s) are activated. The sectors (associated NN’s) that have outputs “1” are considered as the sectors having targets. Then the second stage filtering is activated. The input information to each second stage network is Z , while the output is the filtered Z_{fi} . For each sector having output “1” from the stage 1, the corresponding third stage network(s) are activated. The input information to each third stage network is Z_{fi} , while the output is the actual DoA of the sources.

For a sector Θ_w and a minimum angular resolution of $\Delta\Theta_{\min}$, the number of output nodes is given by

$$J = \left\lceil \frac{\Theta_w}{\Delta\Theta_{\min}} \right\rceil \quad (3.7)$$

DoA estimates are obtained by post processing the neural network outputs of this stage. J output nodes represent bins in a discrete angular sector centered at intervals of width $\Delta\Theta_{\min}$. For example, if Θ_w is a sector of 10 degrees width, and the desired accuracy $\Delta\Theta_{\min}$, is 1 degree, then the number of output nodes is 10. The NN is trained so as to produce “0” or “1” values at the outputs. An output of “1” indicates the presence of a source exactly on that bin and “0” represents no source.

3.3 MN-MUST Algorithm Features

Sampled Data Processing and correlation matrix construction for MN-MUST algorithm is a key first step go through. Even though radial basis function neural network applied to MN-MUST has similarities to [57], training and testing phase of the RBNN for each stage of MN-MUST algorithm have certain differences. Signal and noise models used in this algorithm is similar to [3], to a large extent.

3.3.1. Sampled Data Processing

Because of advances in analog-to-digital converters (ADC) and digital signal processing (DSP); what was once performed in hardware can now be performed digitally and quickly [93]. ADCs, which have resolutions that range from 8 to 24 bits, and sampling rates approaching 20 Giga samples (GSa/s), are now reality [94]. With supercomputing data converters one will be able to sample data at rates up to 100 GSa/s [95]. This makes the direct digitizing of most radio frequency (RF) signals possible in many applications. This allows most of the signal processing to be defined in software near the front end of the receiver [2].

It is assumed that the targets are stationary during the sampling and several samples are available in each period of the signals. 400 snap-shots are used for sampling the data in [57].

3.3.2. Correlation Matrix

Correlation matrix definition and computation is parallel to the one given in [2]. Incoming plane waves induce a random voltage on all M-array elements. The received signal X is a vector and array output voltages in the array are given in Eq. (3.2). $M \times M$ array correlation matrix defined as,

$$\begin{aligned} R &= E\{X(t)X(t)^H\} \\ &= AE\{S(t)S(t)^H\}A^H + E\{N(t)N(t)^H\} \end{aligned} \quad (3.8)$$

The correlation matrix in Eq. (3.8) assumes that we are calculating the ensemble average using the expectation operator $E\{\}$. It should be noted that this is not a vector autocorrelation because we have imposed no time delay in the vector X .

For realistic systems where we have a finite data block, we must estimate the correlation matrix using a time average. Each antenna noise is independent from the signals received and from each other. It has a zero-mean variance σ^2 . Therefore, we can re-express the operation in Eq. (3.8) as

$$R = \frac{1}{T} \int_0^T X(t)X(t)^H dt = \frac{A}{T} \left(\int_0^T S(t)S(t)^H dt \right) A^H + \frac{1}{T} \int_0^T N(t)N(t)^H dt \quad (3.9)$$

Hence the data is sampled data Eq. (3.9) can be written as a series to be expressed as

$$R = \frac{A}{K} \left(\sum_{k=0}^K S(k)S(k)^H \right) A^H + \frac{1}{K} \sum_{k=0}^K N(k)N(k)^H \quad (3.10)$$

$$R = AR_s A^H + R_n \quad (3.11)$$

where

$$R_s = \frac{1}{K} \sum_{k=0}^K S(k)S(k)^H \quad (3.12)$$

$$R_n = \frac{1}{K} \sum_{k=0}^K N(k)N(k)^H \quad (3.13)$$

When the signals are uncorrelated, R_s obviously has to be a diagonal matrix because off-diagonal elements have no correlation. When the signals are partially correlated, R_s is nonsingular. When the signals are coherent, R_s may become singular because the rows are linear combinations of each other. When the signals are uncorrelated and considered as sinusoidal with unit amplitude, then

$$R_s = \frac{1}{2} I_K \quad (3.14)$$

where I_K is a $K \times K$ identity matrix. Noise part of the correlation matrix R_n for zero mean and σ^2 Gaussian noise will be

$$R_n = \sigma^2 I_K \quad (3.15)$$

Eqs (3.14) and (3.15) are used during the simulations will be given in the following chapter with the related signal and noise assumptions.

3.3.3. Signal and Noise Model

Transmission medium is assumed to be isotropic and homogeneous so that the radiation propagates in straight lines. The targets (sources) are assumed to be in the far field of the array. That means a particular source (target) signal is coming to the every array elements in the same incident angle. Basically signals in each element are the summation of plane waves. However there are phase differences for a particular incident wave impinging on each antenna element. The transmission medium is assumed to be non-dispersive so that the signal waveforms do not change as they propagate. It is also assumed that the signal received from a particular target source in each antenna element has basically a phase delay of the carriers.

Antenna elements are considered identical in terms of pattern, polarization, gain and impedance. Mutual coupling is only considered for uniform circular dipole array. Mutual coupling is not taken into account for uniform linear array in the analysis. However, it can be handled easily by multiplying the patterns with appropriate coefficients (mutual coupling matrix). It is also assumed that the antennas and the incident waves are polarization matched. The assumptions made so far are similar to the DF algorithm given in [3].

3.3.4. Radial Basis Function Applied to MN-MUST Algorithm

An overview of neural network can be found in [96]. Radial basis function neural network (RBFNN) can approximate an arbitrary function from an input space of arbitrary dimensionality to an output space of arbitrary dimensionality [92]. RBFNNs The RBNN can be considered as designing neural networks as an interpolation problem in a high-dimensional space [96] and [97]. The mapping from the input space to the output space may be thought of as a hypersurface Γ representing a multidimensional function of the input. During the training phase, the input-output patterns presented to the network are used to perform a fitting for Γ . The architecture consists of three layers; the input layer, a hidden layer of high dimension, and an output layer as shown in Fig. (3.4).

The transformation from the input space to the hidden-unit space is non-linear, whereas the transformation from the hidden layer to the output space is linear. The network represents a mapping from the p -dimensional input space to the m -dimensional output space: $\mathfrak{R}^p \rightarrow \mathfrak{R}^m$. The radial-basis functions (RBF) technique consists of constructing a function F that has the following form

$$F(x) = \sum_1^N w_i \varphi(\|x - x_i\|) \quad (3.16)$$

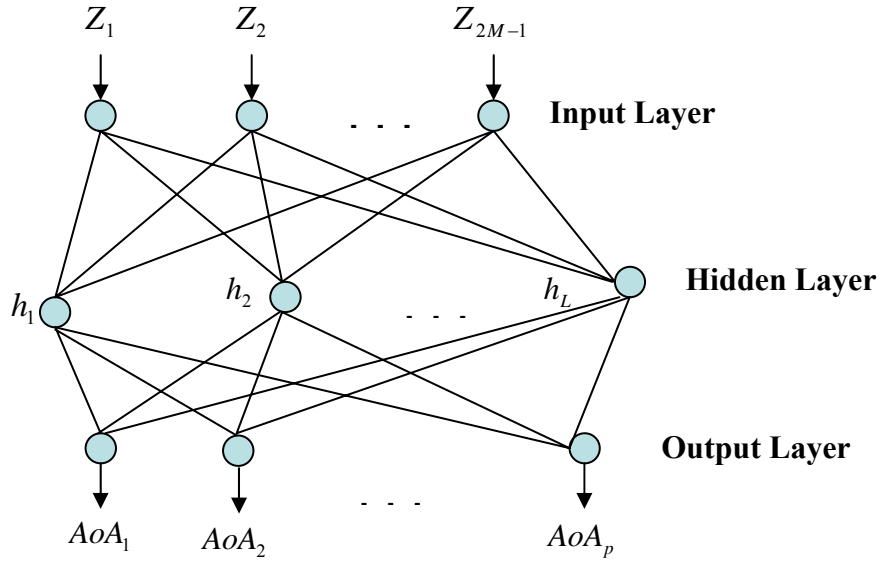


Figure 3.4 Radial basis neural network structure.

where $\| \cdot \|$ denotes the norm, N is a set of arbitrary functions, and x_i are the centers of the radial-basis functions. One of the common and most useful forms for φ is the Gaussian function defined by

$$\varphi(x) = e^{\frac{-x^2}{2\sigma^2}} \quad (3.17)$$

There are several different learning strategies for RBF networks. In this thesis *newrb* function of [98] software is used through the simulations. One can find the proper syntax and training requirements for that function from [98] help box.

Once the training of the RBFNN is accomplished, the training phase is completed and the trained neural network can operate in the performance phase. In the performance phase, the neural network is supposed to generalize, that is, respond to inputs ($X(t)$'s) that it has never seen before, but are drawn from the same distribution as the inputs used in the training set. Hence, during the performance phase the RBFNN produces outputs to previously unseen inputs by interpolating between the inputs used (seen) in the training phase.

3.3.4.1. Detection Stage RBFNN Training and Performance Phase

A. Generation of training data.

- 1) Divide the angular spectrum into P sub-sectors.
- 2) Select a proper angular separation.
- 3) Generate possible targets in any angle in the angular spectrum.
- 4) Evaluate the correlation matrix for each target pairs using Eq. (3.5). N set of source (target) pairs will yield $\{R^n, n = 1, 2, \dots, N\}$.
- 5) Form the vectors $\{b^n, n = 1, 2, \dots, N\}$.
- 6) Normalize the input vectors using Eq. (3.6).
- 7) Generate input output pairs $\{z^n, 0\}$ for source (target) pairs located outside the related sub sector, $\{z^n, 1\}$ for the source pairs inside the related subsector.
- 8) Employ *newrb* of [98] to learn the training set generated in step 7.
- 9) For each sub-sector repeat steps 7 and 8.

B. Performance Phase

- 1) Evaluate the sample correlation matrix using the collected array output measurements Eq. (3.5). If you are using simulation then consider the noise and generate sampled noise data as well and add to the correlation matrix.
- 2) Form the vector b .
- 3) Produce normalized Z using equation (3.6).
- 4) Present input vector Z to the RBFNN's of the detection stage and obtain an output $\{1 \text{ or } 0\}$ for each sub-sector.

3.3.4.2. Spatial Filtering Stage RBNN Training and Performance Phase

A. Generation of training data.

- 1) Divide the angular spectrum in to P sub -sectors.
- 2) Select a proper angular separation.
- 3) Generate possible targets in any angle in the angular spectrum.
- 4) Evaluate the correlation matrix for each target pairs using Eq. (3.5). N set of source (target) pairs will yield $\{R^n, n = 1, 2, \dots, N\}$.
- 5) Evaluate the correlation matrix for each target pairs only for the targets which are in the sub-sector and considering the others as if the do not exist, $\{R_{fp}^n, n = 1, 2, \dots, N\}$. Let the target pair consists of five targets coming from $\{\theta_1, \theta_2, \theta_3, \theta_4, \theta_5\}$. and your sub-sector only has targets $\{\theta_1, \theta_3, \theta_4\}$. Then array correlation matrix $\{R\}$. is computed through Eq. (3.5) considering all 5 signals, while $\{R_{fp}\}$ is computed only considering 3 signals.
- 6) Form the vectors $\{b^n, n = 1, 2, \dots, N\}$. and $\{b_{fp}^n, n = 1, 2, \dots, N\}$.
- 7) Normalize the input vectors using Eq. (3.6).
- 8) Generate input-output pairs $\{Z^N, Z_{fp}^N\}$.
- 9) Employ *newrb* of [98] to learn the training set generated in step 7.
- 10) For each sub-sector repeat steps 5- 9.

B. Performance Phase

- 1) Evaluate the sample correlation matrix using the collected array output measurements using Eq. (3.5). If you are using simulation, then consider the noise and generate sampled noise data as well and add to the correlation matrix.

- 2) Form the vector b .
- 3) Produce normalized Z using Eq. (3.6).
- 4) Present input vector Z to the RBFNN's of the spatial filtering network stage and obtain a filtered output Z_{fp} for each sub-sector. Z_{fp} will be an input to the next stage in the performance phase.

3.3.4.3. DoA Estimation Stage RBNN Training and Performance Phase

A. Generation of training data.

- 1) Generate possible targets in any angle in the sub-sector.
- 2) Evaluate the correlation matrix for each target pairs using Eq. (3.5) for N set of source (target) pairs you like, $\{R^n, n = 1, 2, \dots, N\}$.
- 3) Form the vectors $\{b^n, n = 1, 2, \dots, N\}$.
- 4) Normalize the input vectors using Eq. (3.6).
- 5) Generate input output pairs $\{Z^N, L^N\}$, where L is a vector whose size is given by Eq. (3.7) and the entries are “1” if there is a target in the related angle or “0” if there is no target.
- 7) Employ *newrb* of [98] to learn the training set generated in step 5.
- 8) For each sub-sector repeat steps 1-7.

B. Performance Phase

- 1) Evaluate the sample correlation matrix using the collected array output measurements using Eq. (3.5). If you are using simulation, then consider the noise and generate sampled noise data as well and add to the correlation matrix.

- 2) Form the vector b .
- 3) Produce normalized Z using Eq. (3.6).
- 4) Present input vector Z to the RBFNN's of the spatial filtering network stage (previous stage) and obtain a filtered output Z_{fp} for the related sub-sector. Then present input vector Z_{fp} to the RBFNN's of the DoA stage network and obtain the vector L . L has the information about which one of the discretized angle of the angular sub-sector has targets. Basically the values should be around "1" if there is a target in the related angle or "0" if there is no target.

3.4 MNMUST Algorithm for Circular Array in The Presence of Mutual Coupling

In recent years application of Neural Network (NN) algorithms in both target tracking problem and DoA estimation have become popular because of the increased computational efficiency. The Neural Multiple-Source Tracking (N-MUST) algorithm was presented for locating and tracking angles of arrival from multiple sources [57]. Modified Neural Multiple Source Tracking (MN-MUST) algorithm [58-63] improved the performance of the N-MUST algorithm.

MN-MUST algorithm is established and implemented to ULA(Uniform Linear Array) in the previous section [58]. This section examines MN-MUST algorithm for UCA(Uniform Circular Array) in the presence of mutual coupling. The UCA geometry, antenna elements and induced electromotive force (EMF) model in this thesis is similar to [99].

In smart antenna systems, mutual coupling between elements can significantly degrade the processing algorithms [100]. In this section mutual coupling effects on Modified Neural Multiple Source Tracking algorithm (MN-MUST) have been studied. MN-MUST algorithm applied to UCA geometry. The validity of MN-

MUST algorithm in the presence of mutual coupling has been proved for UCA. The presence of mutual coupling degraded the MN-MUST algorithm performance, as expected.

The MN-MUST algorithm will be formulated for circular array with uniform isotropic elements. Then the problem will be implemented to dipole array in the presence of mutual coupling.

3.4.1 Problem Formulation for Circular Array

The notations and symbols used in this study are parallel to those given in [57] where NN-based multiple source tracking algorithm is introduced. Circular array geometry is similar to the one in [99]. The problem is formulated as follows: M isotropic antenna elements are placed along a circle radius a and separated by a uniform angle $\Delta\Phi$ as shown in Fig. (3.1).. The origin of the coordinate system (The spherical coordinate system is used) is located at the center of the array. Source (target) elevation angles, $\Theta \in [0, \pi/2]$, are measured from the z axis, and azimuth angles, $\Phi \in [0, 2\pi]$, are measured counterclockwise from the x axis on $x - y$ plane.

The angular position of the n -th element of the array is

$$\Phi_n = 2\pi \left(\frac{n}{M} \right), \quad n = 1, 2, \dots, M \quad (3.18)$$

The unit vector from the origin is represented in Cartesian coordinates by

$$\hat{a}_r = \hat{a}_x \sin \theta \cos \phi + \hat{a}_y \sin \theta \sin \phi + \hat{a}_z \cos \theta \quad (3.19)$$

$$\hat{a}_n = \hat{a}_x \cos \phi_n + \hat{a}_y \sin \phi_n \quad (3.20)$$

The vector Δr_n represents the differential distance by which the planar wavefront reaches the n th element of the array relative to the origin, and it is given by

$$\Delta r_n = \hat{a}_r \cdot \hat{a}_n \cos \psi_n \quad (3.21)$$

Since the wavefront is incoming and not radiating outwards, ψ_n can be written as

$$\begin{aligned} \cos \psi_n &= -\hat{a}_r \cdot \hat{a}_n \\ &= -\left(\hat{a}_x \sin \theta \cos \phi + \hat{a}_y \sin \theta \sin \phi + \hat{a}_z \cos \theta \right) \cdot \left(\hat{a}_x \cos \phi_n + \hat{a}_y \sin \phi_n \right) \\ &= -\left(\sin \theta \cos \phi \cos \phi_n + \sin \theta \sin \phi \sin \phi_n \right) \\ &= -\sin \theta (\cos \phi \cos \phi_n + \sin \phi \sin \phi_n) \\ &= -\sin \theta \cos(\phi - \phi_n), \quad n = 1, 2, \dots, M \end{aligned} \quad (3.22)$$

Then Eq. (3.21) becomes

$$\Delta r_n = -\hat{a}_r \cdot \hat{a}_n \sin \theta \cos(\phi - \phi_n), \quad n = 1, 2, \dots, M \quad (3.23)$$

Furthermore, assuming that the wavefront passes through the origin at time $t = 0$, it impinges on the n -th element of the array a relative time delay of

$$\tau_n = -\frac{a}{c} \sin \theta \cos(\phi - \phi_n), \quad n = 1, 2, \dots, M \quad (3.24)$$

where c is speed of light in free space.

The number of sources (targets) is K , where K is not known and it is allowed to exceed M . The angle of incidence of each source is $\{\Theta_{si}, \Phi_{si}\}$, $i = 1, 2, \dots, K$ which are required to be determined. Then the Eq. (3.24) for each single target becomes

$$\tau_n = -\frac{a}{c} \sin \theta_{si} \cos(\phi_{si} - \phi_n), \quad n = 1, 2, \dots, M \quad i = 1, 2, \dots, K \quad (3.25)$$

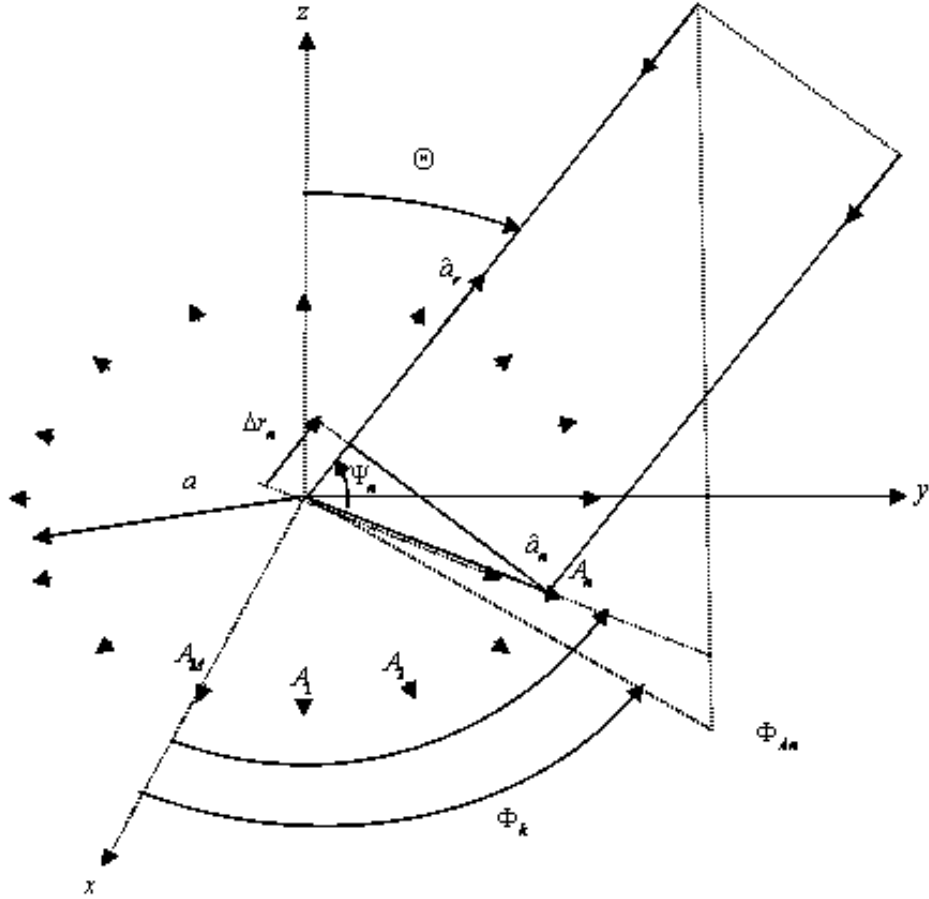


Figure 3.5 Circular Array Structure.

The sources are assumed to be located in the far field of the antenna array, so the difference in the viewing angle of a given source by the different antenna element is neglected. The signal received on each antenna element can be written as

$$X_i(t) = \sum_{m=1}^K S_m(t) e^{-j(i-1)k_m} + n_i(t) \quad i = 1, 2, \dots, M \quad (3.26)$$

where $n_i(t)$ is the noise signal received by the i -th antenna element and $k_m = \frac{\omega_0 a}{c} \sin \theta_{sm} \cos(\phi_{sm} - \phi_i)$, a is the radius of the circular array, c is the speed of light in free-space, and ω_0 is the angular center frequency of the signal.

In matrix form,

$$X(t) = AS(t) + N(t) \quad (3.27)$$

where

$$\begin{aligned} X(t) &= [X_1(t) \quad X_2(t) \quad \dots \quad X_M(t)]^T, \\ N(t) &= [n_1(t) \quad n_2(t) \quad \dots \quad n_M(t)]^T, \\ S(t) &= [S_1(t) \quad S_2(t) \quad \dots \quad S_K(t)]^T, \end{aligned} \quad (3.28)$$

and each entry of A is defined as;

$$A_{im} = e^{-j(i-1)k_m} \quad (3.29)$$

The noise signals, $\{n_i(t), i = 1:M\}$ received at different antenna elements of the array are assumed to be statistically independent zero mean white noise signals with variance σ^2 independent of $S(t)$. The spatial correlation matrix R of the received signal is given by

$$\begin{aligned} R &= E\{X(t)X(t)^H\} \\ &= AE\{S(t)S(t)^H\}A^H + E\{N(t)N(t)^H\} \end{aligned} \quad (3.30)$$

where “ H ” is denoting the conjugate transpose.

3.4.2. Mutual Coupling

The impedance and radiation pattern of an antenna element changes when the element is radiating in the vicinity of other elements causing the maximum and nulls of the radiation pattern to shift [101]. These changes lead to less accurate estimates of the angle of arrival and deterioration in the overall pattern. If these effect are not taken into account by the AoA algorithms (adaptive or others), the overall system performance will degrade. However mutual coupling can be taken into account by using a mutual coupling matrix.

Mutual coupling compensation is used for adaptive algorithms [102-108]. In the MN-MUST algorithm, if mutual coupling is considered during the training phase, then in the performance phase algorithm works accurately.

Under the condition of single-mode elements, the mutual coupling matrix is based on angular independence [109]. Using the fundamental electromagnetic and circuit theory information, mutual coupling matrix can be written as [110]

$$C = (Z_A + Z_L) (Z + Z_L I_M)^{-1} \quad (3.31)$$

where Z_A is the element matrix I_M is the $M \times M$ identity matrix, Z is the mutual impedance matrix, and Z_L is the load impedance (i.e., 50Ω). In general, numerical techniques in electromagnetics, such as the method of moments (MoM), the induced electromotive force (EMF) method, the full-wave electromagnetic computation, can be used to calculate the self and mutual impedances [111-112].

With the presence of array mutual coupling the array output vector Eq. 3-17 can be written as [111]

$$X(t) = CAS(t) + n(t) \quad (3.32)$$

Without loss of generality, we suppose that the signal sources (targets) are uncorrelated and the noises are independent with zero mean with σ^2 variance. Then the correlation matrix Eq. (3-30) becomes

$$\begin{aligned}
 R &= E\{X(t)X(t)^H\} \\
 R &= CAE\{S(t)S(t)^H\}(CA)^H + E\{N(t)N(t)^H\} \\
 R &= CAR_s(CA)^H + \sigma^2 I
 \end{aligned} \tag{3.33}$$

where $R_s = E\{S(t)S(t)^H\}$, and I is the identity matrix.

3.4.3. Problem Formulation in the Presence of Mutual Coupling for Circular Array

The coupling matrix C is symmetric for ULA. In the UCA application since the array follows the rotational symmetry, C is a *Circulant* [113] matrix such as

$$C = \begin{bmatrix}
 c_0 & c_1 & c_2 & \cdot & \cdot & \cdot & c_{M-1} \\
 c_{M-1} & c_0 & c_1 & \cdot & \cdot & \cdot & c_{M-2} \\
 \cdot & \cdot & \cdot & & & & \cdot \\
 \cdot & \cdot & \cdot & \cdot & \cdot & \cdot & \cdot \\
 \cdot & \cdot & \cdot & \cdot & \cdot & \cdot & \cdot \\
 c_1 & c_2 & c_3 & \cdot & \cdot & \cdot & c_0
 \end{bmatrix} \tag{3.34}$$

The coupling matrix can be calculated using the induced electromotive force (EMF) method [114-115].

For an equal length, side-by-side, and identically oriented dipoles, using the induced (EMF) method the self and mutual impedance formula is given by [114]

$$Z_{mn} = \begin{cases} 30[C + \ln(4\beta l) - Ci(4\beta l)] + j30Si(4\beta l), & m = n \\ R_{mn} + jX_{mn} & m \neq n \end{cases} \quad (3.35)$$

where

$$R_{mn} = 30 \left\{ \begin{aligned} & \cos(2\beta l)[Ci(u_0) + Ci(v_0) - 2Ci(u_1) - 2Ci(v_1) + 2Ci(\beta d)] + \\ & + \sin(2\beta l)[-Si(u_0) + Si(v_0) + 2Si(u_1) - 2Si(v_1)] + \\ & + [-2Ci(u_1) - 2Ci(v_1) + 4Ci(\beta d)] \end{aligned} \right\} \quad (3.36)$$

$$X_{mn} = 30 \left\{ \begin{aligned} & \cos(2\beta l)[-Si(u_0) - Si(v_0) + 2Si(u_1) + 2Si(v_1) - 2Si(\beta d)] + \\ & + \sin(2\beta l)[-Ci(u_0) + Ci(v_0) + CSi(u_1) - 2Ci(v_1)] + \\ & + [2Si(u_1) + 2Si(v_1) - 4Si(\beta d)] \end{aligned} \right\} \quad (3.37)$$

$$\begin{aligned} u_0 &= \beta \left(\sqrt{d^2 + 4l^2} - 2l \right) & u_1 &= \beta \left(\sqrt{d^2 + l^2} - l \right) \\ v_0 &= \beta \left(\sqrt{d^2 + 4l^2} + 2l \right) & v_1 &= \beta \left(\sqrt{d^2 + l^2} + l \right) \end{aligned} \quad (3.38)$$

$$Ci(x) = -\int_x^{\infty} \frac{\cos t}{t} dt \quad Si(x) = \int_0^x \frac{\sin t}{t} dt \quad (3.39)$$

d is the horizontal distance between the m_{th} and n_{th} dipole antennas and it is given by

$$d = a \sqrt{(\cos(2\pi m / M) - \cos(2\pi n / M))^2 - (\sin(2\pi m / N) - \sin(2\pi n / M))^2} \quad (3.40)$$

a is the radius of the circular array, M is the total number of dipole antenna elements, $C \approx 0.5772$ is the Euler's constant, $\beta = 2\pi / \lambda$ is the wave number, λ is the wave length, l is the length of the dipole antenna element.

3.5 MN-MUST Algorithm for Cylindrical Microstrip Patch Array

In the previous sections MN-MUST algorithm is established for uniform point source linear array similar to the N-MUST algorithm implementation of [57]. Now, MN-MUST algorithm is applied to uniform dipole circular array in the presence of mutual coupling to examine the performance of the algorithm in the presence of mutual coupling. MN-MUST algorithm is implemented to the somewhat realistic array pattern, in this section.

Cylindrical microstrip patch array is chosen to cover all azimuth angles. Microstrip patch radiation pattern characteristics helps to overcome ambiguity problem for DoA estimation. Even though the pattern of the patch elements of a cylindrical array is not a pencil beam, its directivity is good enough to solve the ambiguity problem arising in uniform patterns of circular arrays. On the other hand directivity characteristics of the pattern has a positive effect on the Spatial Filtering Stage.

Microstrip patch antennas can easily be made to conform to cylindrical surfaces to provide low profile omni directional arrays. A specified array pattern can also be obtained by configuring the geometries [116].

Since the mutual coupling effect on MN-MUST algorithm is already discussed in the previous section for dipole UCA, mutual coupling is not considered for cylindrical microstrip patch array. However, if either mutual coupling matrix or mutual impedance is available then the mutual coupling matrix can easily be inserted to the computation as mentioned in the previous section. Moreover, if MN-MUST algorithm training data is based on measurements, then it is equivalent to the fact that mutual coupling is already considered.

MN-MUST algorithm implementation for a cylindrical microstrip patch array is a practical system solution to the DoA estimation for full azimuth coverage. For instance, the system solution can be implemented in base stations to locate the direction of the mobile user's directions.

The cylindrical patch array used in this section is similar to the one analyzed in [116]. After the element pattern is analyzed, the twelve-element patch array is considered to be implemented in the MN-MUST algorithm.

3.5.1 Cylindrical Microstrip Patch

For the analysis of the array for MN-MUST algorithm, radiation pattern of the patch element is needed. Radiation pattern can be studied by utilizing the cavity model [117].

The geometry of a typical cylindrical patch antenna is shown in Fig. (3.6). $2b$ and $2\theta_0$ define the dimension of the patch in the Z and ϕ directions, respectively. ϕ_0 indicates ϕ -position of the patch, while a and h define the radius of the cylinder and height of substrate, respectively. The position of the coaxial probe feed is indicated by Z_f and ϕ_f . When the coaxial probe feed is modeled by a current density, with an effective width w , the wave equation of the field in the cavity becomes [117]

$$\frac{1}{\rho^2} \frac{\partial^2(\rho E_\phi)}{\partial \rho \partial \phi} - \frac{1}{\rho^2} \frac{\partial^2 E_\rho}{\partial \phi^2} - \frac{\partial^2 E_\rho}{\partial z^2} + \frac{\partial^2 E_z}{\partial z \partial \rho} - k^2 E_\rho = 0 \quad (3.41)$$

where $k^2 = w^2 \mu \epsilon$.

Following the usual cavity model approximation, the electric field is assumed to have only a E_ρ component which is independent of ρ . Equation (3.31) becomes

$$\left[\frac{1}{\rho^2} \frac{\partial^2}{\partial \phi^2} + \frac{\partial^2}{\partial z^2} + k^2 \right] E_\rho = 0 \quad (3.42)$$

For a thin substrates satisfying $h \ll a$, it can be further assumed that $\rho = a + h$ in Eq. (3.42). Using this approximation, the eigenfunctions of E_ρ and the eigenvalues of k satisfying the magnetic wall condition are given by

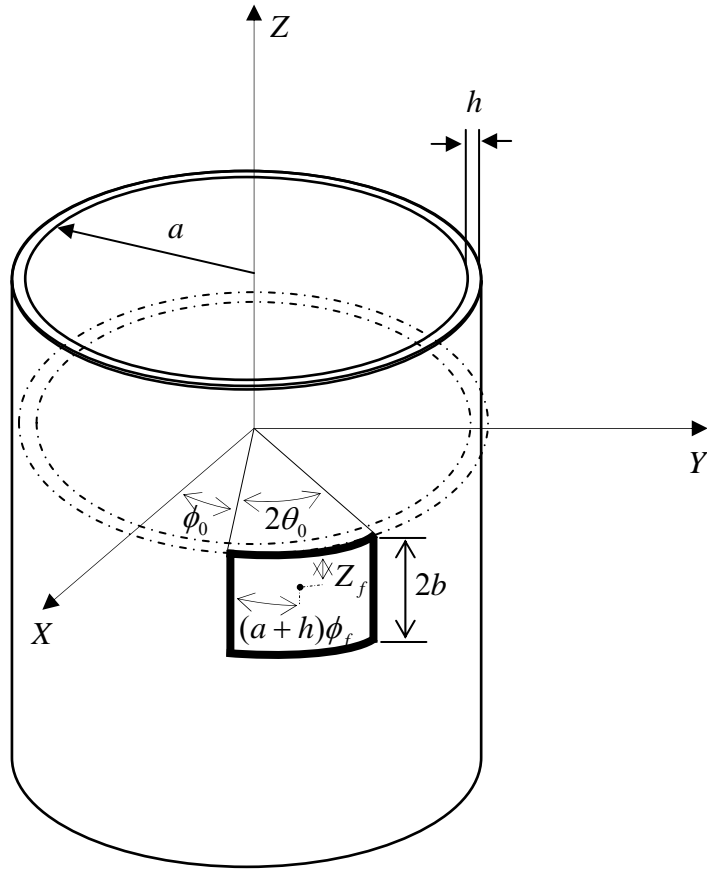


Figure 3.6 Geometry of cylindrical microstrip patch antenna.

$$E_{\rho} = \psi_{mn} = E_0 \cos \left[\frac{m\pi}{2\theta_0} (\phi - \phi_0) \right] \cos \left(\frac{n\pi z}{2b} \right) \quad (3.43)$$

$$k^2 = k_{mn}^2 = \left(\frac{m\pi}{2(a+h)\theta_0} \right)^2 + \left(\frac{n\pi}{2b} \right)^2 \quad (3.44)$$

The expression for the resonant frequencies is

$$f_{mn} = \frac{c}{2\sqrt{\epsilon_r}} \left[\left(\frac{m}{2(a+h)\theta_0} \right)^2 + \left(\frac{n}{2b} \right)^2 \right]^{1/2} \quad (3.45)$$

The equivalent magnetic currents along the edges of the curved patch is obtained from

$$\overline{\mathbf{M}} = E_\rho \hat{\rho} \times \hat{n} \quad (3.46)$$

where E_ρ is given by Eq. (3.43). The problem of magnetic currents radiating in the presence of a cylindrical surface has been considered in [118-125]. Then,

$$E_\theta = E_0 \frac{e^{-jk_0 r}}{\pi r} \sin \theta \sum_{p=-\infty}^{\infty} e^{jp\phi} j^{p+1} f_p(-k_0 \cos \theta) \quad (3.47)$$

$$E_\phi = -\frac{E_0 k_0}{w\mu_0} \frac{e^{-jk_0 r}}{\pi r} \sin \theta \sum_{p=-\infty}^{\infty} e^{jp\phi} j^{p+1} g_p(-k_0 \cos \theta) \quad (3.48)$$

where

$$f_p(u) = \frac{jw \epsilon_0 \overline{M}_\phi(p, u)}{(k_0^2 - u^2) H_p^{(2)'}(a\sqrt{k_0^2 - u^2})} \quad (3.49)$$

$$g_p(u) = \frac{1}{\sqrt{k_0^2 - u^2} H_p^{(2)'}(a\sqrt{k_0^2 - u^2})} \left[-\overline{M}_z(p, u) + \frac{pu \overline{M}_\phi(p, u)}{a(k_0^2 - u^2)} \right] \quad (3.50)$$

$$\overline{M}_\phi(p, u) = \frac{1}{2\pi} \int_0^{2\pi} d\phi \int_{-\infty}^{\infty} dz M_\phi(a, \phi, z) e^{-jp\phi} e^{-juz} \quad (3.51)$$

$$\overline{M}_z(p, u) = \frac{1}{2\pi} \int_0^{2\pi} d\phi \int_{-\infty}^{\infty} dz M_z(a, \phi, z) e^{-jp\phi} e^{-juz} \quad (3.52)$$

$H_p^{(2)}$ is a Hankel function of the second kind and $H_p^{(2)'}$ denotes its derivative.

Evaluating Eqs. (3.49) and (3.50), the resulting components of the far zone electric fields for each cavity mode becomes

$$E_{\theta, mn} = \frac{E_0 h e^{-jk_0 r}}{2\pi^2 r \sin \theta} \left[1 - (-1)^n e^{-jk_0 b \cos \theta} \right] \sum_{p=-\infty}^{\infty} \frac{e^{jp(\phi-\phi_0)} j^{p+1} I(\theta_0, m, -p)}{H_p^{(2)}(k_0 a \sin \theta)} \quad (3.53)$$

$$\begin{aligned}
E_{\phi, mn} = & -j \frac{E_0 h e^{-jk_0 r}}{2\pi^2 r a} I(b, n, -k_0 \cos \theta) \sum_{p=-\infty}^{\infty} \frac{e^{jp(\phi-\phi_0)} j^{p+1}}{H_p^{(2)'}(k_0 a \sin \theta)} \left[1 - (-1)^m e^{-j2p\theta_0} \right] \\
& -j \frac{E_0 h e^{-jk_0 r}}{2\pi^2 r a} \frac{\cos \theta}{k_0 \sin^2 \theta} \left[1 - (-1)^n e^{-j2k_0 b \cos \theta} \right] \sum_{p=-\infty}^{\infty} \frac{e^{jp(\phi-\phi_0)} j^{p+1} p I(\theta_0, m, -p)}{H_p^{(2)'}(k_0 a \sin \theta)}
\end{aligned} \quad (3.54)$$

where

$$I(b, n, -k_0 \cos \theta) = \int_{-2b}^0 \cos\left(\frac{n\pi z}{2b}\right) e^{-juz} dz \quad (3.55)$$

$$I(\theta_0, m, -p) = \int_0^{2\theta_0} \cos\left(\frac{m\pi \phi}{2\theta_0}\right) e^{-jp\phi} d\phi \quad (3.56)$$

The total radiated field is obtained by a summation over all cavity modes, m, n . The infinite summations of Eqs. (3.53) and (3.54) are summations over the cylindrical modes in which the fields have been expanded.

3.5.2 Cylindrical Microstrip Patch Radiation Pattern

The radiation pattern of a cylindrical patch depends on the geometries of the cylinder (a) and the patch (θ_0, b), as well as the characteristics of the substrate (h, ϵ_r) [116]. A software code using [98] is developed by employing the closed form of the Eqns. (3.43-46) to determine the total electric field for chosen fundamental modes.

A cylindrical patch antenna has been chosen as the one presented in [116] to analyze the electrical field pattern. Geometry of the patch is similar the one in Fig. (3-6). Patch has the dimensions $L = 38.3mm$ and $2\theta_0 = 18.3696^\circ$ ($w = 42mm$). Substrate has the height and relative permittivity $h = 1.6mm$, $\epsilon_r = 4.4$, respectively. The radius of the cylinder is $a = 131mm$. The patch has been put into X axis, i.e., $\phi_0 = \theta_0 = 18.3696^\circ / 2$. The resulting electrical field pattern is given in Fig. (3.7) at

1.8 GHz. Normalized azimuth pattern data for “1 degree” resolution is also obtained. The pattern and the data is similar to the one given in [116].

3.5.3 Cylindrical Microstrip Patch Array

A twelve element equally spaced cylindrical patch array is designed to implement the MN-MUST algorithm for full azimuth coverage. The geometry of the array is given in Fig. (3-8). Array is equally spaced in XY -plane ($\theta = 90^\circ$). The patch elements are as the same as the one in the previous section. The excitation point of first antenna element A_1 is located on the X axis, i.e., $\phi_0 = -9.1848^\circ$ according to the notation used in previous section. All of the parameters of the patch elements are the same as in the previous section. The n -th element is located at the angle

$$\phi_{an} = \frac{2\pi n}{12} \quad (3.57)$$

Far zone electric field is given by eqns. (3-53 – 3-56). The overall array electric field total radiation pattern is given in Fig. (3-9).

Twelve cylindrical patch elements are placed along a circle radius a and separated by a uniform angle 30° as shown in Fig. (3.10). A spherical coordinate system is used with its the origin located at the center of the array. Source (target) azimuth angles, $\Phi \in [0, 2\pi]$, are measured counterclockwise from the x axis on $x - y$ plane. Targets (sources) are assumed to be on the $x - y$ plane and $\theta = \pi/2$. DoA estimation is performed only for the azimuth angle. Patch elements are considered to have identical patterns on $x - y$ plane $E_T(\phi_m)$. The signals in each patch antenna element can be expressed as

$$X_i(t) = \sum_{m=1}^K S_m(t) E_T(\phi_m) e^{-jk_m} + n_i(t) \quad i = 1, 2, \dots, 12 \quad (3.58)$$

where $n_i(t)$ is the noise signal received by the i -th antenna element and $k_m = k_0 a \cos(\phi_m - \frac{2\pi(i-1)}{12})$, a is the radius of the cylinder, c is the speed of light in free-space, and ω_0 is the angular center frequency of the signal. In matrix form

$$X(t) = AS(t) + N(t) \quad (3.59)$$

where

$$\begin{aligned} X(t) &= [X_1(t) \quad X_2(t) \quad \dots \quad X_M(t)]^T, \\ N(t) &= [n_1(t) \quad n_2(t) \quad \dots \quad n_M(t)]^T, \\ S(t) &= [S_1(t) \quad S_2(t) \quad \dots \quad S_K(t)]^T, \end{aligned} \quad (3.60)$$

and each entry of A is defined as

$$A_{im} = E_T(\phi_m) e^{-jk_m} \quad (3.61)$$

where

$$E_T(\phi_m) = E_\theta(\phi_m) + E_\phi(\phi_m) \quad (3.62)$$

E_θ and E_ϕ are given in equations 3.53 and 3.54, respectively.

The noise signals, $\{n_i(t), i = 1:M\}$ received at different antenna elements of the array are assumed to be statistically independent zero mean white noise signals with variance σ^2 independent of $S(t)$. The spatial correlation matrix R of the received signal is given by

$$\begin{aligned} R &= E\{X(t)X(t)^H\} \\ &= AE\{S(t)S(t)^H\}A^H + E\{N(t)N(t)^H\} \end{aligned} \quad (3.63)$$

where “ H ” denotes the conjugate transpose.

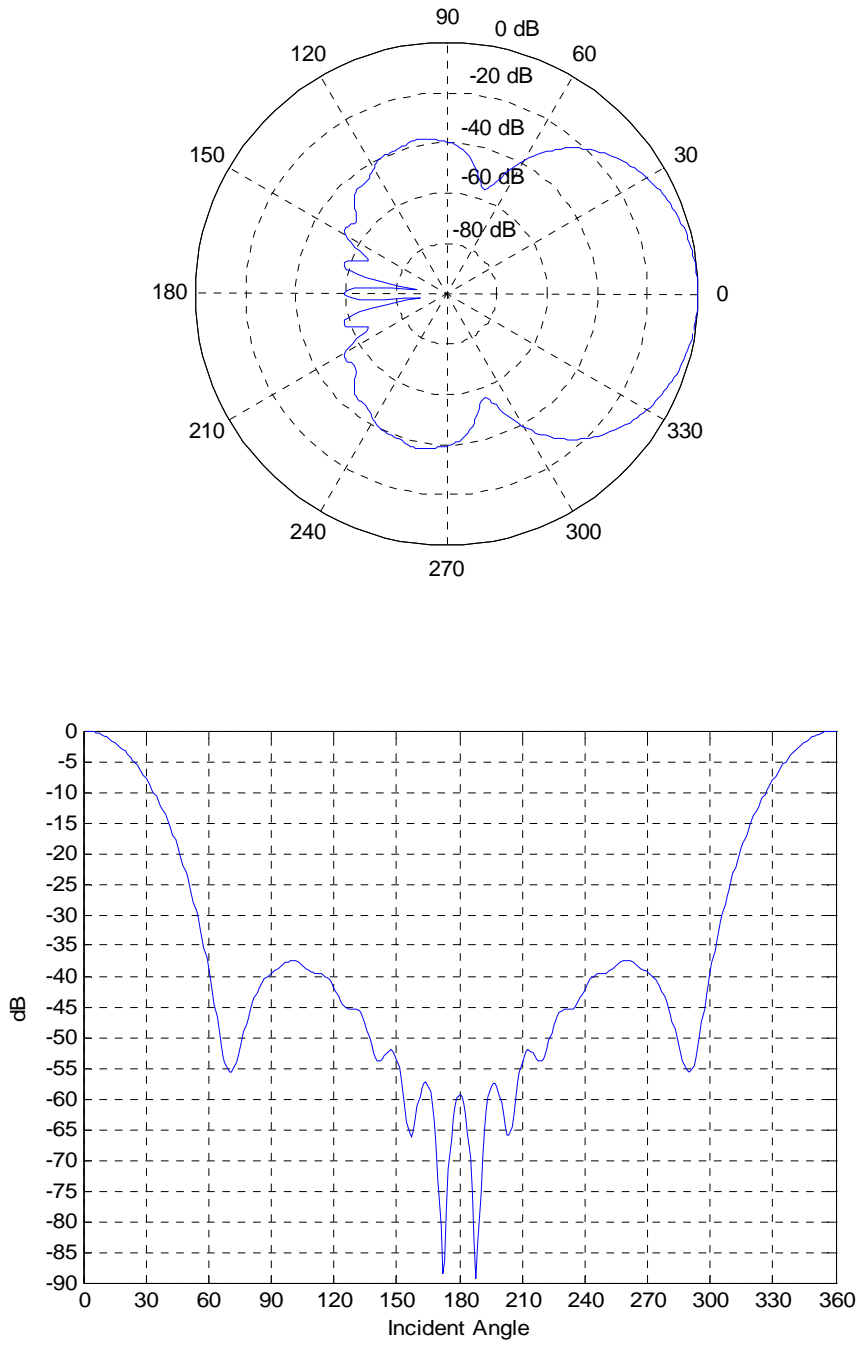


Figure 3.7 The total electrical field pattern of a patch at $\theta = 90^\circ$ (E -plane) with $h = 1.6\text{mm}$, $\epsilon_r = 4.4$, $L = 38.3\text{mm}$, $\theta_0 = 9.1848^\circ$ and $a = 38.3\text{mm}$ $f = 1.8\text{ GHz}$.

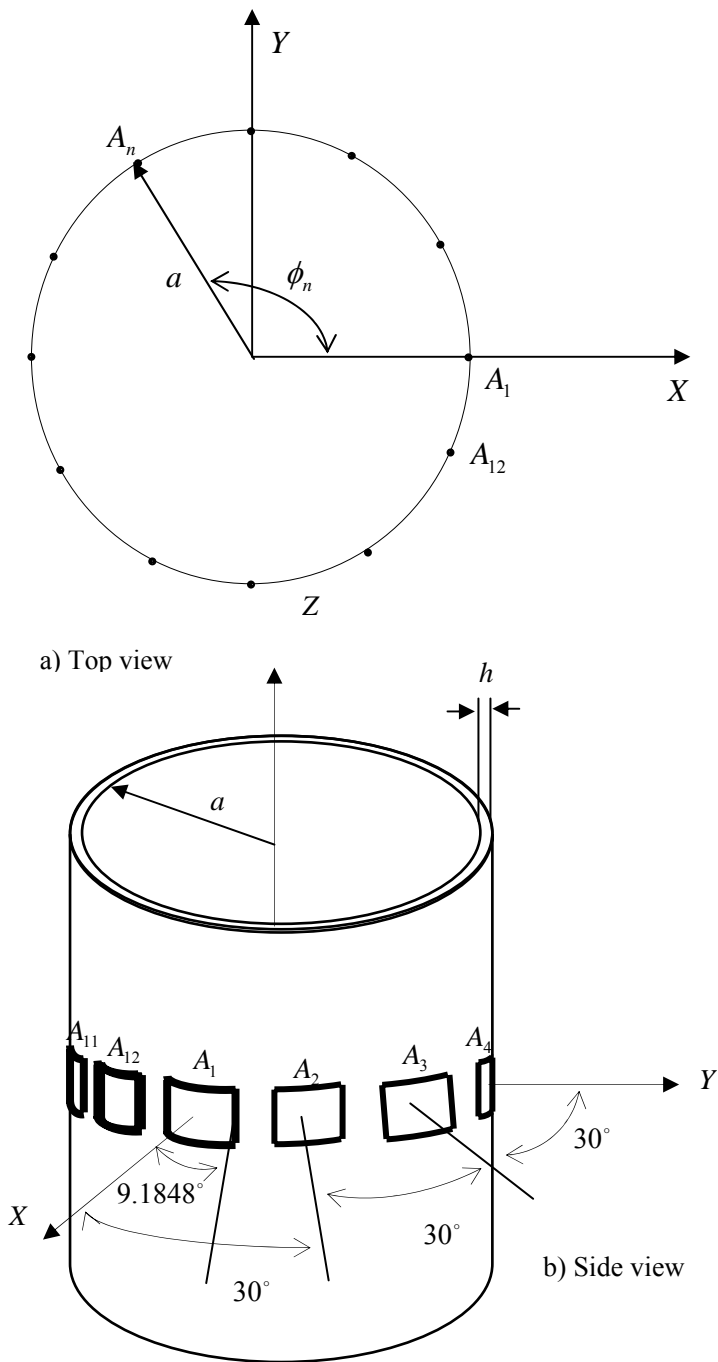


Figure 3.8 The geometry of 12 element uniform cylindrical patch array with $h = 1.6\text{mm}$, $\epsilon_r = 4.4$, $L = 38.3\text{mm}$, $\theta_0 = 9.1848^\circ$ and $a = 38.3\text{mm}$.

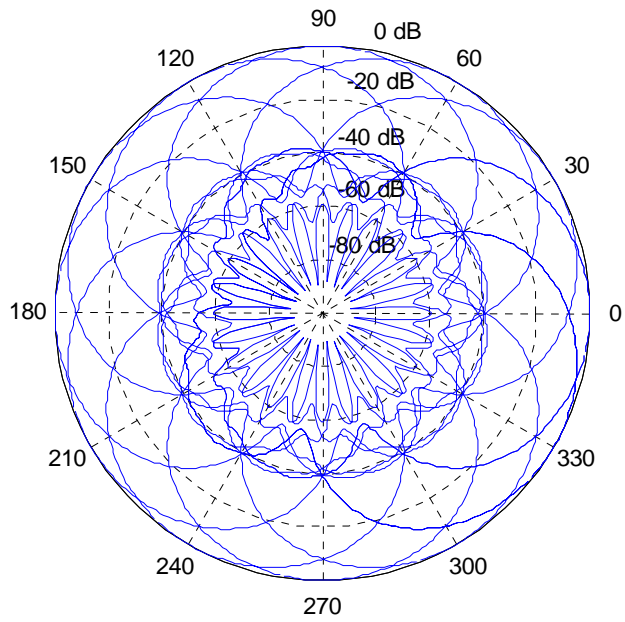


Figure 3.9 The individual element electrical field patterns of 12 element patch array given in Fig. (3.8).

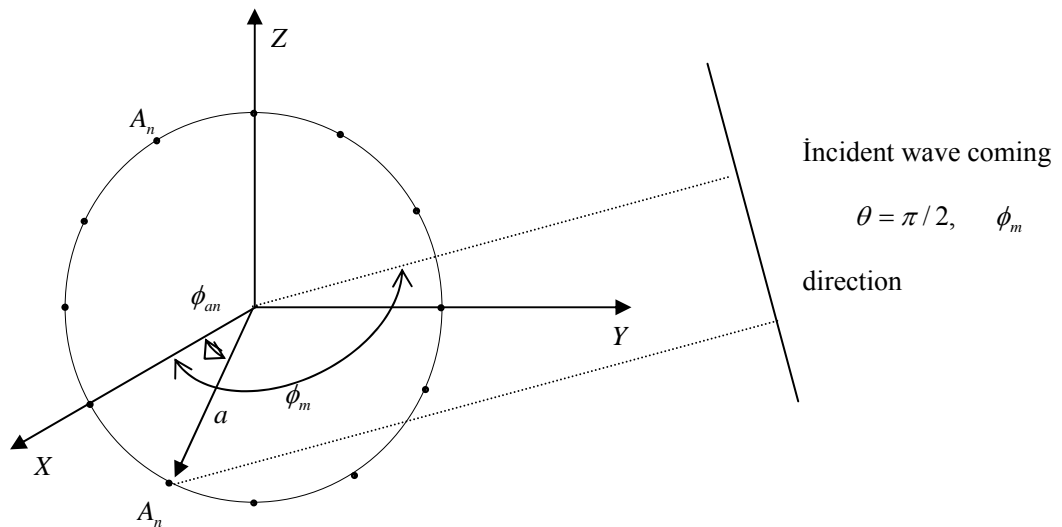


Figure 3.10 Geometry of a circular array (m -th incident wave on n -th antenna element).

3.5.4 MN-MUST Implementation to Cylindrical Array

The twelve cylindrical patch patterns are divided into 12 equal sectors in Fig. (3-11). Sector size is 30° in the azimuth direction. The centers of each sector is located at $[0^\circ \ 30^\circ \ \dots \ 330^\circ]$ degrees, where the patch centers are located. It can be recognized from Fig. (3-11) that each sector has only three antenna elements whose normalized values higher than -20 dB . Cylindrical patch array MN-MUST algorithm structure is given in Fig. (3-12). The adopted algorithm is called CMN-MUST (Cylindrical patch array MN-MUST). CMN-MUST algorithm consists of three stages, detection, reduced order spatial filtering and DoA estimation stage. Detection stage is exactly the same as Section 3.2.1. There are three antenna elements in each sector such as *Sector - i* has the $(i-1)\text{th}$, $i\text{-th}$ and $(i+1)\text{th}$, antenna elements. If we consider only the antenna elements inside the sector of interest, then we do not need to filter out the signals in the antenna elements outside the sector of interest. On the other hand we do not need to have full array for DoA estimation stage for sectors. This reduces spatial filtering and DoA estimation stage NN sizes. Hence the detection stage is not changed, but only reduced order filtering and DoA estimation stages are discussed in detail.

3.5.4.1 Spatial Filtering Stage

This stage is the reduced order form of the spatial filtering stage mentioned in Section 3.2.2. DoA estimation stage needs the signals only from the antenna elements in the sector of interest, then the filtering stage also needs to filter out the signals outside the sector of interest in the antenna elements associated with sector of interest. In otherwords, spatial filter for *Sector - i* will filter out the signals coming outside the *Sector - i* on the $(i-1)\text{th}$, $i\text{-th}$ and $(i+1)\text{th}$, antenna elements.

First (detection) stage is exactly the same as Section 3.2.1, i.e., NN input vector is Z , and its output is either “0” or “1”. The size of Z for a 12 element cylindrical patch array is 24×1 . Input size of spatial filtering stage is reduced by considering the

antenna elements inside the sector of interest only. The NN input for *Sector* $-i$, Z_{Si} can be expressed by using Eq. (3.63) as

$$R = \begin{bmatrix} R_{1-1} & \dots & R_{1-i} & \dots & R_{1-12} \\ \dots & \dots & \dots & \dots & \dots \\ R_{12-1} & \dots & R_{12-i} & \dots & R_{12-12} \end{bmatrix} \quad b = [R_{1-(i-1)} \quad R_{1-i} \quad R_{1-(i+1)}]$$

3.64

$$Z_{Si} = \frac{b}{\|b\|}$$

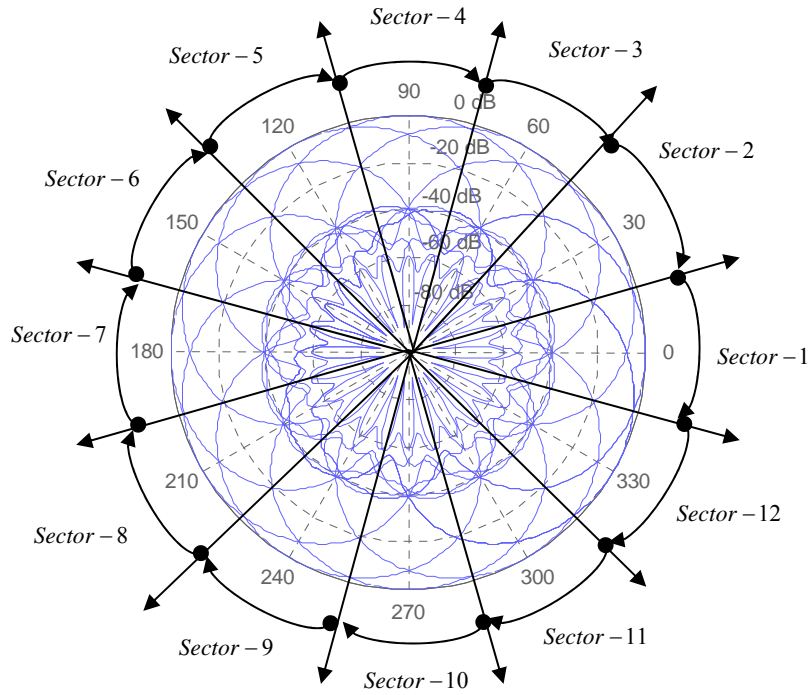


Figure 3.11 The twelve cylindrical patch pattern is divided into 12 equal sectors.

The output of the spatial filter network for *Sector* $-i$ is Z_{fi} which does not include the signals from other sectors on the $(i-1)th$, $i-th$ and $(i+1)th$, in the related antenna elements. In the training phase Z_{fi} pairs are processed discarding the signals

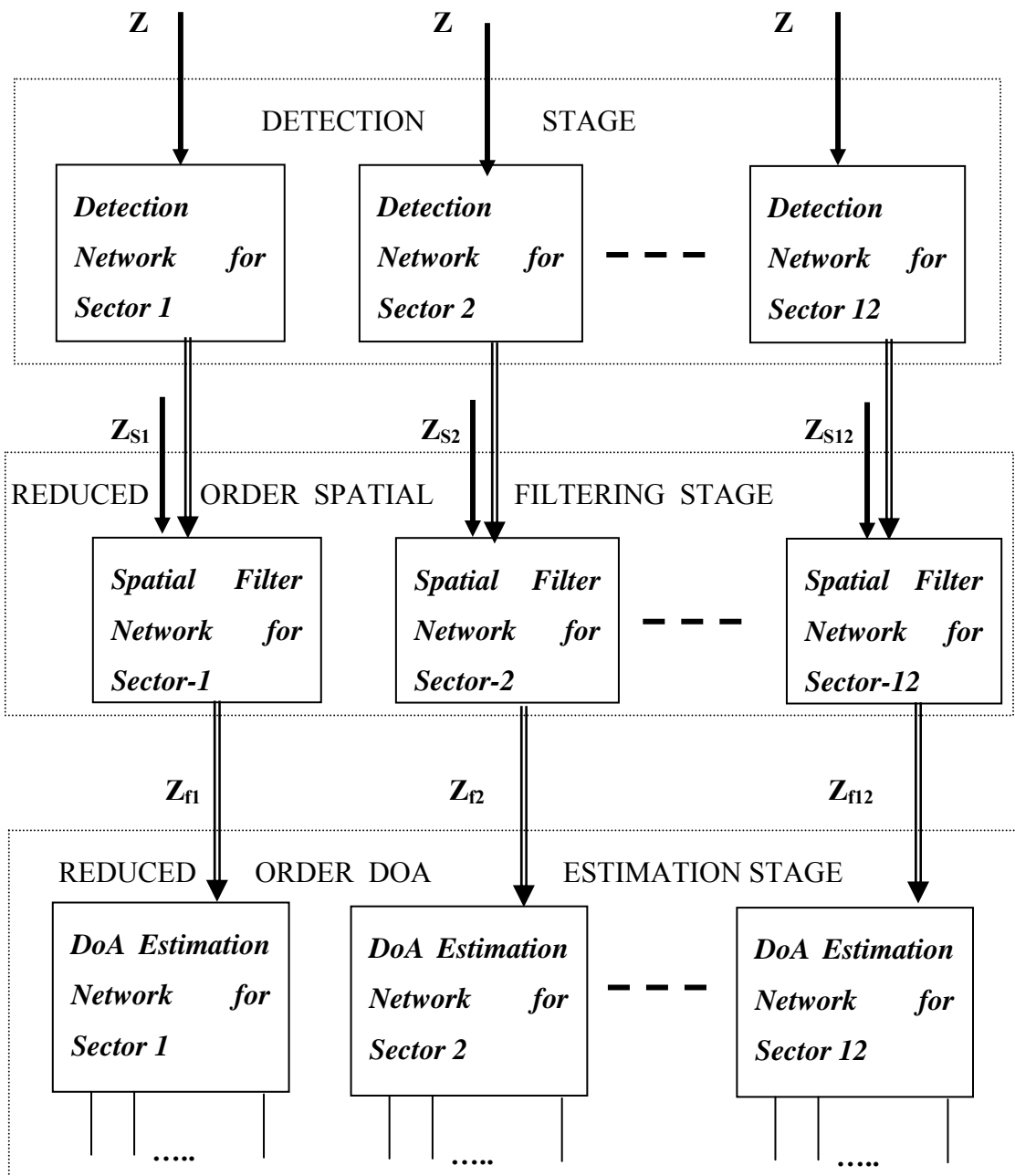


Figure 3.12 The CMN-MUST algorithm architecture.

outside the i -th angular sector. It is assumed that $\{S_1(t), S_2(t), \dots, S_K(t)\}$ are all of the signals impinging on the array and $\{S_t(t), S_q(t), S_l(t)\}$ are the only signals coming into the angular sector- i where $t, q \& l \leq K$. The input of the NN, Z is computed through Eq. (3.64) having $\{S_1(t), S_2(t), \dots, S_K(t)\}$ signals, while the output of NN, Z_{fi} is computed through Eq. (3.64) again, but the signal is $\{S_t(t), S_q(t), S_l(t)\}$ this time. Filtering stage filters out the $\{S_1(t), S_2(t), \dots, S_K(t)\} - \{S_t(t), S_q(t), S_l(t)\}$ signals for the training example. In the training phase NN generalizes the input-output ($Z_{Si} \rightarrow Z_{fi}$) relations in the training phase. In the testing phase, one can have a generalized response to inputs that it has never seen before.

3.5.4.2 Reduced Order Sectoral DoA Estimation Stage

DoA estimation stage consists of a NN that is trained to perform the actual direction of arrival estimation. The sectors (associated NN's) that have outputs "1" are considered as the sectors having targets. When the output of networks of sectors from the first stage is "1", the corresponding second stage network(s) are activated. Then the next stage DoA estimation stage is activated.

First (detection) stage is exactly the same as the one given in Section 3.2.1, i.e., NN input is the vector Z , and its output is either "0" or "1". The filtered Z_{Si} , which is Z_{fi} in spatial filtering stage, will be the input DoA estimation network for Sector $-i$. The size of both the input and output of filtering NN is 6×1 , instead of 24×1 , as given in Section 3.2.2.

Except the structure and size of Z_{fi} the rest of the stage is exactly the same as DoA estimation stage described in Section 3.2.3.

CHAPTER 4

SIMULATIONS

In this Chapter simulation results are presented to demonstrate various performance features of the MN-MUST algorithm. Some of the results of earlier works can be found in [58-63] as well.

MN-MUST algorithm is implemented for a uniform linear array(ULA) consisting of point sources, a six element dipole uniform circular array in the presence of mutual coupling and a twelve element cylindrical patch array. The general performance features of MN-MUST algorithm has been run for ULA. Mutual coupling affects on MN-MUST algorithm has been studied in a six element uniform dipole circular array. The realistic case, array elements having directive patterns has been tested with a twelve element cylindrical patch array.

An important measure of how well a particular method performs is the covariance matrix of estimation errors [3]. The Cramer-Rao bound (CRB) is the most common tool in this respect. There are several studies to calculate CRB in the literature [126-135].

In this thesis CRBs are not computed. However CRBs already calculated for some particular scenarios in similar neural network algorithms [134-135] are used to compare MN-MUST algorithm with other methods and CRBs. For those particular scenarios, MN-MUST algorithm has been run to generate the data.

MN-MUST and N-MUST are run in parallel to generate data for performance comparison such as, NN training, memory requirements, accuracy performance etc.

Various scenarios have been simulated with design parameters such as the number of array elements, number of targets need to be estimated, different positions of the targets, different signal to noise ratio (SNR) levels and RBNN parameters, number of hidden layers, training root mean square (RMS) error, number of training sample etc.

4.1 Simulations Features

The number of antenna elements is an important parameter for DoA algorithms. Simulations are run for ULA, UCA and cylindrical microstrip patch array. The aim of UCA application is to test the algorithm in the presence of mutual coupling. Cylindrical microstrip patch array is implemented to test the effects of directive patterns on the MN-MUST algorithm, so that the number of antenna elements is also constant as twelve for cylindrical microstrip patch array. The effect of antenna elements on MN-MUST algorithm is tested only for ULA with point source elements.

Correlation matrix is evaluated the using the data provided from narrow band receiver from each antenna elements. Because of the advances in ADC, sampling rate is not an issue for the MN-MUST algorithm. The number of snapshots is an important parameter for correlation matrix computations and the noise contribution. The number of snapshots is considered as 400, unless otherwise is stated. The targets (sources) are considered stationary during the time period of the observations (snapshots).

The SNR used in simulations is defined parallel to [3] as,

$$SNR = 10 \log \left(\frac{SP}{\sigma^2} \right)$$

where σ^2 is the average noise power, and SP (Signal Power) is the maximum signal power.

SP is assumed as one for all of the simulations. Noise is generated as zero-mean Gaussian random complex sequence, with uncorrelated real and imaginary parts, each with a variance of $\sigma^2 / 2$.

The number of trials directly influence the confidence level of the assessment. Unless otherwise is stated, the number of trials is chosen as 150 in the simulations to

compute the DoA estimation error RMS value computation. Simulations are run in MATLAB [98] software.

4.2 Cramer-Rao Bound

There are two sources fixed at “0” and “2” degrees in a scenario of [136]. CRBs and MUSIC algorithm DoA estimation RMS error used in this section are taken from Tables III and IV of [136] for three different SNR levels.

RMS error for MN-MUST algorithm for that particular scenario (2 sources) is calculated through a series of simulations. The simulations are run for a ten degree angular sector from -4° to 5° with an angular resolution of 1° . The array is a six element point source uniform linear array with a uniform distance $\lambda/2$. The number of NN neurons is 50, the number of training data pair 60 for the MN-MUST algorithm training. Training is performed with no-noise. MN-MUST algorithm is run for three different SNR levels, i.e., 10 dB , 20 dB and 50 dB . The number of snapshots taken is 200, the number of trails for calculating the variance of estimation error is 300 independent trials.

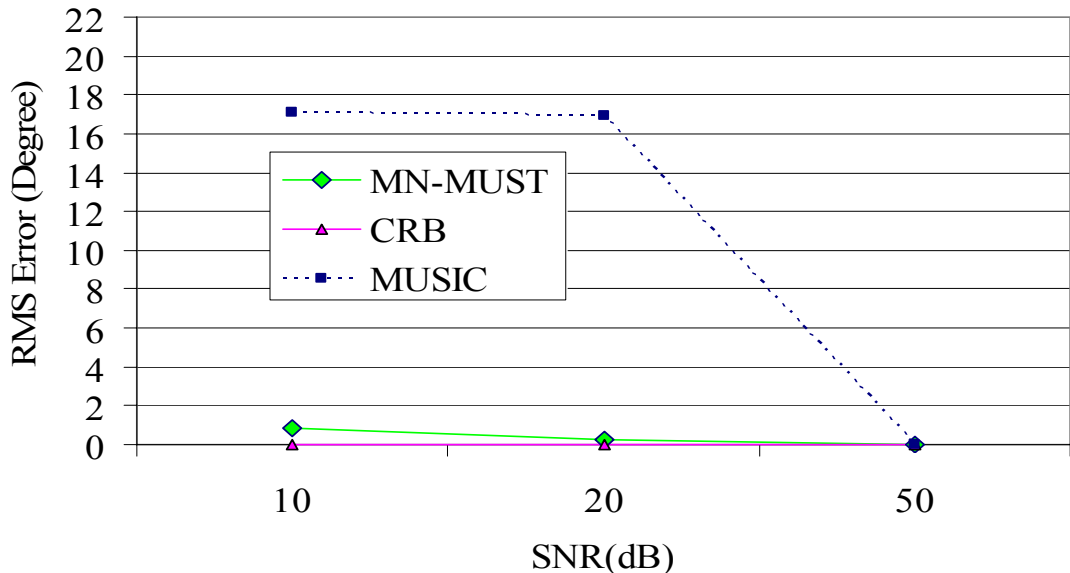


Figure 4.1 MN-MUST performance comparison with MUSIC algorithm and CRB for 0° for three different SNR.

Results for 0° and 2° source are given in Fig. 4.1 and 4.2 respectively. Three different SNRs are considered and the corresponding values of the CRB are also given. It can be observed that for high SNRs, MUSIC algorithm nearly attains the CRB and its variance is far lower than of MN-MUST algorithm. However as the SNR decreases the variance in the error for MUSIC becomes very high. This is due to the fact that the two sources become irresolvable in the MUSIC spectrum at lower SNR and a spurious peak is picked up as a signal source [136]. The neural network based methods perform far better than MUSIC algorithm at lower SNRs since they don't encounter the problem of resolvability. It must be mentioned here that comparisons with the CRB are usually done for studying the performance of unbiased estimators only [136]. The neural network based methods cannot be considered as unbiased estimators since they give a finite error even when there is no noise. However this small error can be reduced to an arbitrarily small level by choosing a smaller error criterion while training.

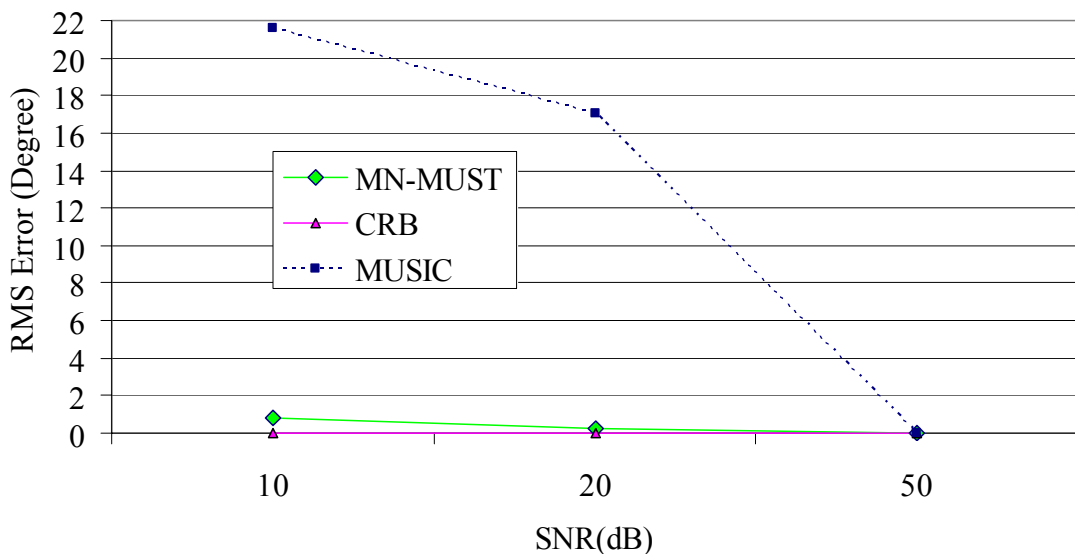


Figure 4.2 MN-MUST performance comparison with MUSIC algorithm and CRB for 2° for three different SNR.

4.3 Neural Network Training Mean Squared Error Effects

Neural network training mean square error plays a major role on the accuracy of MN-MUST algorithm. In order to test that feature, four separate neural networks are trained with four different training mean squared error goal, i.e., 20, 50, 100 and 150 training mean squared error for 3 and 4 sources cases separately. Training is run for three and five element point sources ULA with a uniform $\lambda / 2$ distance. The angular sector is $[21^\circ - 30^\circ]$ with a 1° resolution. DoA estimation RMS testing error for 3 elements and five elements ULA are given in Figures 4-3 and 4-4 respectively.

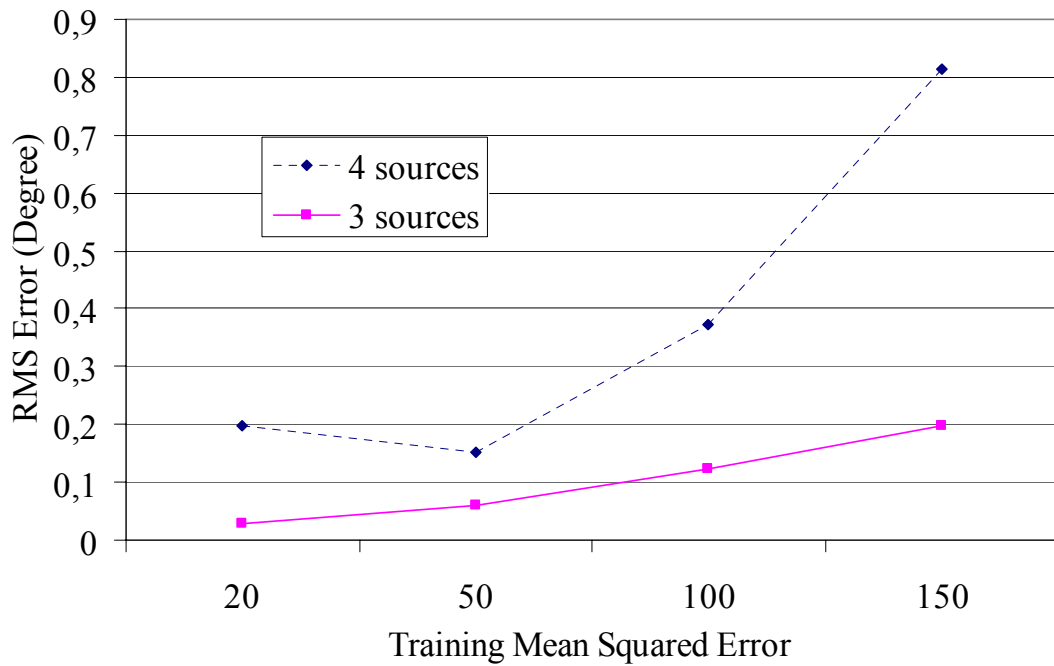


Figure 4.3 DoA estimation RMS error for three elements ULA, three and four sources cases tested on a MN-MUST algorithm DoA estimation stage NN trained under the goal of 20, 50, 100 and 150 mean squared error.

There is a direct link between the training RMS testing error and DoA estimation accuracy. As it is mentioned in the previous section if the training goal is set to a small number then the NN is well trained so that the DoA estimation RMS value is also low. That trend is also observed for the number of sources as well. When the number of sources decreases then the DoA estimation RMS error also decreases.

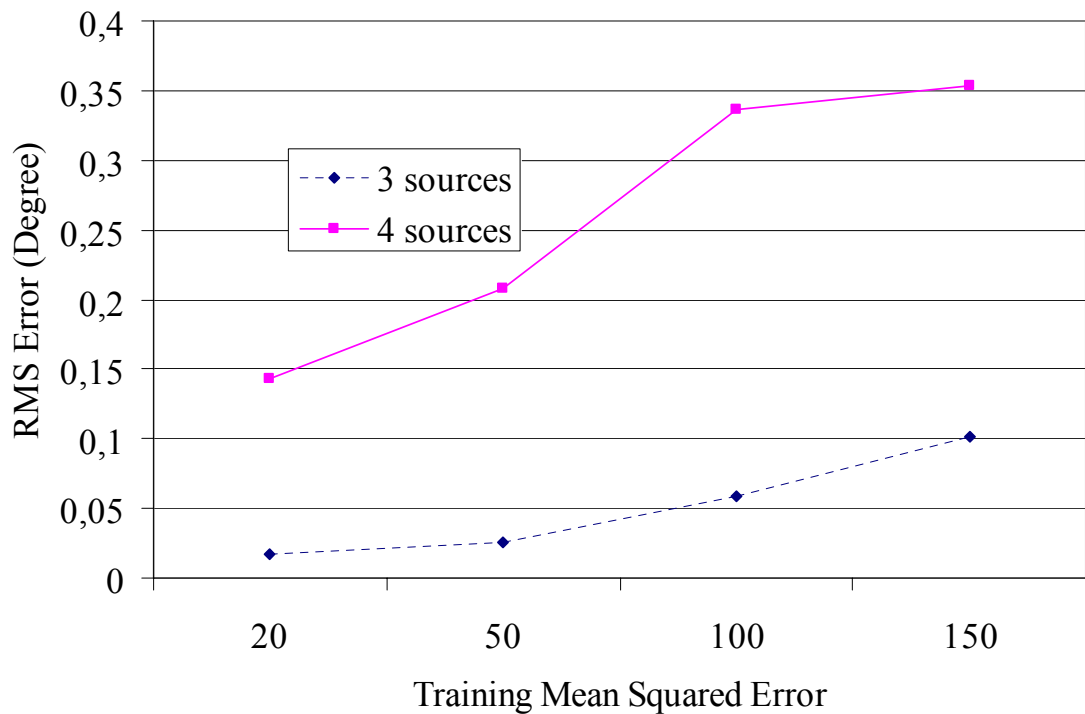


Figure 4.4 DoA estimation RMS error for five element ULA, three and four sources cases tested on a MN-MUST algorithm DoA estimation stage NN trained under the goal of 20, 50, 100 and 150 mean squared error.

4.4 Number of Antenna Elements

The input size of each NN used in MN-MUST algorithm is two times of the number of antenna elements used in the array (ULA and UCA application). This means process cost (time, memory etc.) increases as the number of antenna elements used.

However, the DoA estimation accuracy is supposed to increase as the number of antenna elements increases.

Four separate neural networks are trained for a 3, 5, 8 and 16 element ULA with a uniform $\lambda / 2$ distance and are tested for 3 sources separately. The NN training parameters is set to a constant value for each NN. The angular sector is $[21^\circ - 40^\circ]$ with a 1° resolution. DoA estimation RMS testing error for 3, 5, 8, 10, 12, 14 and 18 antenna elements is given in Figure 4-5.

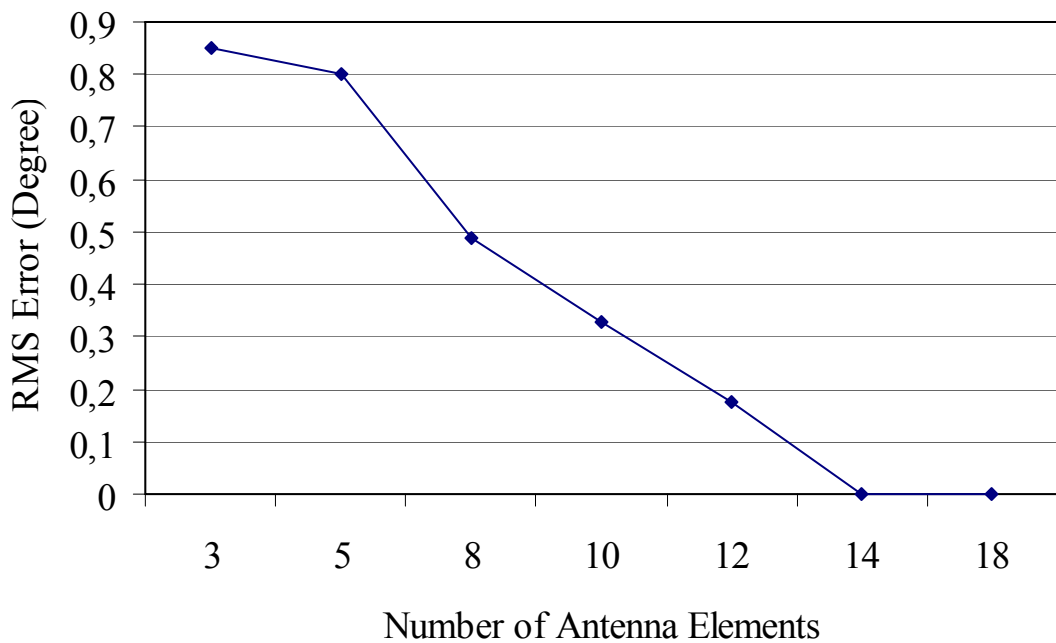


Figure 4.5 DoA estimation RMS error vs. number of antenna elements used in ULA, three source, 20 dB SNR, constant training RBNN parameter.

4.5 MN-MUST and N-MUST Comparison

The use of reduced input size in the NN based system decreases the computational time while keeping the computational accuracy unaffected (Figs 4-6 through 4-8). In Fig. 4-6, neural network training time versus size of the smart antenna structures in N-MUST and MN-MUST algorithms is compared. As the number of array elements

increases the training times of the two systems become drastically different as expected. Fig. 4-7 shows the total training error of both networks within the training times given in Fig. 4-6. The training error threshold is set to the same (one) for all examples for both N-MUST and MN-MUST algorithm. In Fig.4-8 comparison of memory requirements of MN-MUST algorithm and N-MUST algorithm are provided. It is observed that after a certain threshold value in the number of array elements, the MN-MUST algorithm training requires much less memory as well as having high speed for the same training error threshold level.

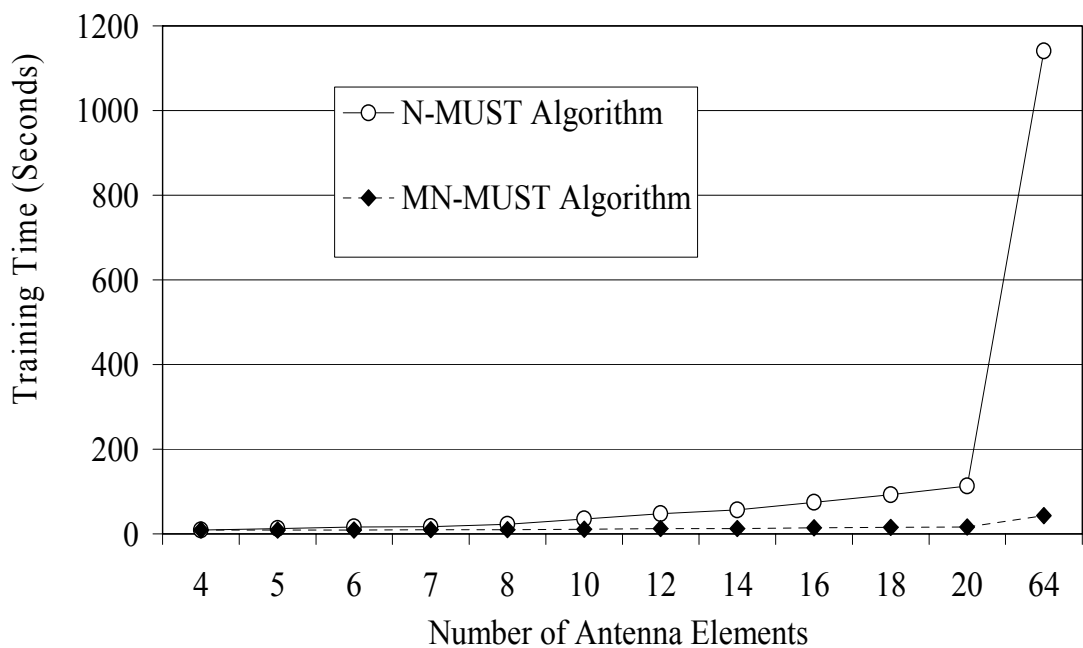


Figure 4.6 Training time vs. antenna elements size (MN-MUST algorithm to N-MUST algorithm)

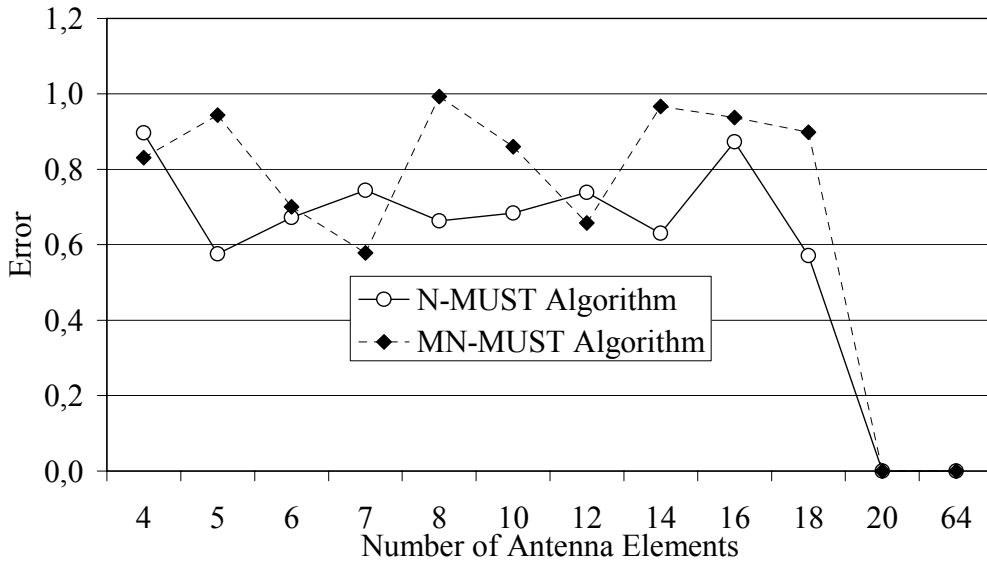


Figure 4.7 Error performance of MN-MUST algorithm and N-MUST algorithm.

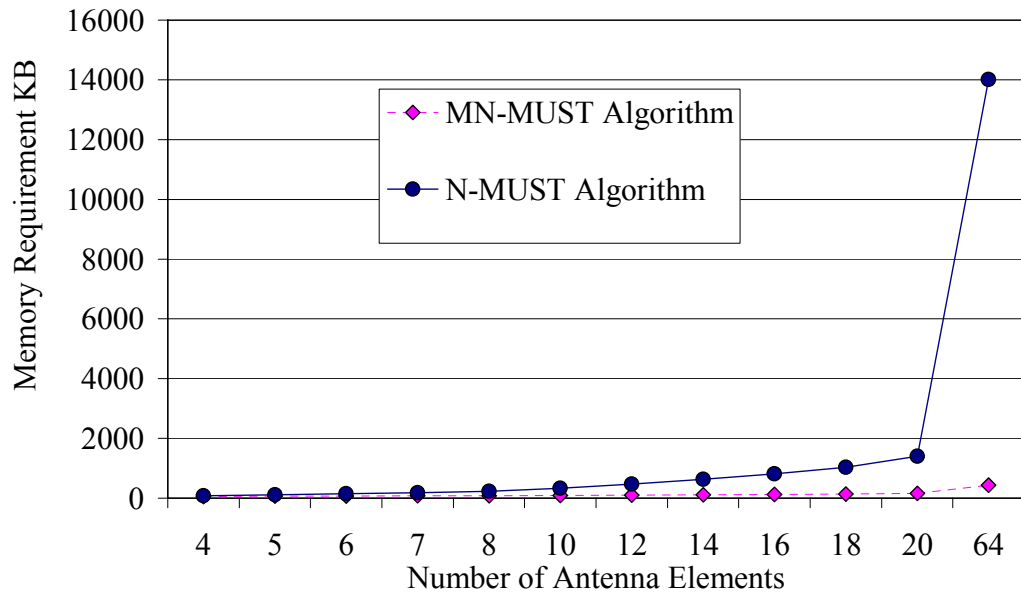


Figure 4.8 Memory requirements comparison of the neural networks for MN-MUST algorithm and N-MUST algorithm.

Performance of the MN-MUST algorithm is demonstrated in Figs 4-9 – 4-11 for some different cases. For this purpose the angular spectrum between 1-30 degrees is divided into 3 angular sectors in 10-degree intervals. The angular resolution is 1 degree within each angular sector. For the first two examples, three stage of MN-MUST algorithm trained for three-target case with a three and five element linear arrays, are used, respectively. Three different detection neural networks are trained to determine whether or not there exists a target in that sector. Three network filters are then trained to annihilate the targets outside the corresponding angular sector. Finally, three separate DoA networks are trained to find the actual targets location within the corresponding sectors.

In the first scenario there exists three targets in three different angular sectors located at 1, 15 and 24 degrees, respectively. The performance of the MN-MUST algorithm is given in Fig. 4-9.

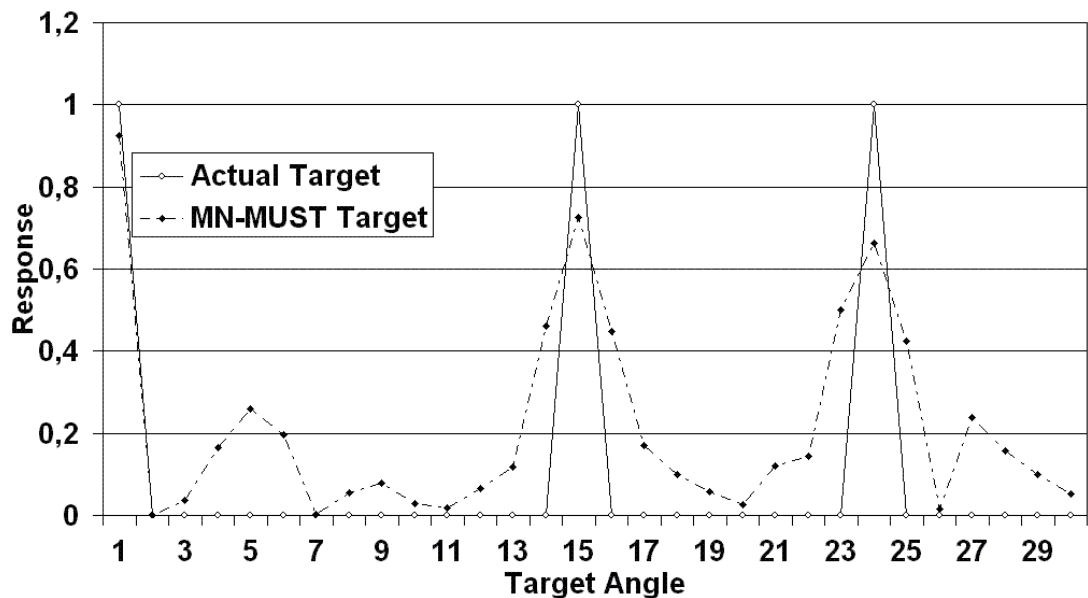


Figure 4.9 Three targets in three sectors in three-element array (Targets are at 1, 15 and 24 degrees)

In the second scenario presented in Fig. 4-10, there exist three targets in one angular sector case located at 22, 24 and 29 degrees, respectively. This scenario is run using a 5 dB Signal to Noise Ratio (SNR) both for MN-MUST and N-MUST algorithms.

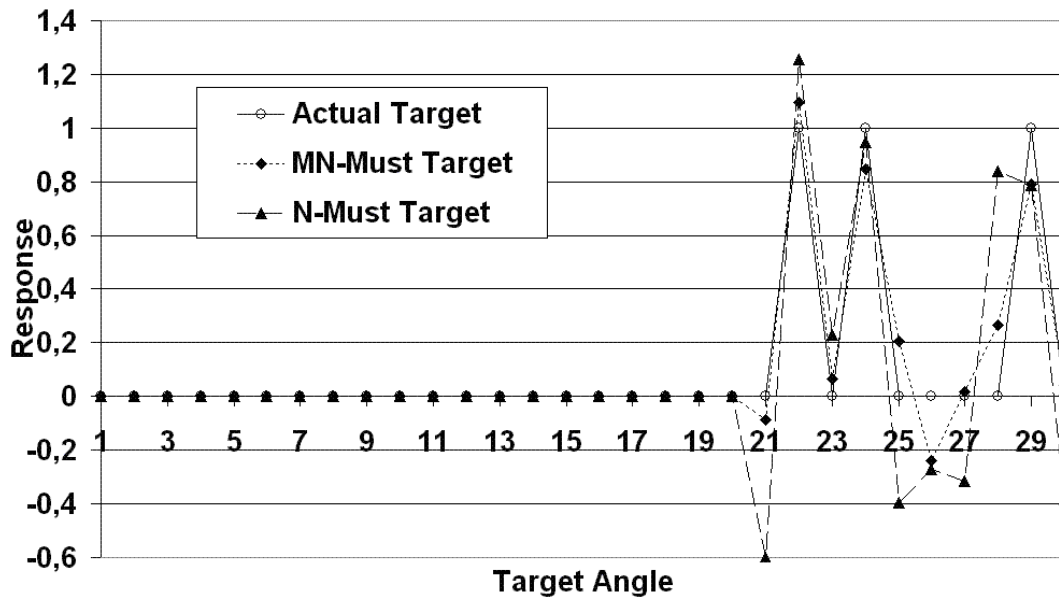


Figure 4.10 Three targets in one sector in five-element array (Targets are at 22, 24 and 29 degrees). Targets are equal power and 5 dB higher than noise power.

In the last scenario MN-MUST algorithm is applied to the case where there exist four targets and a three element antenna array, i.e., the number of targets is greater than the number of antenna elements and 5 dB SNR. The four targets were located at 21, 24, 27 and 29 degrees. The critical point in this application is that all the targets are located within the same angular sector. Simulation results are given in Fig. 4-11.

In all three cases demonstrated in the Figs 4.9 – 4.11, it is observed that the MN-MUST algorithm finds the targets correctly no matter whether the targets are located within the same angular sector or not. In addition, as the number of targets exceeds the number of antenna elements the algorithm can still perform sufficiently well even in a high SNR condition.

The maximum number of targets within an angular sector depends upon the size of the sector and the angular resolution.

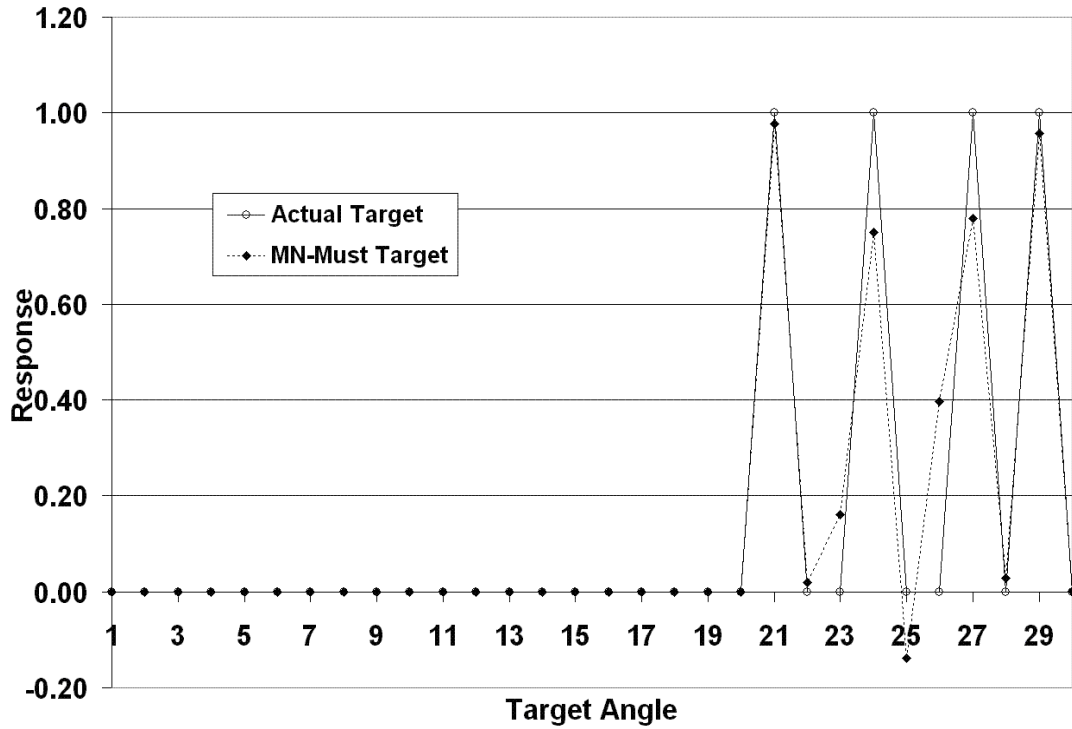


Figure 4.11 Four targets in one sector in three-element array (Targets are at 21, 24, 27 and 29 degrees). Targets are equal power and 5 dB higher than noise power.

4.6 SNR Level

MN-MUST algorithm is compared to conventional methods and CRB in Section 4.1. It is observed that MN-MUST algorithm performs well in low SNR. In order to investigate MN-MUST algorithm performance against noise, two different neural networks have been trained and tested with more than 100 trials.

First Neural network is trained for a 12 elements ULA with a uniform $\lambda / 2$ distance and is tested for 3 sources with 3, 5, 10, 15, 20 and 30 dB SNRs separately. The angular sector is $[21^\circ - 40^\circ]$ with a 1° resolution. DoA estimation RMS testing error for different SNR levels is given in Figure 4-12.

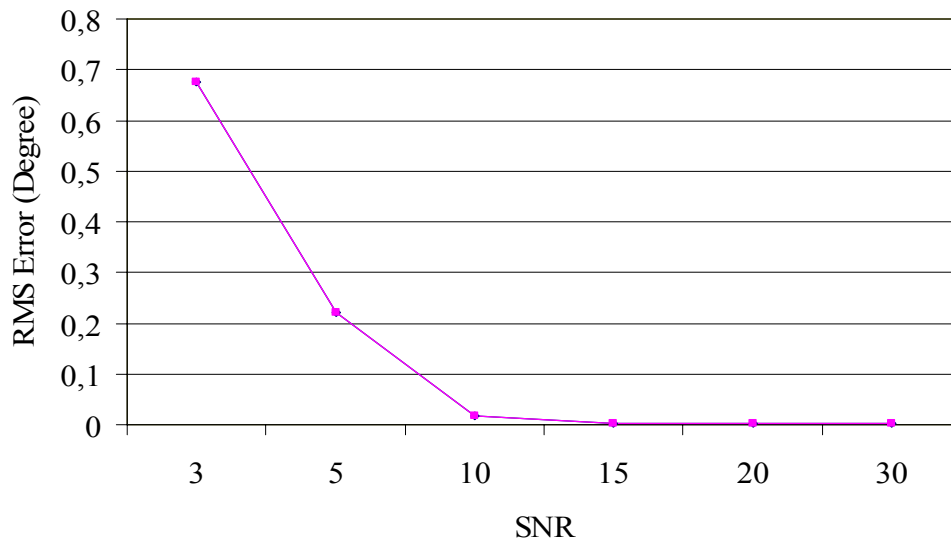


Figure 4.12 Twelve-element ULA , tested for three sources.

Second neural network is trained for a 3 elements ULA with a uniform $\lambda / 2$ distance and is tested for 3 sources with 3, 5, 10, 15, 20 and 30 dB SNRs separately. The angular sector is $[21^\circ - 40^\circ]$ with a 1° resolution. DoA estimation RMS testing error for different SNR levels is given in Figure 4-13.

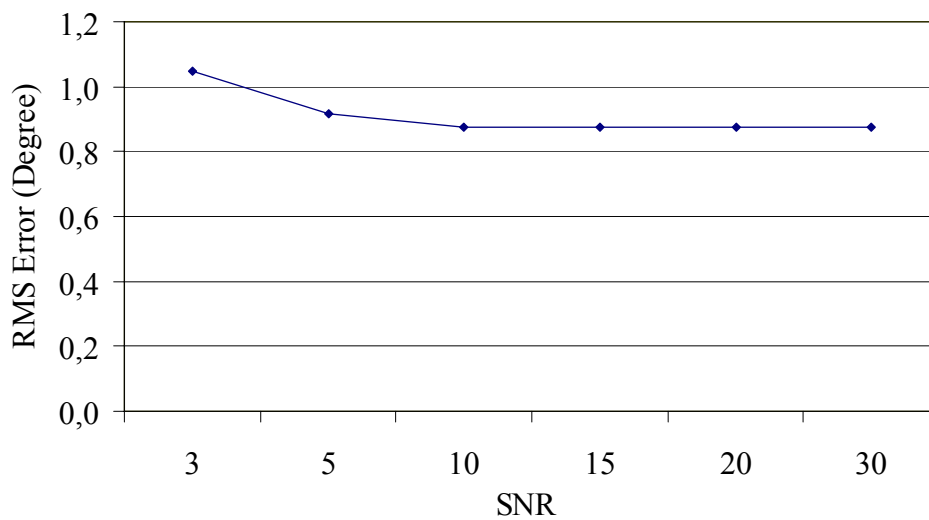


Figure 4.13 Three-element ULA , tested for three sources.

RMS error decreased as the SNR level increased for both simulations. The main difference between two simulations is the offset value between two RMS errors. However, their trends are similar. RMS error decreases when SNR increases, as expected. The RMS error offset value between two simulation exists because of the number of antenna elements used in both ULA. DoA estimation accuracy dramatically increases as the number of antenna elements used in array increase. DoA estimation accuracy of MN-MUST algorithm for low SNR is observed far beyond the conventional algorithms.

4.7 Effect of the Number of Snapshots

MN-MUST algorithm depends on computation of correlation matrix. Correlation matrix computation methodology is given in Section 3.3.2. Correlation matrix value used in the algorithm is the average of values taken in snapshots. During the observation period, targets are assumed stationary. Because of advances in sampling technology, i.e., high speed ADCs, the observation period is short, so the assumption is realistic. An observation on a time instant is called snapshot. The number of snapshots used for neural network algorithms in literature is usually between 50-400.

A neural network trained for a 8-element ULA with a uniform $\lambda / 2$ distance in order to test MN-MUST sensitivity against number of snapshots used. The angular sector is $[21^\circ - 40^\circ]$ with a 1° resolution. NN is tested for 3 sources with 50, 60, 70, 80, 90 and 100 snapshots. The DoA estimation error RMS values for 100 trials are given in Fig. 4.14. RMS value of DoA errors decreased as the number of snapshots reaches 90. The optimum value of snapshots may vary for different ULA or different number of sources. However, during simulations it is observed that snapshots over 100 performs good solutions.

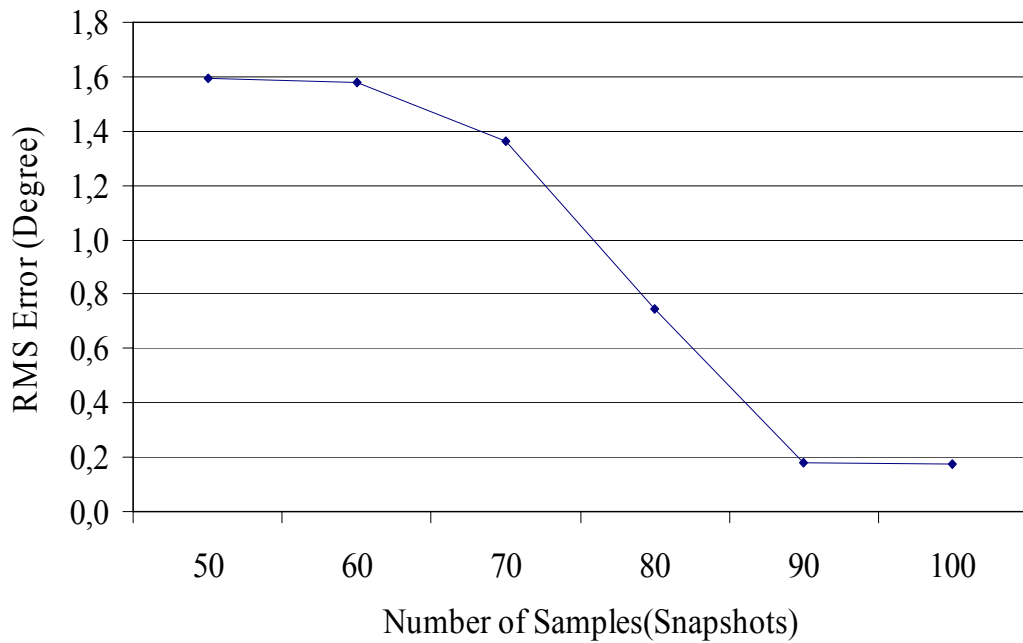


Figure 4.14 RMS value of DoA estimation error vs. number of snapshots for a 8-element ULA with $\lambda / 2$ distance and tested for 3 targets. Targets are equal power and 20 dB higher than noise power

4.8 Effect of Angular Separation of the Targets

Angular resolution is a parameter for MN-MUST algorithm. Angular resolution is the minimum angular separation. A MN-MUST DoA estimation neural network is trained for an eight elements-ULA with a $\lambda / 2$ distance. The angular sector is $[21^\circ - 40^\circ]$ with a 1° resolution. The network tested in 20 DB SNR for different angular separation of three targets. DoA estimation error RMS values are given in Fig. 4.15 for 1° , 2° , 3° , 4° , 5° , 6° , and 7° separations. The number of trials for each case is more than 50. The DoA estimation accuracy gets better as the angular separation gets bigger. But the trend is not smooth. DoA estimation error RMS value for the smallest angular separation, i.e., resolution, is reasonable.

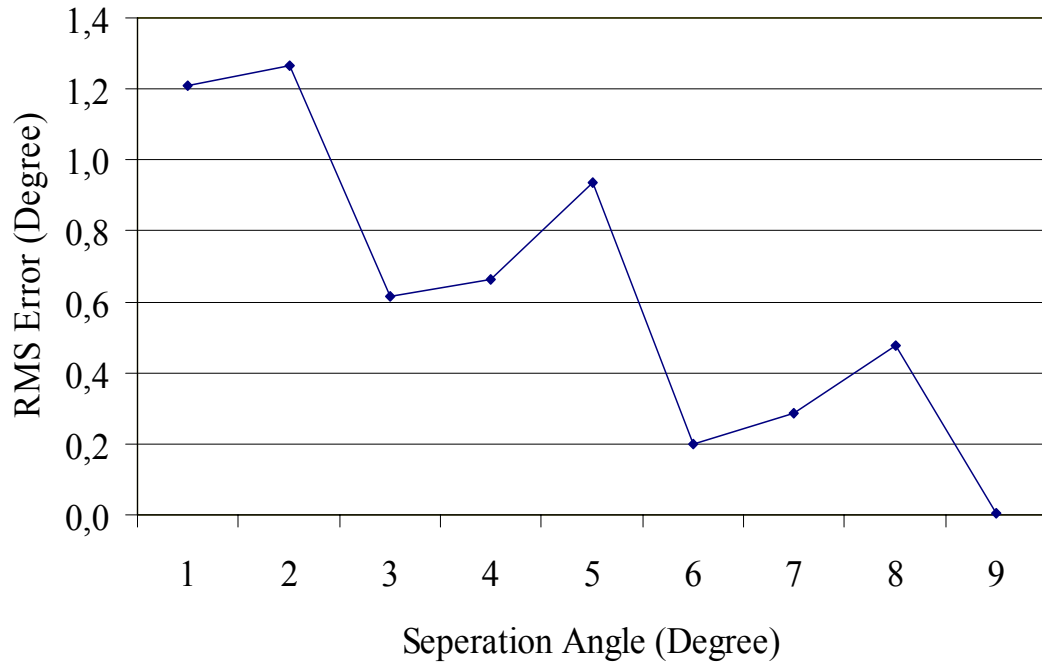


Figure 4.15 RMS value of DoA estimation error vs. angular separation for an 8-element ULA with $\lambda / 2$ distance. There are three targets, equal power and 20 dB higher than noise power.

4.9 Effect of the Mutual Coupling under UCA Implementation

Simulation results are presented to demonstrate MN-MUST algorithm performance in UCA structure in the presence of mutual coupling. Six element half-wave dipole UCA is used for simulation. The coupling impedance is calculated through the formulas derived in Section 3.4.3. The coupling impedance matrix for six element half-wave dipole UCA with a radius of $a = 3\lambda / 2\pi$ is given in Table C.1.

Performance of the MN-MUST algorithm is demonstrated in Figs 4.16 to 4.17 for two different cases. For this purpose the angular spectrum between 21-30 degrees is used in 1 degree separation. In the both cases there exist two targets located at 21 and 25 degrees, respectively. Both scenarios are run using a 20 dB Signal to Noise Ratio.

In the first scenario, MN-MUST DoA networks are trained in the presence of mutual coupling (PMC) to find the actual targets location. Simulation results are provided in Fig. 4.16. It is observed that MN-MUST algorithm performs well if the NN is trained in PMC and is tested in PMC.

In the second scenario, MN-MUST algorithm is trained in the absence of mutual coupling. Then the test phase of MN-MUST algorithm performed in the presence of mutual coupling. The result is given in Fig 4.17. One can observe a significant degradation from Fig 4.16. The degradation of the performance is an expected result.

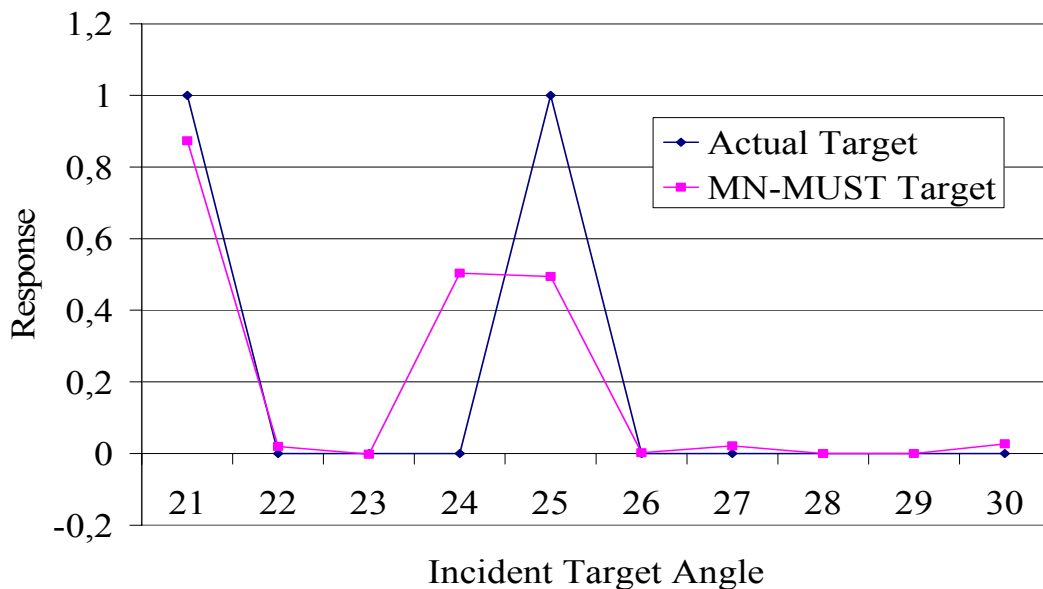


Figure 4.16 Two targets in six-element half-wave dipole uniform circular array (Targets are at 21 and 25 degrees). MN-MUST DoA Networks are trained in PMC.

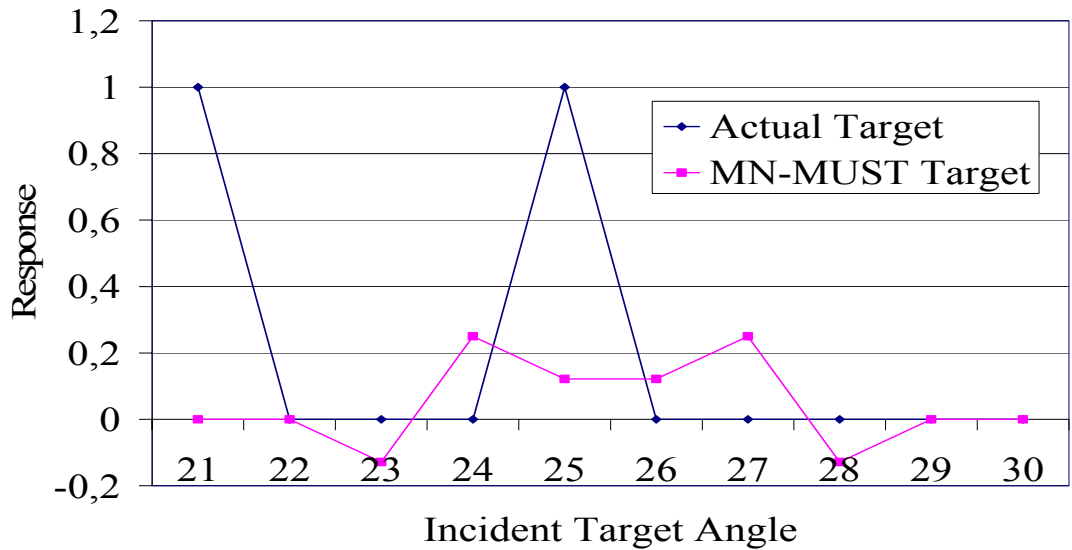


Figure 4.17 Two targets in six-element half-wave dipole uniform circular array (Targets are at 21 and 25 degrees). MN-MUST DoA Networks are trained in the absence of mutual coupling.

4.10 Cylindrical Patch Array Implementation

In order to test MN-MUST algorithm performance in case of a realistic antenna pattern, algorithm is implemented for a twelve element cylindrical patch array. The algorithm is adopted and called CMN-MUST. The array parameters are chosen as $h = 1.6mm$, $\epsilon_r = 4.4$, $L = 38.3mm$, $\theta_0 = 9.1848^\circ$, $a = 38.3mm$ and $f = 1.8 GHz$. It is aimed to cover full azimuth direction. Full azimuth direction is divided into twelve equal sectors. In each sector only three antenna elements whose normalized values more than $-20 dB$ are used. CMN-MUST algorithm consists of three stages; detection, reduced order spatial filtering and DoA estimation stage as MN-MUST does. Detection stage is exactly the same as in MN-MUST.

CMN-MUST algorithm is tested through several simulations. First simulation has two sources in Sector 1. SNR is 20 dB for this simulation. Sector 1 is covering

[$346^\circ - 15^\circ$] angular region and the resolution of DoA estimation stage is set to 1° . Two sources are placed at 348° and 3° . DoA estimation results in polar coordinates are given in Fig. (4.18). Actual targets are shifted 2 units and estimated values are shifted one unit. DoA estimation error RMS values for this example versus 3, 10, 20, 30 and 50 dB SNR levels are given in Fig. (4.19). CMN-MUST algorithm DoA estimation accuracy against SNR is similar to MN-MUST algorithm.

Two targets in two different angular sector case is simulated. CMN-MUST algorithm's detection stage found the targets in Sector-1 and Sector-6. Then the spatial filter for Sector-1 is run to filter out the signal outside the Sector-1. The filtered output applied to the DoA estimation stage of Sector-1. The DoA estimation results and actual targets are given in Fig. (4-20). The target in Sector-6 can be found in a similar way. Hence it is identical to the one in Sector-1, and it was not run. CMN-MUST algorithm performs similarly as the MN-MUST algorithm. However, 12 elements patch is sufficient to cover full 360 degrees of azimuth angle and only three antenna elements are used in each spatial filtering and DoA estimation stages.

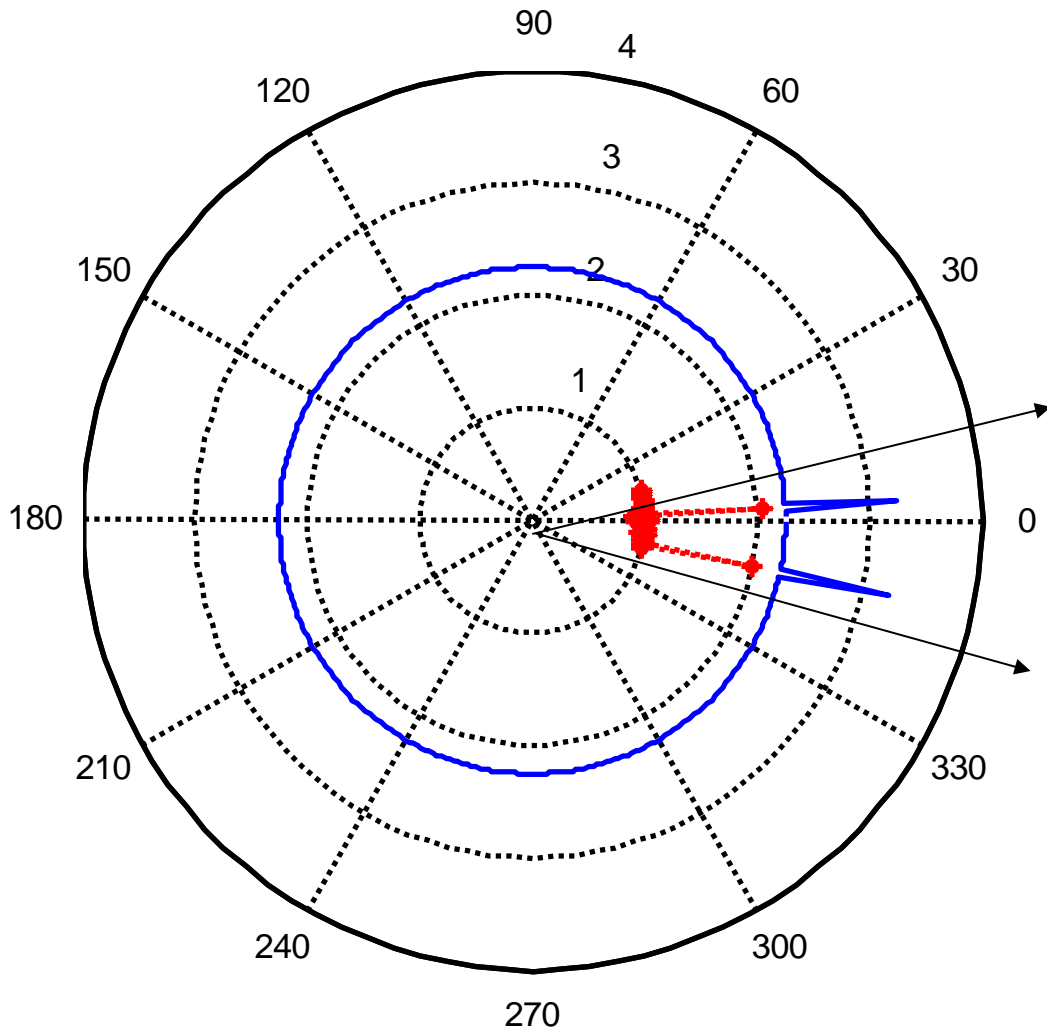


Figure 4.18 DoA estimation two targets are in angular Sector 1 (Targets are at 348 and 3 degrees). CMN-MUST DoA estimation stage of Sector-1 run with a 30 dB SNR level (estimated values of the targets is the one close to the center).

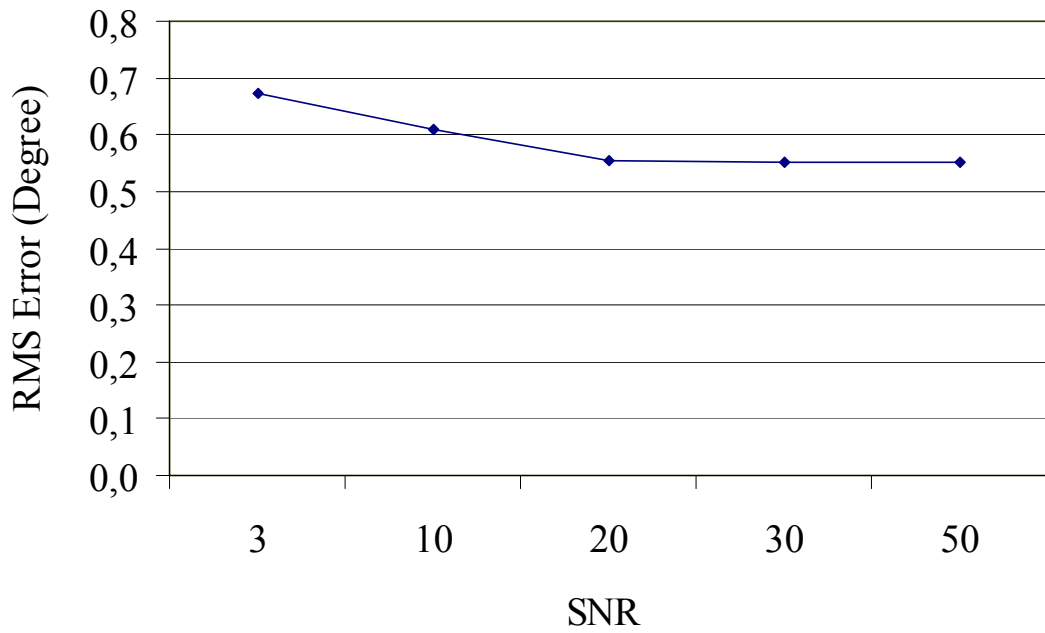


Figure 4.19 CMN-MUST DoA estimation error RMS values vs. 20, 30, 50 dB SNR. Two target case run for angular Sector 1.

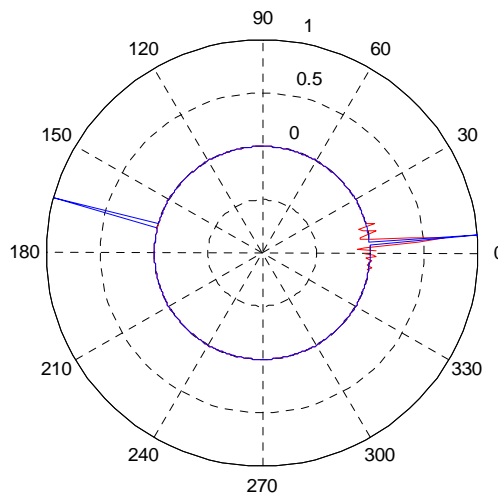


Figure 4.20 Two targets are in two different sectors. The spatial filtering stage run after the detection stage for Sector 1. The filtered output is the input for DoA estimation stage for Sector 1. DoA estimation results for Sector 1 and actual targets in the same axes (targets at 5 and 164 degrees). SNR is 30 dB.

CHAPTER 5

CONCLUSIONS

In this thesis a neural network-based algorithm (MN-MUST) is proposed for real time multiple source tracking problem based on a previously reported work (N-MUST) [57]. MN-MUST algorithm performs DoA estimation in three stages which are the detection, filtering and DoA estimation stages. The main contributions of this proposed system are: reducing the input size for the uncorrelated source case (reducing the training time) of NN system without degradation of accuracy and insertion of a nonlinear spatial filter to isolate each one of the sectors where sources are present, from the others. Focusing on each sub-sector independently improves the accuracy of the overall system.

It is also observed that the MN-MUST algorithm finds the targets correctly no matter whether the targets are located within the same angular sector or not. In addition as the number of targets exceeds the number of antenna elements the algorithm can still perform sufficiently well.

An important measure of how well a particular method performs is the covariance matrix of estimation errors. Estimation error RMS value is compared to Cramer-Rao bound and MUSIC algorithm for a uniform linear point source array. MN-MUST algorithm demonstrated a better performance than MUSIC algorithm for low SNR level. The neural network based methods perform far better than MUSIC algorithm at lower SNRs since they don't encounter the problem of resolvability.

MN-MUST algorithm performance is compared with the N-MUST algorithm in the sense of accuracy, training and performance times and memory requirements. The proposed algorithm had a similar accuracy performance as N-MUST algorithm while having a fast training and performance phases. MN-MUST algorithm had a good performance when there are targets in different angular sectors with the help of inserted spatial filters; while N-MUST algorithm fails when there are targets in different angular sectors. It is observed from simulation results that MN-MUST

algorithm improves N-MUST algorithm and also is successful in cases where N-MUST fails.

The performance of MN-MUST algorithm is discussed with a series of simulations for varying uniform linear arrays with point sources. The parameters such as, antenna elements number in array, SNR levels, sampling number, neural network training parameters are investigated in terms of their influence on DoA RMS error. It is observed that when the number of antenna elements increases then the RMS error decreases, it also has a similar trend for sampling number, angular separation of the sources,

The proposed algorithm is also examined for a uniform circular dipole array in the presence of mutual coupling. Mutual coupling for a uniform circular dipole array is calculated by using the induced EMF method. It has been proved that the MN-MUST algorithm for smart real time multiple source tracking problem can effectively be used in the presence of mutual coupling for both ULA and UCA geometries. Simulation results of MN-MUST algorithm in the presence of mutual coupling for a six element half-wave dipole UCA geometry are provided. Results demonstrate the success of the MN-MUST algorithm performance in the presence of mutual coupling. Similar to adaptive algorithms MN-MUST algorithm is also sensitive to mutual coupling. When the MN-MUST algorithm is performed in the absence of mutual coupling, then in the test phase the MN-MUST algorithm fails as expected.

In order to test the MN-MUST algorithm performance in case of a realistic antenna pattern, algorithm is implemented to a twelve element cylindrical patch array. It is aimed to cover full azimuth direction. Full azimuth direction is divided into twelve equal sectors. In each sector only three antenna elements whose normalized values more than -20 dB are used. Because of those characteristics, MN-MUST algorithm is adopted for cylindrical array geometry. The adopted algorithm is called CMN-MUST (Cylindrical patch array MN-MUST). CMN-MUST algorithm consists of three stages; detection, reduced order spatial filtering and DoA estimation stage as MN-MUST does. Detection stage is exactly the same as in MN-MUST. There are

three antenna elements in each sector, such as *Sector - i* has the $(i - 1)th$, $i - th$ and $(i + 1)th$, antenna elements. If we consider the antenna elements inside the sector of interest only, then we do not need to filter out the signals in the antenna elements outside the sector of interest. In addition we do not need the full array for DoA estimation stage for sectors. This reduces spatial filtering and DoA estimation stage NN size.

It is demonstrated through computer simulations that the performance of the proposed MN-MUST algorithm is quite satisfactory and MN-MUST algorithm is applicable for real time target tracking and DoA estimation problems.

Proposed algorithm is implemented in two dimensional DoA estimation. Future works will be focused on three dimensional DoA estimation of the proposed algorithm.

Proposed algorithm is implemented in two dimensional DoA estimation. Future works will be focused on three dimensional DoA estimation.

REFERENCES

- [1] Godara, L., C, “Application of antenna arrays to mobile communications, Part II: Beam-forming and direction-of-arrival considerations”, Proceedings of IEEE, Vol. 85, pp. 1195-1245, Aug 1997.
- [2] Gross, F., *Smart Antennas for Wireless Communications*, Newyork: McGraw-Hill, 2005.
- [3] Koç, A.T., *Direction Finding with a Uniform Circular Array via Single Shapshot Processing*, Ankara: Middle East Technical University, Ph.D. Thesis, January 1996.
- [4] K.L. Du, A.K.Y. Lai, K.K.M. Cheng, and M. N. S. Swamy, “Neural methods for antenna array signal processing: A review”, Signal Processing, vol. 82, pp. 547–561, 2002.
- [5] Wang, Y.M.; Ma, Y.L., “The performance of neural network for high resolution direction-of-arrival estimation”, 1991 International Conference on Circuits and Systems Proc., vol. 1, pp. 301 - 304, June 1991
- [6] Yang, Z.-K.; Yin, Q.-Y.; Liu, Q.-G.; Zou, L.-H., “Neural networks for direction finding via a stochastic model”, 1991. IEEE International Sympoisum on Circuits and Systems Proc., vol. 5, pp. 2546 - 2549, June 1991
- [7] Yang, J.; Wu, Q.; Reilly, J.P.; “A neural network for direction finding in array processing”, 1992 IEEE International Conference on Acoustics, Speech, and Signal Processing Proc., vol. 2, pp. 313 - 316, March 1992
- [8] Yupeng Chen; Chaohuan Hou; “High resolution adaptive bearing estimation using a complex-weighted neural network”, 1992 IEEE International Conference on Acoustics, Speech, and Signal Processing Proc., vol. 2, pp. 317 - 320, March 1992
- [9] Burel, G.; Rondel, N., “Neural networks for array processing: from DOA estimation to blind separation of sources”, 1993. 'Systems Engineering in the Service of Humans', Conference Proc., vol. 2, pp. 601 - 606, Oct 1993

- [10] Sheng Lin; Qin-Ye Yin, "Searching over DOA parameter space via neural networks", IEEE 1994 International Symposium on Circuits and Systems Proc., vol. 6, pp. 295 - 298, June 1994
- [11] Lo, T.; Leung, H.; Litva, J., "Radial basis function neural network for direction-of-arrivals estimation", IEEE Signal Processing Letters, vol. 1, pp. 45 - 47, Feb. 1994
- [12] Yang, W.-H.; Chan, K.-K.; Chang, P.-R., "Complex-valued neural network for direction of arrival estimation", IEEE Electronics Letters, vol. 30, pp. 574 - 575, March 1994
- [13] Sheng Lin; Qin-Ye Yin, "Performance analysis of Hopfield neural networks for DOA estimation", 1994 IEEE International Symposium on Circuits and Systems Proc., vol. 6, pp. 395 - 398, June 1994
- [14] Lee, C.S., "Non-linear adaptive techniques for DOA estimation-a comparative analysis", Electronic Technology Directions to the Year 2000 Proc., vol. 4, pp. 72 - 77, May 1995
- [15] Shun-Hsyung Chang; Tong-Yao Lee; Wen-Hsien Fang, "High-resolution bearing estimation via unitary decomposition artificial neural network (UNIDANN)", 1995 International Conference on Acoustics, Speech, and Signal Processing Proc., vol. 5, pp. 3607 - 3610, May 1995
- [16] Colnet, B.; Di Martino, J.-C, "Source localization with recurrent neural networks", 1996 IEEE International Conference on Acoustics, Speech, and Signal Processing Proc., vol. 6, pp. 3073 - 3076, May 1996
- [17] Deergha Rao, K., "Narrowband direction finding using complex EKF trained multilayered neural networks", 1996. 3rd International Conference on Signal Processing Proc., vol. 2, pp. 1377 - 1380, Oct 1996
- [18] Arslan, G.; Gurgen, F.; Sakarya, F.A.; "Application of neural networks to bearing estimation", 1996 Proceedings of the Third IEEE Int. Conference on Electronics, Circuits, and Systems Proc., vol. 2, pp. 647 - 650, Oct. 1996

- [19] Hirari, M.; Hayakawa, M., "DOA estimation using blind separation of sources", 1997. Proceedings of the IEEE Signal Processing Workshop on Higher-Order Statistics, pp. 311 - 315, July 1997
- [20] Zhong Ding Lei; Xiu Kun Huang; Shu Jing Zhang, M., "A novel algorithm for wideband DOA estimates based on neural network", IEEE International Conference on Neural Networks Proc., vol. 4, pp. 2167 - 2170, June 1997.
- [21] Alspector, J.; Norgand, J.D.; Parish, J., "Spatio-temporal equalization for wireless communication", 1998 IEEE Radio and Wireless Conference Proc., pp. 165 - 168, Aug. 1998
- [22] Jung Sik Jeong; Araki, K.; Takada, J.-I., "A neural network for direction of arrival estimation under coherent multiple waves", The 1998 IEEE Asia-Pacific Conference on Circuits and Systems Proc., pp. 495 - 498, Nov 1998
- [23] Hirari, M.; Gotoh, K.; Hayakawa, M., "DOA estimation of distributed sources using neural networks", IEEE Signal Processing Proceedings, vol. 1, pp. 335 - 338, Oct. 1998.
- [24] Kar-Ann Toh; Chong-Yee Lee, "Efficient network training for DOA estimation", 1999 IEEE International Conference on Systems, Man, and Cybernetics Proc., vol. 5, pp. 383 - 388, Oct 1999
- [25] Voulgarelis, A.; Popescu, I.; Naornita, I.; Constantinou, P., "Implementation of a direction-of-arrival finding antenna using neural networks", 2000. Proceedings of the Second International Symposium of Trans Black Sea Region on Applied Electromagnetism, vol. 1, pp. 22, June 2000
- [26] Ching-Sung Shieh; Chin-Teng Lin, "Direction of arrival estimation based on phase differences using neural fuzzy network", IEEE Transactions on Antennas and Propagation., vol. 48, pp. 1115 - 1124, July 2000
- [27] Tong Xinhai; Wang Huali; Gan Zhongmin, "Satellite interference location based on RBF neural network method", 2000. 5th International Conference on Signal Processing Proc., vol. 1, pp. 445 - 449, Aug 2000

- [28] Badidi, L.; Radouane, L., "A neural network approach for DOA estimation and tracking", 2000. Tenth IEEE Workshop on Statistical Signal and Array Proc., pp. 434 - 438, Aug 2000
- [29] Badidi, L.; Radouane, L., "A neural network approach for DOA estimation and tracking", 2000. Tenth IEEE Workshop on Statistical Signal and Array Proc., pp. 434 - 438, Aug 2000
- [30] Li Yang; Hu Ming; Liyang Liwan; Pan Weifeng; Chen Yaqin; Feng Zhenghe, "Efficient implementation of DOA estimation for DS-CDMA systems with smart antennas", 2000. International Conference on Communication Technology Proc., vol. 1, pp. 160 - 163, Aug 2000
- [31] Girma, D.; Lazaro, O., "Quality of service and grade of service optimisation with distributed DCA schemes based on Hopfield neural network algorithm", 2000 IEEE 52nd Vehicular Technology Conference Proc., vol. 3, pp. 1142 - 1147, Sept. 2000
- [32] Maruyama, T.; Kuwahara, Y., "Estimation of propagation structure by means of Hopfield neural network", 2001. IEEE Antennas and Propagation Society International Symposium Proceedings, vol. 1, pp. 476 - 479, July 2001
- [33] de Araujo Dourado, O., Jr.; Neto, A.D.D., "Neural networks of modular structure applied to linear and planar antennas array", 2001 SBMO/IEEE MTT-S International Microwave and Optoelectronics Conference Proc., vol. 1, pp. 295 - 298, Aug. 2001
- [34] De Araujo Dourado Junior, O.; Doria Neto, A.D.; da Mata, W., "Intelligent system to find multiple DOA", IEEE 2002 Antennas and Propagation Society International Symposium Proc., vol. 4, pp. 668 - 671, June 2002
- [35] Feng Wenjiang; Yu Ping; Yang Shizhong, "Blind parameter estimation on array antenna CDMA communication syst", 2002 3rd International Conference on Microwave and Millimeter Wave Technology Proc., 4A, pp. 681 - 684, Aug. 2002

- [36] Wang Jie-gui; Luo Jing-qing; Lv Jiu-ming, "Passive tracking based on data association with information fusion of multi-feature and multi-target", 2003 Int. Conference on Neural Networks Proc.,vol. 1, pp. 686 - 689, Dec. 2003
- [37] Li Qiong; Ye Zhongfu; Gan Long, "DOA and Doppler frequency estimation with sensor gain and phase uncertainties", 2003 Int. Conference on Neural Networks Proc.,vol. 2, pp. 1314 - 1317, Dec. 2003
- [38] Coviello, C.M.; Sibul, L.H.; Yoon, P.A., "Algebraic DOA estimation and tracking using ULV decomposition", 2003 Int. Conference on Neural Networks Proc.,vol. 2, pp. 1310 - 1313, Dec. 2003
- [39] Xian Feng; Jianguo Huang; Qunfei Zhang; Haiyan Wang, "A novel DOA estimation method and its focusing matrices for multiple wide-band sources", 2003 Int. Conf. on Neural Networks Proc.,vol. 2, pp. 1306 - 1309, Dec. 2003
- [40] Hongfeng Qin; Jianguo Huang; Qunfei Zhang, "A novel joint estimator of direction-of-arrival and time-delay for multiple source localization", 2003 Int. Conf. on Neural Networks Proc.,vol 2., pp. 1294 - 1297, Dec. 2003
- [41] Zhilong Shan; Fei Ji; Gang Wei, "Extending music-like algorithm for DOA estimation with more sources than sensors", 2003 Int. Conf. on Neural Networks Proc.,vol 2. , pp. 1281 - 1284, Dec. 2003
- [42] Suleesathira, R., "Close direction of arrival estimation for multiple narrowband sources", 2003 Int. Conf. on Neural Networks Proc.,vol. 2, pp. 1277 - 1280, Dec. 2003
- [43] Chen Hongguang; Li biao; Shen Zhenkang, "Efficient network training method for two-dimension DOA estimation", The Fourth International Conference on Computer and Information Technology Proceedings, pp. 1028 - 1032, Sept 2004
- [44] Kuwahara, Y.; Matsumoto, T., "Experiments on direction finder using RBF neural network with post-processing", IEEE Electronics Letters, vol. 41, pp. 602 - 603, May 2005

- [45] Matsumoto, T.; Kuwahara, Y., “Experiments of direction finder by RBF neural network with post processing”, IEEE 2005 Antennas and Propagation Society International Symposium Proc., vol 4A, pp. 10 - 13, July 2005
- [46] Danneville, E.; Brault, J.-J.; Laurin, J.-J., “Implementation of an MLP-based DOA system using a reduced number of MM-wave antenna elements”, IEEE IJCNN '05. Proceedings, vol. 5, pp. 3220 - 3225, Aug 2005
- [47] Lima, C.A.M.; Junqueira, C.; Suyama, R.; Von Zuben, F.J.; Romano, J.M.T., “Least-squares support vector machines for DOA estimation: a step-by-step description and sensitivity analysis”, 2005 IEEE International Joint Conference on Neural Networks Proc., vol. 5, pp. 3226 - 3231, Aug. 2005
- [48] Lima, C.A.M.; Junqueira, C.; Suyama, R.; Von Zuben, F.J.; Romano, J.M.T., “Least-squares support vector machines for DOA estimation: a step-by-step description and sensitivity analysis”, 2005 IEEE International Joint Conference on Neural Networks Proc., vol. 5, pp. 3226 - 3231, Aug. 2005
- [49] Bertrand, H.; Grenier, D.; Roy, S., “Experimental Antenna Array Calibration with ADaptive LInear Neuron (ADALINE) Network”, IEEE 63rd Vehicular Technology Conference 2006, vol. 48, pp. 2706 - 2711, - 2006
- [50] Pour, Hamed Movahedi; Atlasbaf, Zahra; Hakkak, Mohammad, “Evaluation of an MLP-based Direction of Arrival System Using Genetic Algorithm for Training”, IEEE Wireless and Microwave Technology Conference Proc., pp. 1 - 5, Dec. 2006
- [51] Vigneshwaran, S.; Sundararajan, N.; Saratchandran, P., “Direction of Arrival (DoA) Estimation Under Array Sensor Failures Using a Minimal Resource Allocation Neural Network”, IEEE Transactions on Antennas and Propagation., vol. 55, pp. 334 - 343, Feb 2007
- [52] Southall, H., L., J.A. Simmers, and T.H. O'Donnell, “Direction Finding in Phased arrays with a neural network beamformer”, IEEE Transaction on Antennas and Propagation, Vol. 43, December 1995, pp.1369-1374.

- [53] El Zooghby, A.H.; Christodoulou, C.G.; Georgiopoulos, M.; “Performance of radial-basis function networks for direction of arrival estimation with antenna arrays”, IEEE Transactions on Antennas and Propagation., vol. 45, pp. 1611 - 1617, Nov 1997.
- [54] El Zooghby, A.H.; Christodoulou, C.G.; Georgiopoulos, M., “Antenna array signal processing with neural networks for direction of arrival estimation”, The 1997 IEEE Antennas and Propagation Society International Symposium Proc., vol. 4, pp. 2274 - 2277, July 1997
- [55] El Zooghby, A.H.; Christodoulou, C.G.; Georgiopoulos, M., “Multiple sources neural network direction finding with arbitrary separations”, 1998 IEEE-APS Conference on Antennas and Propagation for Wireless Communications Proc., pp. 57 - 60, Nov 1998
- [56] El Zooghby, A.H.E.L.; Southall, H.L.; Christodoulou, C.G., “Experimental validation of a neural network direction finder”, 1999. IEEE Antennas and Propagation Society International Symposium Proc., vol. 3, pp. 1592 - 1595, July 1999
- [57] El Zooghby, A.H.; Christodoulou, C.G.; Georgiopoulos, M., “A neural network-based smart antenna for multiple source tracking”, IEEE Transactions on Antennas and Propagation, vol. 48, pp. 768 - 776, May 2000
- [58] Çaylar, S., K. Leblebicioğlu, G. Dural, “Akıllı Anten Dizileri ile Hedef İzlemede Yapay Sinir Ağları Kullanan Yeni bir Sistem”, Proc. of URSI 2004 National Symposium, pp. 112-114, September 2004.
- [59] Çaylar, S., K. Leblebicioğlu, G. Dural, “A New Neural Network Approach to the Target Tracking Problem with Smart Structure”, Proc. of 2006 IEEE AP-S International Symposium and USNC/URCI meeting, pp. 1121 – 1124, July 2006.
- [60] Çaylar, S., K. Leblebicioğlu, and G. Dural , “A New Neural Network Approach to the Target Tracking Problem with Smart Structure”, Radio Sci., 41, RS5004, doi:10.1029/2005RS003301, 3 October 2006.

- [61] Çaylar, S., K. Leblebicioğlu, and G. Dural , “Modified Neural Multiple Source Tracking Algorithm in The Presence of Mutual Coupling”, Proc. of 2007 IEEE AP-S International Symposium, June 2007.
- [62] Çaylar, S., K. Leblebicioğlu, G. Dural, “A Neural Network Method for Direction of Arrival Estimation with Uniform Circular Dipole Array in The Presence of Mutual Coupling ”, Proc. of RAST 2007, pp. 537-540, June 2007.
- [63] Çaylar, S., K. Leblebicioğlu, G. Dural, “Direction of Arrival Estimation Algorithm with Uniform Linear and Circular Array”, Proc. of SIU 2007, June 2007.
- [64] Bartlett, M., *An Introduction to Stochastic process with Special References to Methods and Application*, Cambridge University Press, New York, 1961
- [65] Capon, J., “High-Resolution Frequency-wavenumber Spectrum Analysis”, Prococeedings of the IEEE, vol. 70, pp. 1408-1418, Aug 1969.
- [66] Van Trees, H., *Optimum Array Processing: Part IV of Detection, Estimation, and Modulation Theory*, Willey Interscience, New York, 2002.
- [67] Makhoul, J., “Linear Prediction: A Tutorial review”, Prococeedings of the IEEE, vol. 63, pp. 561-580, 1975.
- [68] Burg, J. P., “Maximum entropy spectral analysis,” presented at the 37th Annu. Meeting, Society Exploration Geophysics, Oklahoma City, OK, 1967.
- [69] Burg, J. P., “The relationship between maximum Entropy Spectra and maximum likelihood spectra”, Geophysics, vol. 37, pp. 375-376, April 1972.
- [70] Barabell, A., “Improving the resolution of eigenstructured based direction finding algorithms”, in Proc. ICASSP, Boston, MA,1983, pp. 336–339.
- [71] Pisarenko, V.F., “The retrieval of harmonics from a covariance function”, Geophysical Journal of the Royal Astronomical Society, vol. 33 pp. 347-366, 1973.
- [72] J. J. Fuch, “Rectangular Pisarenko method applied to source localization,” IEEE Trans. Signal Process., vol. 44, pp 2377–2383, 1996.

- [73] Reddi, S. S., “Multiple source location—A digital approach,” IEEE Trans. Aerosp. Electron. Syst., vol. AES-15, pp. 95–105, 1979.
- [74] Kumaresan, R. and D. W. Tufts, “Estimating the angles of arrival of multiple plane waves,” IEEE Trans. Aerosp. Elect. Systems, vol. AES-19, pp. 134–139, 1983.
- [75] Ermolaev, V. T. and A. B. Gershman, “Fast algorithm for minimum-norm direction-of-arrival estimation,” IEEE Trans. Signal Processing, vol. 42, pp. 2389–2394, 1994.
- [76] Schmidt, R. O., “Multiple emitter location and signal parameter estimation,” IEEE Trans. Antennas Propagat., vol. AP-34, pp. 276–280, 1986.
- [77] Roy, R. and T. Kailath, “ESPRIT—Estimation of signal parameters via rotational invariance techniques”, IEEE Trans. Acoust., Speech, Signal Processing, vol. ASSP-37, pp. 984–995, 1989.
- [78] Liberti, J., and T. Rappaport, *Smart Antennas for Wireless Communication*, Printice Hall, Newyork, 1999.
- [79] G. Cybenko, “Approximation by superposition of a sigmoid function”, Math. Control, Signals Systems, vol. 12, pp.303–314, 1989.
- [80] K.M. Homi, K.M. Stinchcombe, H. White, “Multilayer feedforward networks are universal approximators”, Neural Networks, vol.2, pp. 359–366, 1989.
- [81] P.C.J. Hill, P.D. Wells, “Antenna beamforming for EW using adaptive layered networks”, Proceedings of the IEE Colloquium on Signal Processing in Electronic Warfare, London, UK, , pp. 2/1–2/5, January 1994
- [82] P.D. Wells, P.C.J. Hill, “Adaptive antenna beamforming using artificial neural networks”, Proceedings of the IEEE Workshop on Neural Network Applications and Tools, Liverpool, UK, pp. 1–5, September 1993.
- [83] J.J. Hopfield, D.W. Tank, “Neural computation of decisions in optimization problems”, Biol. Cybern., vol. 52, pp. 141–152, 1985.

- [84] T. Poggio, F. Girosi, “Networks for approximation and learning”, Proc. IEEE 78, vol. 9, pp 1481–1497, 1990.
- [85] J. Park, I.W. Sanberg, “Universal approximation using radial basis function networks”, Neural Comput., vol. 3, pp.246–257, 1991.
- [86] B. Kosko (Ed.), *Neural Networks for Signal Processing*, Prentice-Hall, Englewood Cliffs, NJ, 1992.
- [87] S. Li, T.J. Sejnowski, “Adaptive separation of mixed broadband sound sources with delays by a beamforming Herault–Jutten network”, IEEE J. Oceanic Eng. 20, vol. 1, pp 73-79, 1995
- [88] E. Oja, “ A simplified neuron model as a principal component analyzer”, J. Math. Biol., vol. 15, pp. 267–273, 1982.
- [89] B.K. Bose, “Fuzzy logic and neural networks in power electronics and drives”, IEEE Ind. Appl. Mag. 6, vol. 3, pp. 57–63, 2000.
- [90] J.S. Roger Jang, C.I. Sun, “Neuro-fuzzy modelling and control”, Proc. IEEE 83, pp. 378–406, 1995.
- [91] C.F. Juang, C.T. Lin, “An on-line self-constructing neural fuzzy inference network and its application”, IEEE Trans.Fuzzy Systems, vol. 6, , pp. 12–32, Jan 1998.
- [92] El Zooghby, A., *Smart Antenna Engineering*, Norwood:Artech House, 2005.
- [93] Walden, R.H. “Performance Trends for Analog-to-Digital Converters”, IEEE Comm. Mag. pp. 96-101, Feb. 1999
- [94] Litva, J., and T.Kwok-Yeung Lo, *Digital Beamforming in Wireless Communications*, Artech House, Boston, MA, 1996.
- [95] J. Rosa, “Superconductor Digital RF Development for Software Radio”, IEEE Comm. Mag. pp. 174, Feb. 2001
- [96] Haykin, S., *Neural Networks: A Comprehensive Foundation*, Newyork: Macmillan, 1994.

- [97] Mulgrew, B. "Applying Radial Basis Functions", IEEE Signal Processing Mag., vol. 13, pp. 50-65, Mar. 1996.
- [98] Neural Network Toolbox, *MATLAB*, Version 7.0, The Mathworks, Inc., Copyright 1999-2004.
- [99] Zhiyong, H., C. A. Balanis, and C. R. Birtcher, "Mutual coupling compensation in UCAs: simulations and experiment", IEEE Trans. on Ant. and Prop., 54, 3082-3086, Nov. 2006.
- [100] Panayiotis Ioannides and Constantine A. Balanis, "Uniform Circular Arrays for Smart Antennas", IEEE Antennas and Propagation Magazine, Vol. 47, No.4, August 2005, pp.192-206.
- [101] Balanis, C., A., Panayiotis I. Ioannides, *Introduction to Smart Antennas*, New Jersey: Morgan & Claypool Publisher, 2007.
- [102] I. J. Gupta and A. A. Ksienski, "Effect of mutual coupling on the performance of adaptive arrays," IEEE Trans. Antennas Propagat., vol. AP-31, no. 5, pp. 785–791, Sept. 1983.
- [103] H. Steyskal and J. S. Herd, "Mutual coupling compensation in small array antennas," IEEE Trans. Antennas Propagat., vol. 38, no. 12, pp. 1971–1975, Dec. 1990.
- [104] T. Svantesson, "Direction finding in the presence of mutual coupling," Thesis for the degree of Licentiate of Engineering, Chalmers University of Technology, School of Electrical and Computer Engineering, Department of Signals and Systems, Göteborg, Sweden, Tech. Rep., 1999.
- [105] T. Su and H. Ling, "On modeling mutual coupling in antenna arrays using coupling matrix," Microw. Opt. Technol. Lett., vol. 28, no. 4, pp. 231–237, Feb. 2001.
- [106] H. T. Hui, "Improved compensation for the mutual coupling effect in a dipole array for direction finding," IEEE Trans. Antennas Propagat., vol. 51, no. 9, pp. 2498–2503, Sept. 2003.

- [107] Z. Huang, C. A. Balanis, and C. R. Birtcher, "Mutual coupling compensation in UCAs: Simulations and experiment," *IEEE Trans. Antennas Propagat.*, vol. 54, no. 11, pp. 3082–3086, Nov. 2006.
- [108] Adve, R.S., and T. K. Sarkar "Compensation for the Effects of Mutual Coupling on Direct Data Domain Adaptive Algorithms," *IEEE Trans. Antennas Propagat.*, vol. 48, no. 1, pp. 86–94, January 2000.
- [109] Dandekar, K.R., "Experiment study of mutual coupling compensation in smart antenna applications", *IEEE Transactions on Wireless Commun.*, vol. 1, pp. 480-487, July 2002.
- [110] Gupta, I.J., and A.K. Ksienski "Effect of Mutual Coupling on the performance of adaptive arrays", *IEEE Transaction on Antennas and Propagation*, vol. 31, pp.785-791, May. 1983.
- [111] Lin, M., Z. Gong, and L. Yang "A Method for DOA Estimation with Mutual Coupling Present", 2005 *IEEE Int. Symp. On Microwave, Antenna, Propagat and EMC Tech.s for Wireless Comm. Proceedings*, pp. 996–999, 2005.
- [112] Wyglinski, A.M., and S.D. Blostein "On Uplink CDMA cell capacity: mutual coupling and scattering effects on beam forming", *IEEE Transaction on VT*, vol.52, pp. 289-304, March 2003.
- [113] Wax, M., and J. Sheinvald, "Direction finding of coherent signals via spatial smoothing for uniform circular arrays", *IEEE Trans. on Ant. and Prop.*, 42, 613-620, May 1994.
- [114] Panayiotis I., and Constantine A. Balanis, " Mutual Coupling in adaptive circular arrays", *Proc. 2004 IEEE Antennas and Propagation Symposium*, pp. 403-406.
- [115] Panayiotis, I., and C. A. Balanis, " Uniform Circular Arrays for Smart Structure", *IEEE Trans. on Ant. and Prop.*, vol. 48, pp. 768-776, May 2000.
- [116] Niemand, P., *Null Synthesis and Implementation of Cylindrical Microstrip Patch Arrays*, Pretoria:University of Pretoria, Ph.D. Thesis, Nov 2004.

- [117] Luk, K., K. Lee and J.S. Dahele, “ Analysis of the Cylindrical-Rectangular Patch Antenna”, IEEE Trans. on Ant. and Prop.,vol. 37, no.2, pp. 143-147, Feb 1989.
- [118] Carver, K.R. and J.W. Mink, “ Microstrip Antenna Technology”, IEEE Trans. on Ant. and Prop.,vol. 29, no.1, pp. 2-24, Jan 1981.
- [119] Richard, W.F., Y.T. Lo, D.D. Harrison, “ An improved Theory for Microstrip Antennas and Applications”, IEEE Trans. on Ant. and Prop.,vol. 29, no.1, pp. 38-46, Jan 1981.
- [120] Krowne, C.M., “ Cylindrical-rectangular Microstrip Antenna”, IEEE Trans. on Ant. and Prop.,vol. 31, no.1, pp. 194-199, Jan 1983.
- [121] Harrington, R.F., *Time-harmonic Electromagnetic Fields*, Newyork:McGraw-Hill, 1961.
- [122] Ashkenazy, J., S. Shtrikman, D. Treves, “ Electric Surface Current Model for the Analysis of Microstrip Antennas on Cylindrical Bodies”, IEEE Trans. on Ant. and Prop.,vol. 33, no.3, pp. 295-300, March 1985.
- [123] Da Silva, C. M., F. Lumini, “ Analysis of Cylindrical Arrays of Microstrip Rectangular Patches”, Electronics Letters,vol. 27, no.9, pp. 778-779, April 1991.
- [124] Pozar, D.M. and D.H. Schaubert, *Microstrip Antennas*, Newyork, IEEE Press, 1995.
- [125] Josefsson, L. and P. Persson, *Conformal Array Antenna Theory and Design*, Hoboken, NJ, John Wiley & Sons, IEEE Press, 2006.
- [126] Hao Ye; DeGroat, D.; “Maximum likelihood DOA estimation and asymptotic Cramer-Rao bounds for additive unknown colored noise”, IEEE Transactions on Signal Processing,vol. 43, pp. 938 - 949, April 1995.
- [127] Delmas, J.-P.; Abeida, H.; “Cramer-Rao bounds of DOA estimates for BPSK and QPSK Modulated signals”, IEEE Transactions on Signal Processing,vol. 54, pp. 117 - 126, Jan. 2006.

- [128] Satish, A.; Kashyap, R.L., “Maximum likelihood estimation and Cramer-Rao bounds for direction of arrival parameters of a large sensor array”, IEEE Transactions on Antennas and Propagation, vol. 44, pp. 478 - 491, April 1996.
- [129] Doroslovacki, M.I.; Larsson, E.G., “Nonuniform linear antenna arrays minimising Cramer-Rao bounds for joint estimation of single source range and direction of arrival”, IEE Proceedings of Radar, Sonar and Navigation, vol. 152, pp. 225 - 231, Aug. 2005.
- [130] Satish, A.; Kashyap, R.L.; “Cramer-Rao bounds and estimation of direction of arrival for narrowband signals”, IEE Proceedings of Acoustics, Speech, and Signal Processing, 1993, vol. 4, pp 532 – 535, 27-30 April 1993.
- [131] Gazzah, H.; Marcos, S.; “Cramer-Rao bounds for antenna array design”, IEEE Transactions on Signal Processing, vol. 54, pp 336 – 345, Jan. 2006.
- [132] Crassidis, J.L. and J.L. Junkins; *Optimal Estimation of Dynamic Systems*, New York, CRC Press Company, 2004.
- [133] Weis, A.J. and E. Weinstein, “Lower Bounds in Parameter Estimation-Summary of results”, Proceedings of ICASSP 1986, pp. 569-572, 1986.
- [134] Van Trees, H.L., *Detection, Estimation, and Modulation Theory : Part I*, New York, Wiley, 1968.
- [135] Ghogho, M., O. Besson, A. Swami, “Estimation of Directions of Arrival of Multiple Scattered Sources”, IEEE Trans. on Signal Processing., vol. 49, pp. 2467-2480, Nov 2001.
- [136] Vigneshwaran, S., Narasimhan Sundararajan, “Direction of Arrival (DoA) Estimation Under Array Sensor Failures Using a Minimal Resource Allocation Neural Network”, IEEE Trans. on Ant. and Prop., vol. 55, 334-343, Feb 2007.

APPENDIX A
CORRELATION MATRIX

Ignoring the noise each entry of the correlation matrix given by Eq. 3.5 can be written as,

$$R_{il} = E\{X_i X_l^H\} \quad (\text{A1})$$

$$X_i(t) = \alpha_i S(t) \quad \text{and} \quad X_l(t) = \alpha_l S(t) \quad (\text{A2})$$

where

$$S(t) = [s_1(t) \quad s_1(t) \quad \dots \quad s_1(t)]^T,$$

$$\alpha_i = [e^{-j(i-1)k_1} \quad e^{-j(i-1)k_2} \quad \dots \quad e^{-j(i-1)k_K}],$$

and $\alpha_l = [e^{-j(l-1)k_1} \quad e^{-j(l-1)k_2} \quad \dots \quad e^{-j(l-1)k_K}]$ respectively.

$$\begin{aligned} R_{il} &= E\{X_i X_l^H\} \\ &= E\{\alpha_i S(t) (\alpha_l S(t))^H\} \\ &= \alpha_i E\{S(t) S(t)^H\} \alpha_l^H \\ &= \frac{R_{11}}{R_{11}} \alpha_i E\{S(t) S(t)^H\} \alpha_l^H \\ &= \frac{1}{R_{11}} \alpha_i E\{S(t) S(t)^H\} \alpha_1^H \alpha_1 E\{S(t) S(t)^H\} \alpha_l^H \end{aligned} \quad (\text{A4})$$

Let's define the P matrix as,

$$P = E\{S(t) S(t)^H\}. \quad (\text{A5})$$

The i -th row and l -th column entry of the matrix P , is $P_{il} = E\{S_i(t) S_l(t)^*\}$ where $*$ represents complex conjugate. Hence if the source signals $\{S_1(t), S_2(t), \dots, S_K(t)\}$ are assumed to be uncorrelated then:

$$E\{S_i(t)S_l(t)^*\} = \frac{E\{S_1(t)S_i(t)^*\}^* E\{S_1(t)S_l(t)^*\}}{E\{S_1(t)S_1(t)^*\}} \quad (\text{A6})$$

Then,

$$P_{il} = \frac{P_{li}^* P_{ll}}{P_{11}} \quad (\text{A7})$$

Providing Eq. A7 one can write,

$$\alpha P \alpha^H \beta P \gamma^H = \beta P \alpha^H \alpha P \gamma^H \quad (\text{A8})$$

where α, β and γ are $1 \times K$ row vector have non zero entries.

Using the property in Eq. A8, Eq. A4 becomes,

$$\begin{aligned} R_{il} &= E\{X_i X_l^H\} \\ &= \frac{1}{R_{11}} \alpha_1 P \alpha_1^H \alpha_i P \alpha_i^H \\ &= \frac{1}{R_{11}} \alpha_i P \alpha_1^H \alpha_1 P \alpha_i^H \\ &= \frac{1}{R_{11}} \alpha_i E\{S(t)S(t)^H\} \alpha_1^H \alpha_1 E\{S(t)S(t)^H\} \alpha_i^H \\ &= \frac{1}{R_{11}} R_{li}^H R_{ll} \end{aligned} \quad (\text{A9})$$

$$R_{il} = \frac{1}{R_{11}} R_{li}^H R_{ll} \quad i = 2, 3, \dots, M \quad \text{and} \quad l = 1, 2, \dots, M \quad (\text{A10})$$

Eq. A10 -shows that all entries of R starting from second row are the combination of the entries in the first row of correlation Matrix. Eventually first row of R is enough to represent the overall correlation matrix when the sources are uncorrelated.

APPENDIX B

MUTUAL IMPEDANCE MATRIX FOR 6 ELEMENT CIRCULAR ARRAY WITH HALF-WAVELENGTH DIPOLES

The mutual impedance matrix of a six element uniform circular array with halfwavelength dipoles is calculated for a circular radius of $a = \frac{3\lambda}{2\pi}$ using the equations described in Chapter 3 section 3.4.3(eqs 3-25 through 3-30). $Ci(x)$ and $Si(x)$ are calculated through the MATLAB functions. The impedance matrix for the subject array is given in Table 3.1.

Table C.1 Coupling Impedance Matrix for a 6 elements halfwavelength dipole array with a radius $a = \frac{3\lambda}{2\pi}$.

73.13 + 42.54i	223.85 - 32.36i	195.54 + 14.65i	174.22 + 18.94i	195.54 + 14.65i	223.85 - 32.36i
223.85 - 32.36i	73.13 + 42.54i	223.85 - 32.36i	195.54 + 14.65i	174.22 + 18.94i	195.54 + 14.65i
195.54 + 14.65i	223.85 - 32.36i	73.13 + 42.54i	223.85 - 32.36i	195.54 + 14.65i	174.22 + 18.94i
174.22 + 18.94i	195.54 + 14.65i	223.85 - 32.36i	73.13 + 42.54i	223.85 - 32.36i	195.54 + 14.65i
195.54 + 14.65i	174.22 + 18.94i	195.54 + 14.65i	223.85 - 32.36i	73.13 + 42.54i	223.85 - 32.36i
223.85 - 32.36i	195.54 + 14.65i	174.22 + 18.94i	195.54 + 14.65i	223.85 - 32.36i	73.13 + 42.54i

VITA

The author was born in Posof, Ardahan, Turkey, on March 15, 1969. He received the B.Sc. degree from Hacettepe University, Ankara, M.Sc. degree from Middle East Technical University, Ankara in 1991 and 1996, respectively. He focused on navigation systems and rate gyros during his M.Sc. degree studies.

He joined Turkish Air Force 1987, as a student. He has been a Turkish Air Force officer since his graduation from Hacettepe University. He had worked in 3 rd Air Supply and Maintenance Center (ASMC), in Ankara, from 1991 to 2003 as an engineer officer in communication, avionics, electronics and fuze design areas. He had worked for AWACS program management, in The Netherlands, as a test officer from 2003 to 2006. In 2006, he was back in 3 rd ASMC where he is still working on.

His current interest are smart antennas, neural network based direction of arrival algorithms. He is a co-author of the bellows papers. He likes to play chess.

1. Çaylar, S., K. Leblebicioğlu, G. Dural, “Akıllı Anten Dizileri ile Hedef İzlemede Yapay Sinir Ağları Kullanan Yeni bir Sistem”, Proc. of URSI 2004 National Symposium, pp. 112-114, September 2004.
2. Çaylar, S., K. Leblebicioğlu, G. Dural, “A New Neural Network Approach to the Target Tracking Problem with Smart Structure”, Proc. of 2006 IEEE AP-S International Symposium and USNC/URCI meeting, pp. 1121 – 1124, July 2006.
3. Çaylar, S., K. Leblebicioğlu, and G. Dural , “A New Neural Network Approach to the Target Tracking Problem with Smart Structure”, Radio Sci., 41, RS5004, doi:10.1029/2005RS003301, 3 October 2006.
4. Çaylar, S., K. Leblebicioğlu, and G. Dural , “Modified Neural Multiple Source Tracking Algorithm in The Presence of Mutual Coupling”, Proc. of 2007 IEEE AP-S International Symposium, June 2007.
5. Çaylar, S., K. Leblebicioğlu, G. Dural, “A Neural Network Method for Direction of Arrival Estimation with Uniform Circular Dipole Array in The Presence of Mutual Coupling ”, Proc. of RAST 2007, pp. 537-540, June 2007.